

İSTANBUL TECHNICAL UNIVERSITY ★ INSTITUTE OF SCIENCE AND TECHNOLOGY

**APPLICABILITY OF EQUAL ENERGY ASSUMPTION TO
THE OUT-OF-PLANE RESPONSE OF STEEL ARCH
BRIDGES**

**Master Thesis by
Civil Eng. Osman Tunc CETINKAYA**

Department : Civil Engineering

Programme: Structural Engineering

May 2005

**APPLICABILITY OF EQUAL ENERGY ASSUMPTION TO
THE OUT-OF-PLANE RESPONSE OF STEEL ARCH
BRIDGES**

**Master Thesis by
Civil Eng. Osman Tunç ÇETİNKAYA
(501011087)**

Date of submission : 3 May 2005

Date of defence examination: 30 May 2005

Supervisor (Chairman): Prof. Dr. Hasan BODUROĞLU

Members of the Examining Committee Prof. Dr. Reha ARTAN

Prof. Dr. Faruk YÜKSELER (YTÜ)

MAY 2005

**EŞDEĞER ENERJİ VARSAYIMININ ÇELİK KEMER
KÖPRÜLERİN DÜZLEM DIŞI DAVRANIŞLARINA
UYGULANABİLİRLİĞİ**

**YÜKSEL LİSANS TEZİ
İnş. Müh. O. Tunç ÇETİNKAYA
(501011087)**

**Tezin Enstitüye Verildiği Tarih : 3 Mayıs 2005
Tezin Savunulduğu Tarih : 30 Mayıs 2005**

**Tez Danışmanı : Prof.Dr. Hasan BODUROĞLU
Diğer Jüri Üyeleri Prof.Dr. Reha Artan
Prof.Dr. Faruk YÜKSELER (YTÜ)**

MAYIS 2005

PREFACE

I would like to express my heartfelt gratitude to my academic adviser Prof. Dr. Hasan BODUROGLU for his great support to my studies. I appreciate his unlimited tolerance to my long stay in Japan.

I want to express my deep thanks to Associate Professor Shozo NAKAMURA of Nagasaki University for his support to my work and for being very kind to me. He gave me very valuable advices.

I would like to express my sincere appreciation to Prof. Kazuo TAKAHASHI of Nagasaki University for his invaluable support.

I owe too much to my friends in the Structural Engineering Laboratory of the Civil Engineering Department of Nagasaki University. They really made my laboratory life very enjoyable. The atmosphere of the laboratory was very motivating to pursue my studies.

I am also very grateful to Eng. Gülçin GÜLEY, Civil Engineering Department Secretary of ITU, for her kind assistance.

I thank my dear family supporting me with their affection even from the other side of the world. Their trust was the greatest motivation for my studies.

TABLE OF CONTENTS

PREFACE	iii
LIST OF TABLES	vi
LIST OF FIGURES	vii
NOTATIONS	ix
SUMMARY	xi
ÖZET	xii
1 INTRODUCTION	1
1.1 Background and Objectives	1
1.2 Literature Review	3
1.3 Contents and Structure of the Thesis	5
2 OUTLINE OF THE CURRENT JAPANESE SEISMIC DESIGN CODE	6
2.1 Principles of Seismic Design	6
2.2 Verification of Seismic Performance	8
2.2.1 Verification of Seismic Performance Based on Static Analysis	11
2.2.1.1 Seismic Performance Verification for Level 1 Earthquake Ground Motion	11
2.2.1.2 Seismic Performance Verification for Level 2 Earthquake Ground Motion	14
2.2.2 Verification Methods of Seismic Performance Based on Dynamic Analysis	15
3 ANALYSIS PROCEDURE	19
3.1 Outline of the Research	19
3.2 Modeling	20
3.2.1 Determination of Structural Parameters and Generation of Models	20
3.2.2 Fiber Modeling	23
3.2.3 Modal Analysis	29
3.2.4 Determination of Damping Parameters	32
3.2.5 Input Ground Motions	34
3.3 Numerical Analysis	37
3.3.1 Examination Procedure	37
3.3.2 Pushover Analysis	38
3.3.3 Linear and Nonlinear Dynamic Response Analysis	41
3.3.4 Application of Equal Energy Assumption	44
3.3.5 Evaluation of Estimation Accuracy	44

4 APPLICABILITY OF EQUAL ENERGY ASSUMPTION	45
4.1 Estimation Accuracy of the Equal Energy Assumption	45
4.2 Relationship between Accuracy of the Estimation and some Parameters	48
4.3 Approximation of $\delta_{SP}/\delta_{DP} - \mu_E$ Relationship	52
4.4 Correction Functions for Equal Energy Assumption	53
4.5 Validity of the Correction Functions	56
5 CONCLUDING REMARKS	60
REFERENCES	62
APPENDIXES	65
CURRICULUM VITAE	88

LIST OF TABLES

	<u>Page No.</u>
Table 2.1. Seismic Performance of Bridges.....	7
Table 2.2. Design Earthquake Ground Motions and Seismic Performance of Bridges.....	8
Table 2.3. Standard Values of the Design Horizontal Seismic coefficient for Level 1 Earthquake Ground Motion, k_{h0}	13
Table 2.4. Standard Values of the Design Horizontal Seismic Coefficient for Level 2 Earthquake Ground Motion, k_{hc0}	15
Table 2.5. Standard Acceleration Response Spectra for Level 1 Earthquake Ground Motion (S_0).....	17
Table 2.6. Standard Acceleration Response Spectra for Level 2 Earthquake Ground Motion.....	18
Table 3.1. Structural Parameters of the Analyzed Models.....	21
Table 3.2. Eigenvalue Analysis Results for Model 1, 2 and 3.....	30
Table 3.3. Eigenvalue Analysis Results for Model 4, 5, 6.....	31
Table 3.4. Rayleigh Damping Coefficients of the Analyzed Models.....	33
Table 3.5. Input Ground Motions For the Dynamic Response Analysis.....	34
Table D.1. Numerical Analysis Results for Model 1.....	74
Table D.2. Numerical Analysis Results for Model 2.....	75
Table D.3. Numerical Analysis Results for Model 3.....	76
Table D.4. Numerical Analysis Results for Model 4.....	77
Table D.5. Numerical Analysis Results for Model 5.....	78
Table D.6. Numerical Analysis Results for Model 6.....	79
Table E.1. Average Estimation Results for Model 1.....	80
Table E.2. Average Estimation Results for Model 2.....	81
Table E.3. Average Estimation Results for Model 3.....	82
Table E.4. Average Estimation Results for Model 4.....	83
Table E.5. Average Estimation Results for Model 5.....	84
Table E.6. Average Estimation Results for Model 6.....	85
Table F.1. Lower Bound Estimation Results for Model 1.....	86
Table F.2. Lower Bound Estimation Results for Model 2.....	86
Table F.3. Lower Bound Estimation Results for Model 3.....	86
Table F.4. Lower Bound Estimation Results for Model 4.....	87
Table F.5. Lower Bound Estimation Results for Model 5.....	87
Table F.6. Lower Bound Estimation Results for Model 6.....	87

LIST OF FIGURES

	<u>Page No.</u>
Figure 2.1. Seismic Design Flowchart.....	10
Figure 2.2. Earthquake Zones.....	13
Figure 3.1. Outline of the Analysis Procedure.....	19
Figure 3.2. Model 1.....	22
Figure 3.3. Element 14.....	23
Figure 3.4. Element 79.....	24
Figure 3.5. Integration Point Configurations of the Cross-Sections.....	24
Figure 3.6. Finite Element Mesh.....	26
Figure 3.7. Material Models for Steel.....	27
Figure 3.8. Boundary and Connection Conditions.....	28
Figure 3.9. Ground Acceleration Record of Level 2 Type 1 Earthquake for Ground Type 1.....	35
Figure 3.10. Ground Acceleration Record of Level 2 Type 1 Earthquake for Ground Type 2.....	36
Figure 3.11. Flowchart of the Numerical Analysis Procedure.....	37
Figure 3.12. Reference Point and the Load Distribution Pattern.....	38
Figure 3.13. Force Displacement Relationship for Model 1.....	39
Figure 3.14. Force Displacement Relationship for Model 2.....	39
Figure 3.15. Force Displacement Relationship for Model 3.....	39
Figure 3.16. Force Displacement Relationship for Model 4.....	40
Figure 3.17. Force Displacement Relationship for Model 5.....	40
Figure 3.18. Force Displacement Relationship for Model 6.....	40
Figure 3.19. Displacement Distributions for Pushover and Dynamic Response analyses (Model 1, 2 and 3).....	42
Figure 3.20. Displacement Distributions for Pushover and Dynamic Response Analyses (Model 4, 5 and 6).....	43
Figure 3.21. Equal Energy Assumption.....	44
Figure 4.1. Numerical Analysis Results for Model 1.....	45
Figure 4.2. Numerical Analysis Results for Model 2.....	46
Figure 4.3. Numerical Analysis Results for Model 3.....	46
Figure 4.4. Numerical Analysis Results for Model 4.....	47
Figure 4.5. Numerical Analysis Results for Model 5.....	47
Figure 4.6. Numerical Analysis Results for Model 6.....	48
Figure 4.7. δ_{SP}/δ_{DP} – Natural Frequency Relationship.....	49
Figure 4.8. $\delta_{SP}/\delta_{DP} - \mu_E$ Relationships for Individual Ground Motions.....	51
Figure 4.9. $\delta_{SP}/\delta_{DP} - \mu_E$ Relationships for Average Response Displacements	52
Figure 4.10. Approximation of $\delta_{SP}/\delta_{DP} - \mu_E$ Relationship.....	53
Figure 4.11. Correction Results for the Average Response Displacements.....	56
Figure 4.12. Correction Results for the Individual Ground Motions.....	56
Figure 4.13. Average Estimation Results by the Proposed Correction Functions.....	58

Figure 4.14.	Lower Bound Estimation Results by the Proposed Correction Functions.....	59
Figure A.1.	Model 2.....	65
Figure A.2.	Model 3.....	66
Figure A.3.	Model 4.....	67
Figure A.4.	Model 5.....	68
Figure A.5.	Model 6.....	69
Figure B.1.	Predominant Eigenmodes. (Model 1, Model 2).....	70
Figure B.2.	Predominant Eigenmodes. (Model 3, Model 4).....	71
Figure B.3.	Predominant Eigenmodes. (Model 5, Model 6).....	72
Figure C.1.	The specified response spectrum for level 2 Type 2 Earthquake Ground Motions.....	73

NOTATIONS

k_{hc}	: Design horizontal seismic coefficient for Level 2 Earthquake Ground Motion.
k_{hc0}	: Standard value of the design horizontal seismic coefficient for Level 2 Earthquake Ground Motion.
c_s	: Force reduction factor.
c_z	: Modification coefficient.
μ_a	: Allowable ductility factor for the structural system having a plastic force displacement relation.
S	: Acceleration response spectra for Level 1 Earthquake Ground Motion.
S_I	: Acceleration response spectra for Level 2 Type I Earthquake ground motion.
S_{II}	: Acceleration response spectra for Level 2 Type II Earthquake ground motion.
c_z	: Modification factor for zones.
c_D	: Modification factor for damping ratio.
S_0	: Standard acceleration response spectra for Level 1 Earthquake Ground Motion.
S_{I0}	: Standard acceleration response spectra for Level 2 Type I Earthquake Ground Motion.
S_{II0}	: Standard acceleration response spectra for Level 2 Type II Earthquake Ground Motion.
u	: Displacement in x direction degree of freedom.
v	: Displacement in y direction degree of freedom.
w	: Displacement in z direction degree of freedom.
Φ_x	: Rotation around x axis degree of freedom.
Φ_y	: Rotation around y axis degree of freedom.
Φ_z	: Rotation around z axis.
η	: Warping degree of freedom.
σ_y	: Yield displacement.
E	: Young Modulus.
ν	: Poisson's ratio.
E'	: Strain hardening slope.
C	: Rayleigh damping matrix.
M	: Mass matrix.
K	: Stiffness matrix.
α	: Mass matrix multiplier.
β	: Stiffness matrix multiplier
h_n	: Damping ratio of mode n
w_n	: Angular frequency of mode n .
f_n	: Natural vibration frequency of mode n .
A_{\max}	: Maximum ground acceleration.
T	: Duration of input ground motion.

δ_{DE}	: Maximum elastic dynamic response.
δ_{DP}	: Maximum inelastic dynamic response.
δ_{SP}	: Estimated maximum nonlinear dynamic response.
$\{\mathbf{H}_i\}$: Lateral force matrix of pushover analysis.
$\{\phi_i\}$: Eigenvector.
m_i	: Mass component of the structural mass matrix.
ϕ_i	: Transverse component of the eigenvector.
E_{DE}	: Strain energy stored in elastic system.
E_{DP}	: Strain energy stored in inelastic system.
μ	: Ductility factor.
μ_E	: Estimated ductility factor.
$f(\mu_E)$: Approximation function of $\delta_{SP}/\delta_{DP}-\mu_E$ relationship.
C	: Correction function.
μ_C	: Corrected ductility factor.
δ_{SP}'	: Corrected estimated maximum inelastic response.

APPLICABILITY OF EQUAL ENERGY ASSUMPTION TO THE OUT-OF-PLANE RESPONSE OF STEEL ARCH BRIDGES

SUMMARY

Japanese seismic design code for highway bridges specifies the Ductility Design Method, which is based on static analysis considering the material and geometrical nonlinearity, as the design method against severe earthquakes such as the Great Kanto Earthquake and the Hyogo-Ken Nanbu Earthquake. The method employs equal energy assumption for the prediction of maximum inelastic seismic response. However, the application of this method is limited because the applicability of equal energy assumption is not clear to some types of structures with complex dynamic behavior such as steel portal frame bridge piers and deck-type steel arch bridges. For these structures time taking and costly dynamic response analysis is required in the seismic design.

In this thesis, the applicability of the equal energy assumption to the out-of-plane inelastic response prediction of deck-type steel arch bridges is numerically evaluated for 6 models by performing eigenvalue analysis, pushover analysis, and elastic and inelastic dynamic response analysis. The models are generated by setting the Arch Rise/Span Length ratio and the distance between the arch ribs as the main structural parameters. Although safety side estimation was achieved by the assumption, the results were too conservative in many cases. For the applicability of the assumption some tendencies were found and correction functions were established to improve the accuracy based on these tendencies. The validity of the proposed correction functions for the estimation of maximum inelastic seismic response without the need of inelastic dynamic response analysis was evidenced on the studied bridge models.

EŞDEĞER ENERJİ VARSAYIMININ ÇELİK KEMER KÖPRÜLERİN DÜZLEM DIŞI DAVRANIŞLARINA UYGULANABİLİRLİĞİ

ÖZET

Japon Karayolu Köprüleri Deprem Yönetmeliği`nde büyük Kanto depremi, Kobe depremi gibi şiddetli depremlere karşı tasarım yöntemi olarak “Süneklik Tasarım Yöntemi” adında malzeme ve geometrik doğrusal olmayan davranışı göz önüne alan statik analizlere dayanan basitleştirilmiş bir tasarım yöntemi verilmektedir. Yöntemde maksimum doğrusal olmayan şekil değiştirmelerin hesabında Eşdeğer Enerji Varsayımı kullanılmaktadır. Ancak bu varsayımın uygulanabilirliği çerçeve sistemli ayaklı köprüler, çelik kemer köprüler gibi karmaşık dinamik davranış gösteren yapılar için sınırlıdır. Bu sebeple Japon Deprem Yönetmeliği, yönetmelikte karmaşık köprü sınıfına giren bu tür köprülerin sismik tasarımı için zaman alıcı ve pahalı doğrusal olmayan dinamik analiz yöntemlerinin kullanılmasını zorunlu kılmıştır. Bu çalışmada eşdeğer enerji varsayımının tabliyesi kemer üzerinde bulunan çelik kemer köprülerin maksimum doğrusal olmayan davranışının hesabında kullanılabilirliği 6 model üzerinde, serbest titreşim, pushover ve de doğrusal ve doğrusal olmayan dinamik davranış analizi (time history) yapılarak denenmiştir. Modellerin oluşturulmasında taşıyıcı kemerlerin basıklığı ve de aralarındaki mesafe temel parametreler olarak seçilmiştir. Elde edilen sonuçlara göre hesaplanan şekil değiştirmeler güvenli tarafta olmasına rağmen birçok durumda hesaplanan değerler ekonomik güvenlik marjını aşarak gerçek şekil değiştirmelerin çok üzerinde bulunmuştur. Ancak varsayımın uygulanabilirliğine ilişkin bazı ilişkiler bulunmuş ve bu ilişkilere dayanarak bazı düzeltme fonksiyonları geliştirilmiştir. Bu fonksiyonların kullanılabilirliği çelik kemer köprü modelleri üzerinde numerik olarak gösterilmiştir.

1 INTRODUCTION

1.1 Background and Objectives

Hyogo-ken Nanbu earthquake of 17 January 1995, which was more severe earthquake than that considered in the design code for structures, caused destructive damage of many structures [1]. The steel bridges were not the exceptions. A variety of damages including the collapse of steel bridge piers and local buckling of stiffened box and pipe sections was observed. After the earthquake, many efforts to improve the seismic performance of steel structures have been made in Japan. These efforts have started from the most common and simple structures such as cantilever steel piers and portal frame piers. The strength and ductility of these structures for cyclic loading was examined experimentally or numerically [2-5]. By the time the trend is shifted to clarify the inelastic seismic behavior of more rare but complicated structures such as steel truss [6], arch [7-14] and elevated [15,16] bridges. Recently more attention is being attracted to the development and application of vibration control devices to the structures [17]. Some outcomes have been introduced into the revised version of Japanese seismic design code for highway bridges (JRA code) [18, 19]. The design ground motion was also revised and two-level seismic design method is specified respectively for moderate (called Level-I) and extreme (called Level-II) ground motions [18, 19].

Steel arch bridges were generally treated as structures for which the earthquake loading is not predominant as they are normally built in mountain areas having few possibilities to experience strong earthquakes in Japan, where ocean-type earthquakes are common. Moreover even if experienced, the earthquake excitation was thought to be not crucial as they are structures having relatively long natural period and generally built on rock foundations. Therefore the conventional design had been made by considering only the moderate earthquakes for which the structure should be in elastic range. However the adoption of Level-II ground motions in the design for all bridges in Japan made it necessary also to understand the inelastic

behavior of steel arch bridges as severe earthquake loading could be the critical situation. There are some earlier papers studying the seismic response of steel arch bridges [7-14]. Usami *et al.* [12] investigated the inelastic seismic performance of a typical upper-deck steel arch bridge subjected to major earthquakes. It is found that seismic responses are small under longitudinal ground motion input but severe plasticization and insufficient performance is observed for transverse excitation. This study has proven that Level-II ground motion can be critical for deck-type steel arch bridges.

Meanwhile, design became complicated compared to the conventional practice, by making it compulsory to evaluate the inelastic behavior of the bridge. The powerful nonlinear dynamic response (time-history) analyses is the most rigorous way for the seismic response estimation. However, it is time consuming, which hampers its wide application to everyday design. It is desirable to conduct the seismic design without the need of dynamic response analysis. JRA code specifies a simplified method called the Ductility Design Method which is based on static analysis. It is a force-based design procedure utilizing elastic analysis and force reduction factor to account for the inelastic behavior. The force reduction factor is calculated by equal energy assumption [20] which assumes the elastic energy stored in the elastic and inelastic systems are identical. However the application of this method is limited only to simple structures as the applicability of equal energy assumption is not clear for structures with complicated dynamic response characteristics. In the JRA code simple dynamic behavior implies that structure is a system with a predominant first vibration mode and possible location of primary plastic hinge can be easily foreseen. This confines the method applicable only to reinforced concrete piers and steel piers with in-filled concrete. For the other structures referred as complicated structures by the JRA code (including the steel arch bridges) dynamic response analysis should be conducted for the seismic performance verification.

The main aim of this research is to develop a seismic design method for deck-type steel arch bridges that is based on static analysis. For this purpose applicability of the equal energy assumption as a prediction tool of the maximum inelastic response is examined. Factors affecting the estimation accuracy of the equal energy assumption are evaluated and correction functions are developed to improve the estimation accuracy. Validity of these correction functions is evaluated for their availability to

substitute the inelastic dynamic response analysis in order to simplify the seismic design for deck-type steel arch bridges.

1.2 Literature Review

The equal energy assumption is proposed by Veletsos and Newmark [20] in a research studying the effect of the inelastic behavior on the response of simple systems to earthquake motions. They have compared the dynamic responses of single degree of freedom linear and nonlinear systems and try to relate the nonlinear response to the linear response. Two possible approaches are presented for the relation of linear and nonlinear systems. One of the possibilities is to relate the dynamic response of the nonlinear system to that of the corresponding linear system by considering the maximum relative displacements of the two systems are equal. This approach is called the equal displacement assumption. The other approach is to compute the displacements for the nonlinear system by equating the energy at the maximum deformation of this system to the maximum strain energy in corresponding linear system. This approach is called the equal energy assumption. It was found that the two procedures give nearly identical results for small values of ductility factor. However, for the larger values the differences were appreciable.

There are some earlier researches regarding the applicability of the equal energy assumption to steel bridges. Usami *et al.* [21] examined the applicability of the equal energy and equal displacement assumptions based on the results of pseudo-dynamic tests of cantilever columns of steel bridge piers. In this study, fairly good estimation of nonlinear response was achieved by using the equal energy assumption, while the response estimated by the equal displacement assumption was much smaller than the test results.

Nakajima *et al.* [22] investigated the applicability of the equal energy assumption to the seismic design of steel portal frames. The paper states that the assumption can be used as a safety side estimation of the maximum nonlinear response, but the estimated maximum displacement can be much larger than the one obtained by elasto-plastic dynamic response analysis.

Nakamura *et al.* [23] also investigated the applicability of the equal energy assumption to steel portal frames. In this study it is found that the equal energy

assumption results in conservative side prediction of the maximum response. But in many cases the results were too conservative. Some correction functions are suggested to improve the estimation accuracy. Additionally, a static analysis method to predict the maximum nonlinear response of steel portal frame bridge piers is presented.

Lu *et al.* [13, 14] investigated the applicability of a capacity and demand prediction procedure based on a nonlinear pushover analysis and an equivalent single-degree-of-freedom system approximation for seismic performance evaluation of steel arch bridges. The procedure is presented as a simplified method to estimate the out-of plane nonlinear seismic demand without performing dynamic response analysis of the actual multi-degree-of-freedom system but using the pushover analysis and conducting dynamic response analysis of the equivalent single-degree-of-freedom system. It is found that the proposed pushover-analysis-based procedure results in acceptable accuracy for the prediction of the seismic demand.

1.3 Contents and Structure of the Thesis

This thesis is composed of 5 chapters as explained below.

Chapter 1 gives the objective of the research. Previous researches about the equal energy assumption and simplification of seismic design method for steel arch bridges are summarized as the background of this study.

Chapter 2 briefly explains the main concepts of the current Japanese Seismic Design Code for highway bridges.

In Chapter 3, the analysis procedure conducted throughout the research is described in details. First the generation of models and the analysis considerations are explained in the modeling section. Then the main steps of the numerical analysis which are the pushover analysis, linear and nonlinear dynamic response analysis and the application of the equal energy assumption to predict the maximum seismic response are explained.

Chapter 4 discusses the estimation accuracy of the equal energy assumption and evaluates the applicability of the assumption for the prediction of maximum seismic response. As it is found that the estimation resulted in poor accuracy in many cases, some correction functions are developed to improve the estimation accuracy. The improved estimation accuracy results are presented and the validity of the proposed correction functions is demonstrated.

Chapter 5 presents the concluding remarks of the research.

2 OUTLINE OF THE CURRENT JAPANESE SEISMIC DESIGN CODE

2.1 Principles of Seismic Design

Two levels of design earthquake ground motions are specified for the seismic design of a bridge: The first level corresponds to an earthquake with high probability of occurrence during the bridge service life (called “Level 1 Earthquake Ground Motion”), and the second level corresponds to an earthquake with less probability of occurrence during the bridge service life but strong enough to cause critical damage (called “Level 2 Earthquake Ground Motion”). For the Level 2 Earthquake Ground Motion, two types of earthquake ground motions having different characteristics shall be taken into account, namely, Type I of a plate boundary earthquake with large magnitude like the great Kanto Earthquake and Type II of an inland direct strike type earthquake like the Hyogo-ken nanbu earthquake. Type I represents the one with large amplitude and longer duration, while Type II motion is the one with strong accelerations and shorter duration.

Depending on the social functions, roles for disaster reduction efforts after an earthquake, and influences of function losses, bridges are classified into two groups: bridges of standard importance (Class A), and bridges of high importance (Class B).

Seismic performances of bridges as a target of seismic design are classified into three levels in view of the seismic behavior of the bridge:

- 1) Seismic Performance Level 1 “Performance level of a bridge keeping its sound functions during an earthquake”: The structure should behave in an elastic manner without any essential damage. The bridge shall be protected safely from unseating, no emergency repair is needed to recover the functions soon after the earthquake, and also repair work which may take a long time can be easily conducted.
- 2) Seismic Performance Level 2 “Performance level of a bridge sustaining limited damages during an earthquake and capable of recovery within a short period”: This performance can ensure not only the safety of unseating prevention, but also

capability of recovering the functions soon after the event as well as reparability by a comparatively easy long-term repair work.

3) Seismic Performance Level 3 “Performance Level of a bridge sustaining no critical damage during an earthquake”: The safety against unseating should be ensured, but does not cover the functions necessary for serviceability and reparability for seismic design.

Table 2.1 summarizes items of Seismic Performances 1 to 3 in view of safety, serviceability and reparability for seismic design. Safety implies performance to avoid loss of life due to unseating of superstructure during an earthquake. Serviceability means that a bridge is capable of keeping its bridge functions such as fundamental transportation function, role of evacuation routes and emergency routes for rescue, first aid, medical services, firefighting and transportation of emergency goods to refugees. Reparability denotes capability of repairing seismic damages.

Table 2.1: Seismic Performance of Bridges

Seismic Performance	Seismic Safety Design	Seismic Serviceability Design	Seismic Reparability Design	
			Emergency Reparability	Permanent Reparability
Seismic Performance Level 1 : Keeping the sound functions of bridges	To ensure the safety against girder unseating	To ensure the normal functions of the bridges	No repair work is needed to recover the functions	Only easy repair works are needed
Seismic Performance Level 2: Limited damages and recovery	Same as above	Capable of recovering functions within a short period after the event	Capable of recovering functions by emergency repair works	Capable of easily undertaking permanent repair works
Seismic Performance Level 3: No critical damages	Same as above	—	—	—

A performance based design approach is specified which targets one of the above seismic performance levels for the seismic behavior of the bridge depending on its importance and levels of design earthquake motions. According to this approach the seismic design should conform to the following.

1) Both Class A and Class B bridges shall be designed so that the Seismic Performance Level 1 is ensured to the Level 1 Earthquake Ground Motion.

2) To the Level 2 Earthquake Motion Class A bridges shall be designed so that the Seismic Performance Level 3 is ensured, while Class B bridges should be designed so that the Seismic Performance Level 2 is ensured.

These target performance levels for different bridge classes and ground motion levels are summarized in **Table 2.2**.

Table 2.2: Design Earthquake Ground Motions and Seismic Performance of Bridges

Earthquake Ground Motions		Class A Bridges	Class B Bridges
Level 1 Earthquake Ground Motion (highly probable during the bridge service life)		Keeping sound functions of bridges (Seismic Performance Level 1)	
Level 2 Earthquake Ground Motion	Type I Earthquake Ground Motion (a plate boundary type earthquake with a large magnitude)	No critical damages (Seismic Performance Level 3)	Limited seismic damages and capable of recovering bridge functions within a short period (Seismic Performance Level 2)
	Type-II (an inland direct strike type earthquake like Hyogo-ken Nanbu Earthquake)		

2.2 Verification of Seismic Performance

In verifying the seismic performance, the limit state of each structural member shall be appropriately determined in accordance with the target performance level of the bridge. Limit states for Seismic Performance Level 1 shall be properly established so that the mechanical properties of the bridge are maintained within the elastic ranges. For each structural member the stress induced by an earthquake shall not exceed its allowable value. For the limit states of performance level 2 and performance level 3 plastic behavior is also taken into account. The structural member, in which the generations of plastic behavior are allowed, deforms plastically within a range of easy functional recovery for performance level 2. The limit states for performance level 3 are generated in a way that the plastic behavior is allowed to take place within a range of the ductility limit of the member without the concern of functional recovery.

The verification shall be performed so that the state of each structural member of a bridge due to the design seismic force does not exceed its limit state. The general verification procedure is illustrated in **Figure 2.1**. The verification is carried out first for Level 1 Earthquake Ground Motions and then for Level 2 Earthquake ground motion by employing either static analysis or dynamic response analysis. Static Analysis is applicable to bridges which have no complicated seismic behavior. For the bridges with complicated seismic behavior dynamic analysis are required.

2.2.1 Verification of Seismic Performance Based on Static Analysis

In static analysis, responses can be obtained by substituting reactions induced in structures or ground due to effects of earthquake with static loads so that seismic behavior could be comparatively simply estimated. The method is applicable only to bridges without complicated seismic behavior which means that the structure is a system with a predominant first vibration mode and clear location where primary plastic behavior generates in case of level 2 earthquake motions is easy to predict.

Static-analysis-based verification methods include two kinds of approaches, Seismic Performance Verification for Level 1 Earthquake Ground Motion and Seismic Performance Verification for Level 2 Earthquake Ground Motion called as "Seismic Coefficient Method" and "Ductility Design Method" in the previous editions of the JRA [1] code, respectively. The former refers to the design method in which vibration characteristics of elastic range is considered while the latter is the method in which deformation property and dynamic strength of nonlinear zone of a structure is taken into account. Both of the approaches employ design horizontal seismic coefficients that convert the dynamic forces into static ones. Static inertia forces obtained by multiplying these coefficients with the structural weight are applied to the structure in lateral direction in order to estimate the seismic response.

2.2.1.1 Seismic Performance Verification for Level 1 Earthquake Ground Motion

In the verification for Level 1 Earthquake Ground Motion, the first mode of vibration in elastic range of the objective structure is taken into account and associated elastic responses can be estimated by substituting seismic reactions with static ones. Stresses or displacements resulted from the responses is then confirmed to be less than each allowable value of the limit states for Seismic Performance Level 1.

The design horizontal seismic coefficient to be used for this method is defined by equation (2.1) in terms of the standard value of the design horizontal seismic coefficient presented in **Table 2.3**. However, if the value obtained from this equation is less than 0.1, the seismic coefficient is set to 0.1

$$k_h = c_z k_{h0} \quad (2.1)$$

where,




k_h : Design horizontal seismic coefficient.

k_{h0} : Standard value of the design horizontal seismic coefficient for Level 1 Earthquake Ground Motion shown in **Table 2.3**.

c_z : Modification coefficient for zone, as shown in **Figure 2.2**

Table 2.3: Standard Values of the Design Horizontal Seismic coefficient for Level 1 Earthquake Ground Motion, k_{h0}

Ground Condition	k_{h0} value for natural period T (sec)		
	Group I (stiff)	$T < 0.1$ $k_{h0} = 0.431T^{1/3}$ But $k_{h0} \geq 0.16$	$0.1 \leq T \leq 1.1$ $k_{h0} = 0.2$
Group II (Moderate)	$T < 0.1$ $k_{h0} = 0.427T^{1/3}$ But $k_{h0} \geq 0.20$	$0.2 \leq T \leq 1.3$ $k_{h0} = 0.25$	$1.3 < T$ $k_{h0} = 0.298T^{2/3}$
Group III (soft)	$T < 0.1$ $k_{h0} = 0.430T^{1/3}$ But $k_{h0} \geq 0.24$	$0.34 \leq T \leq 1.5$ $k_{h0} = 0.3$	$1.5 < T$ $k_{h0} = 0.393T^{2/3}$

Legend	Zoning	Correction factor c_z
	A	1.0
	B	0.85
	C	0.7

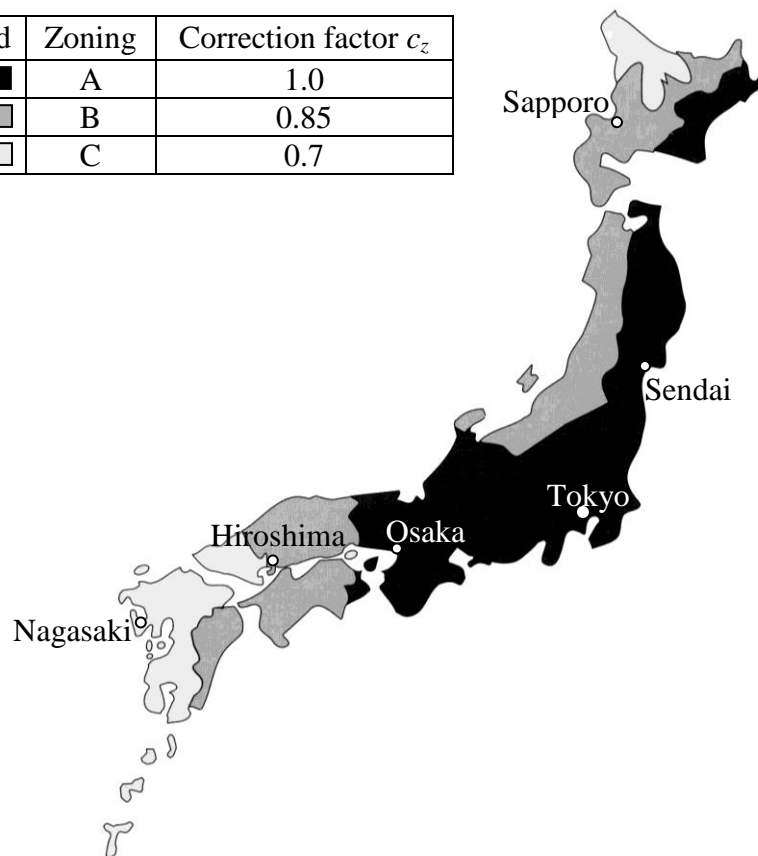


Figure 2.2 Earthquake Zones

2.2.1.2 Seismic Performance Verification for Level 2 Earthquake Ground Motion

In verification of Level 2 Earthquake Ground Motion by the static analysis, the plastic behavior is considered since the target seismic performance levels are level 2 and level 3 depending on the class of the bridge. The dynamic inelastic response generated in the bridge is estimated with the equal energy assumption of one-degree-of freedom system, and ductility or strength is taken into account within plastic ranges of the members by reducing the static inertia force applied to the structure.

The design horizontal seismic coefficient to be used for this method is calculated by Equation (2.2). For Ground Motion Type I, when the product of the standard value of the design horizontal seismic coefficient (k_{hc0}) and modification factor for zones (c_z) is less than 0.3, design horizontal seismic coefficient shall be obtained by multiplying the force reduction factor (c_s) by 0.3. In addition, when the design horizontal seismic coefficient is less than 0.4 times the modification factor for zones (c_z), the design horizontal seismic coefficient shall be equal to 0.4 times c_z .

$$k_{hc} = c_s c_z k_{hc0} \quad (2.2)$$

where

k_{hc} : Design horizontal seismic coefficient for Level 2 Earthquake Ground Motion.

k_{hc0} : Standard value of the design horizontal seismic coefficient for Level 2 Earthquake Ground Motion shown in **Table 2.4**.

c_s : Force reduction factor as in equation (2.3)

c_z : Modification coefficient for zone.

For a structural system that can be modeled as a one degree-of-freedom vibration system having a plastic force-displacement relation, force reduction factor is calculated as Equation (2.3) based on the equal energy assumption.

$$c_s = \frac{1}{\sqrt{2\mu_a - 1}} \quad (2.3)$$

where

μ_a : Allowable ductility factor for the structural system having a plastic force displacement relation.

Table 2.4: Standard Values of the Design Horizontal Seismic Coefficient for Level 2 Earthquake Ground Motion, k_{hc0}

(a) Type-I Ground Motions			
Ground Condition	k_{hc0} value for natural period T (sec)		
Type I (stiff)	$k_{hc0}=0.7$ for $T \leq 1.4$		$k_{hc0}=0.876T^{2/3}$ for $T > 1.4$
Type II (Moderate)	$k_{hc0}=1.51T^{1/3}$ ($k_{hc0} \geq 0.7$) for $T < 0.18$	$k_{hc0}=0.85$ For $0.18 \leq T \leq 1.6$	$k_{hc0}=1.16T^{2/3}$ For $T > 1.6$
Type III (soft)	$k_{hc0}=1.51T^{1/3}$ ($k_{hc0} \geq 0.7$) For $T < 0.29$	$k_{hc0}=1.0$ For $0.29 \leq T \leq 2.0$	$k_{hc0}=1.59T^{2/3}$ For $T > 2.0$
(b) Type-II Ground Motions			
Ground Condition	k_{hc0} value for natural period T (sec)		
Type I (stiff)	$k_{hc0}=4.46T^{2/3}$ For $T \leq 0.3$	$k_{hc0}=2.0$ For $0.3 \leq T \leq 0.7$	$k_{hc0}=1.24T^{4/3}$ For $T > 0.7$
Type II (Moderate)	$k_{hc0}=3.22T^{2/3}$ For $T < 0.4$	$k_{hc0}=1.75$ For $0.4 \leq T \leq 1.2$	$k_{hc0}=2.23T^{4/3}$ For $T > 1.2$
Type III (soft)	$k_{hc0}=2.38T^{2/3}$ For $T < 0.5$	$k_{hc0}=1.50$ For $0.5 \leq T \leq 1.5$	$k_{hc0}=2.57T^{4/3}$ For $T > 1.5$

2.2.2 Verification Methods of Seismic Performance Based on Dynamic Analysis

In verification of seismic performance for bridges with complicated seismic behavior, a dynamic analysis shall be applied to obtain the seismic response. “Bridges with

complicated seismic behavior” indicate bridges that the application of the static analysis is limited because of the reasons given below.

- i) In case that vibration modes primarily affecting responses of the bridge differ considerably from ones assumed by the static analysis method.
- ii) There are more than 2 types of vibration modes contributing to responses of the bridge.
- iii) In verification of seismic performance for Level 2 Earthquake Ground Motion, plural plastic hinges are expected or locations of plastic hinges cannot be specified due to complicated structure.
- iv) In case the application of equal energy assumption is not clear for the verification of seismic performance for Level 2 Earthquake Ground Motion.

Depending on the above issues, bridges that should be verified with the dynamic analysis method are as follows.

- 1) Bridges with longer natural periods (generally more than 1.5s), or bridges with higher piers (generally more than 30m)
- 2) Bridges of horizontal force distributed structure with rubber bearings
- 3) Seismically-isolated bridges
- 4) Rigid-frame bridges
- 5) Bridges with steel piers in which plasticity are allowed
- 6) Bridge with cables such as cable-stayed bridges or suspension bridges
- 7) Deck-type or half-through-type arch bridges
- 8) Curved bridges with a large angle between ends of superstructure at a small curvature.

During the verification of seismic performance by dynamic method, the maximum response values such as sectional force and displacement occurred in each structural member, which are obtained from dynamic response analysis results, shall be kept below the allowable values. The methods of dynamic response analysis include time history method and acceleration response spectrum method. The verification of seismic performance for each level of ground motion should be conducted by using the average seismic response for at least three input ground motions.

The ground motions used in the dynamic response analysis are spectral fitted to the following response spectra for Level 1 and Level 2 ground motions respectively;

$$S = c_z \cdot c_D \cdot S_0 \quad (2.4)$$

$$S_I = c_z \cdot c_D \cdot S_{I0} \quad (2.5)$$

$$S_{II} = c_Z \cdot c_D \cdot S_{II0} \quad (2.6)$$

where

- S_I : Acceleration response spectra for Level 1 Earthquake Ground Motion
 S_{II} : Acceleration response spectra for Level 2 Type I Earthquake Ground Motion.
 S_{II} : Acceleration response spectra for Level 2 Type II Earthquake Ground Motion.
 c_Z : Modification factor for zones.
 c_D : Modification factor for damping ratio. It is calculated by Equation (2.7) in accordance with the damping ratio h .
 S_0 : Standard acceleration response spectra (cm/sec²) for Level 1 Earthquake Ground Motion given in **Table 2.5** in accordance with fundamental period T .
 S_{I0} : Standard acceleration response spectra (cm/sec²) for Level 2 Type I Earthquake Ground Motion given in **Table 2.6(a)** in accordance with fundamental period T .
 S_{II0} : Standard acceleration response spectra (cm/sec²) for Level 2 Type II Earthquake Ground Motion given in **Table 2.6(b)** in accordance with fundamental period T .

The standard acceleration spectra are given for damping ratio $h=0.05$. When the considered modal damping ratio h_i of the structure is different from this value, the spectra is modified by c_D computed as:

$$c_D = \frac{1.5}{40h_i + 1} + 0.5 \quad (2.7)$$

Table 2.5 Standard Acceleration Response Spectra for Level 1 Earthquake Ground Motion (S_0)

Ground Condition	Response Acceleration S_{I0} (cm/sec ²)		
Group I (stiff)	$T < 0.1$ $S_0 = 431T^{1/3}$ But $S_0 \geq 160$	$0.1 \leq T \leq 1.1$ $S_0 = 200$	$1.1 < T$ $S_0 = 220/T$
Group II (Moderate)	$T < 0.2$ $S_0 = 427T^{1/3}$ But $S_0 \geq 200$	$0.2 \leq T \leq 1.3$ $S_0 = 250$	$1.3 < T$ $S_0 = 325/T$
Group III (soft)	$T < 0.34$ $S_0 = 430T^{1/3}$ But $S_0 \geq 240$	$0.34 \leq T \leq 1.5$ $S_0 = 300$	$1.5 < T$ $S_0 = 450/T$

Table 2.6 Standard Acceleration Response Spectra for Level 2 Earthquake Ground Motion

(a) Type-I Ground Motion

Ground Condition	Response Acceleration S_{I0} (cm/sec ²)		
Type I (stiff)	$S_{I0}=700$ for $T_i \leq 1.4$		$S_{I0}=980/T_i$ for $T_i > 1.4$
Type II (Moderate)	$S_{I0}=1505T_i^{1/3}$ ($S_{I0} \geq 700$) For $T_i < 0.18$	$S_{I0}=850$ For $0.18 \leq T_i \leq 1.6$	$S_{I0}=1360/T_i$ For $T_i > 1.6$
Type III (soft)	$S_{I0}=1511T_i^{1/3}$ ($S_{I0} \geq 700$) For $T_i < 0.29$	$S_{I0}=1000$ For $0.29 \leq T_i \leq 2.0$	$S_{I0}=2000/T_i$ For $T_i > 2.0$

(b) Type-II Ground Motions

Ground Condition	Response Acceleration S_{II0} (cm/sec ²)		
Type I (stiff)	$S_{II0}=4463T_i^{2/3}$ For $T_i \leq 0.3$	$S_{II0}=2000$ For $0.3 \leq T_i \leq 0.7$	$S_{II0}=1104/T_i^{5/3}$ For $T_i > 0.7$
Type II (Moderate)	$S_{II0}=3224 T_i^{2/3}$ For $T_i < 0.4$	$S_{II0}=1750$ For $0.4 \leq T_i \leq 1.2$	$S_{II0}=2371/T_i^{5/3}$ For $T_i > 1.2$
Type III (soft)	$S_{II0}=2381T_i^{2/3}$ For $T_i < 0.5$	$S_{II0}=1500$ For $0.5 \leq T_i \leq 1.5$	$S_{II0}=2948/T_i^{5/3}$ For $T_i > 1.5$

3 ANALYSIS PROCEDURE

3.1 Outline of the Research

The main steps of the analysis procedure are illustrated in **Figure 3.1**. First the steel arch bridge models are generated considering some structural parameters in order to have models representing a general deck-type steel arch bridge behavior. The generated models are investigated by fiber modeling using beam finite elements. Then numerical analyses are conducted to study the applicability of the equal energy assumption for the maximum inelastic response estimation. The applicability of the assumption is evaluated as a next step and correction functions are set in order to improve the accuracy of the estimation. Finally the validity of the proposed correction functions is evaluated. These steps are explained in detail in the following sections.

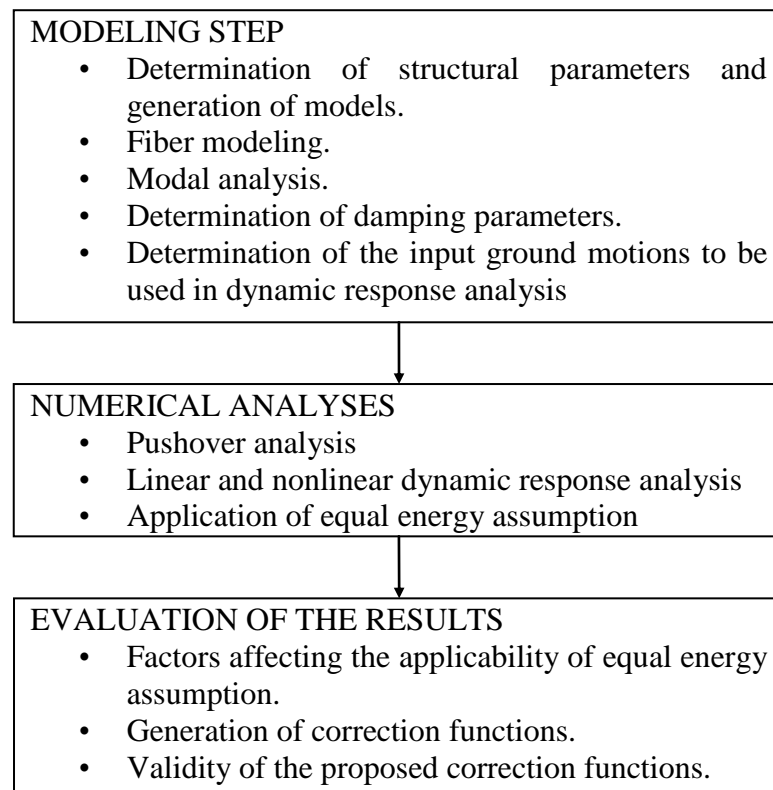


Figure 3.1: Outline of the Analysis Procedure

3.2 Modeling

3.2.1 Determination of Structural Parameters and Generation of Models

The applicability of equal energy assumption is studied numerically on 6 deck-type steel arch bridge models. The structural parameters that are thought to affect the applicability of the assumption are the Arch Rise/ Span Length ratio and the distance between the arch ribs. Model 1 shown in **Figure 3.2** is used as a template model to generate 6 parametric models. This bridge was adopted by the JSSC committee as a representative model for nonlinear behavior investigation under major earthquakes [24]. The parametric models are generated by using JSP-15W [25] preliminary design software for steel arch bridges. This software determines the necessary cross-sections of the arch ribs, stiffening girder and vertical members considering the design specifications. During the calculation only the vertical loads and impact factor are taken into account. Having used this software for the generation of the new models, only the cross sections of the arch rib, stiffening girder and the vertical members are changed. The transverse and diagonal members are kept the same with the template Model 1. It is assumed that these members don't have significant influence to the estimation accuracy results of the equal energy assumption. As it will be explained in detail later in **Section 3.3**, the assessment of the accuracy of the assumption is based on the comparison of the estimation results of equal energy assumption with that of the dynamic response analysis. The individual effects of these members are thought to be negligible for the evaluation of the applicability of equal energy assumption as they are considered to be the same for in both dynamic response analysis and application of equal energy assumption.

The structural parameters are summarized in **Table 3.1**. Models 2, 3, 4 are generated from the Model 1 by changing the only the Arch Rise. Models 5 and 6 are generated from Model 1 by changing only the distance between the two arch ribs. The generation process was carefully conducted in order to keep the newly generated models within realistic limits. The selected Arch Rise /Span Length ratios have their applications in existing steel arch bridges. The template Model 1 and newly generated Models 2, 3, 4 carry two-lane traffic. The distance between the arch ribs is widened in order to carry a deck having three lanes for Model 5, and four lanes for model 6. By this way realistic steel arch bridge models are generated to be studied by

numerical analysis. Models 1, 2, 3 and 4 constitute the pattern demonstrating the effect of Arch Rise/Span Length ratio, whereas Models 1, 5 and 6 demonstrate the effect of the distance between the arch ribs on the applicability of equal energy assumption.

Newly generated models 2, 3, 4, 5, 6 are illustrated in **Appendix A**, respectively. Also the cross-sections of the main structural elements are shown in the figures. Box type section is used for the arch rib and side column. I-section is adopted for the stiffening girder. The cross section of the arch rib near its support and that of the stiffening girder in the span center are shown in the figures. Uniform box section is used for the side columns.

Table 3.1: Structural Parameters of the Analyzed Models

Model No.	Span Length (m)	Arch Rise (m)	$\frac{\text{Arch Rise}}{\text{Span Length}}$	Distance between the Arch Ribs (m)
Model 1	114	16.87	0.15	6.0
Model 2	114	22.80	0.20	6.0
Model 3	114	34.20	0.30	6.0
Model 4	114	45.60	0.40	6.0
Model 5	114	16.87	0.15	9.5
Model 6	114	16.87	0.15	13

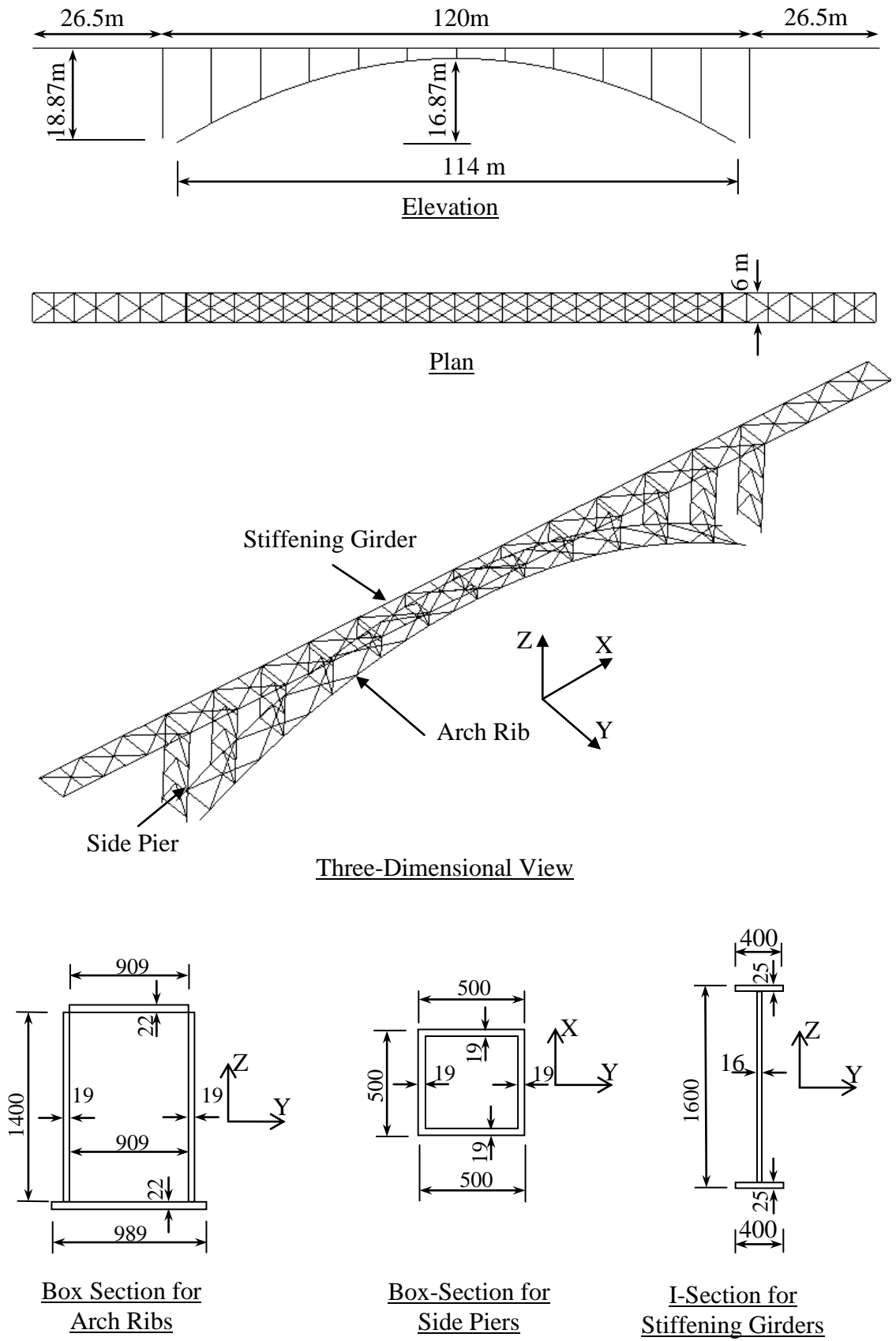
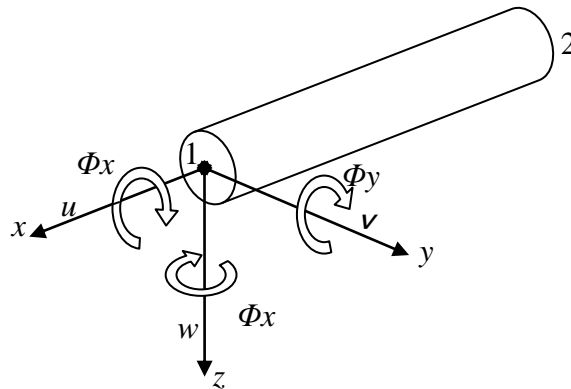


Figure 3.2: Model 1

3.2.2 Fiber Modeling

The bridges are modeled and analyzed using the general purpose MARC [26] nonlinear finite element analysis software. Three dimensional beam elements of type 14 and 79 provided in the MARC element library are employed to model the structural members. Element 14 (See **Figure 3.3**) is a straight beam element with no warping of the section but including twist. It is a closed section beam based on Euler-Bernoulli beam theory. Element 14 is adopted for the box sections (arch ribs and side piers). There are two nodes per element. The degrees of freedom associated with each node are three global displacements and three global rotations. Element 79 (See **Figure 3.4**) is used for the I-shaped sections. It is an open section straight beam element that includes warping and the twisting of the section. It is composed of two nodes where 7 degree of freedom, 3 for global displacements, 3 for global rotations and one for warping of the section is associated to each of them.



Degrees of Freedom	
Node 1	Node 2
u	u
v	v
w	w
Φ_x	Φ_x
Φ_y	Φ_y
Φ_z	Φ_z

Figure 3.3 Element 14

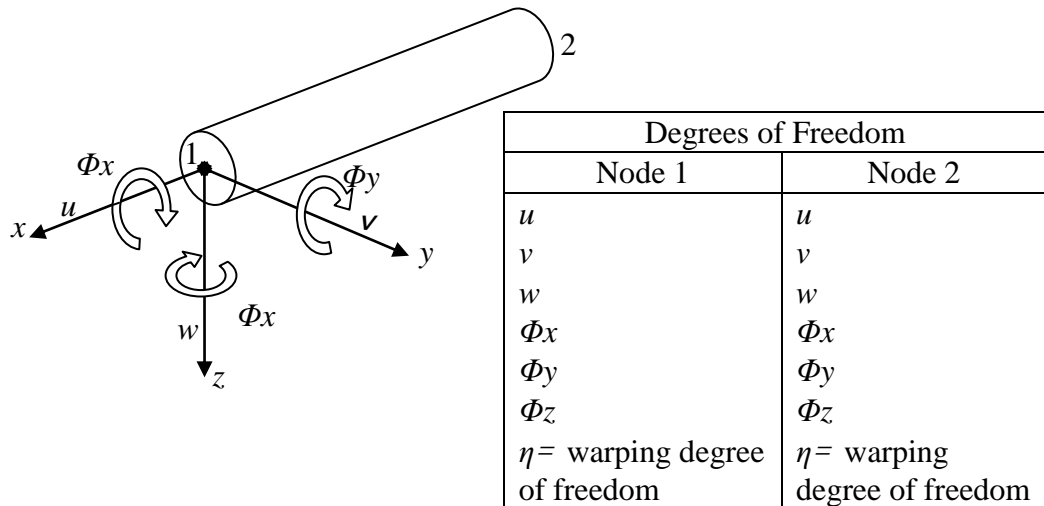


Figure 3.4: Element 79

3 dimensional fiber modeling is used to consider the material nonlinearity. For the box sections of the arch ribs 26 integration points are specified, for the side columns 24 integration points, and for the I-shaped sections 25 integrations points are selected as illustrated in **Figure 3.5**. The integration points are the points where the stress-strain relationship is defined and used for numerical integration of section's stiffness and for output results. Geometrical nonlinearity is also taken into account in the Finite Element Analysis. Updated Lagrangian Formulation is employed to consider the large displacements.

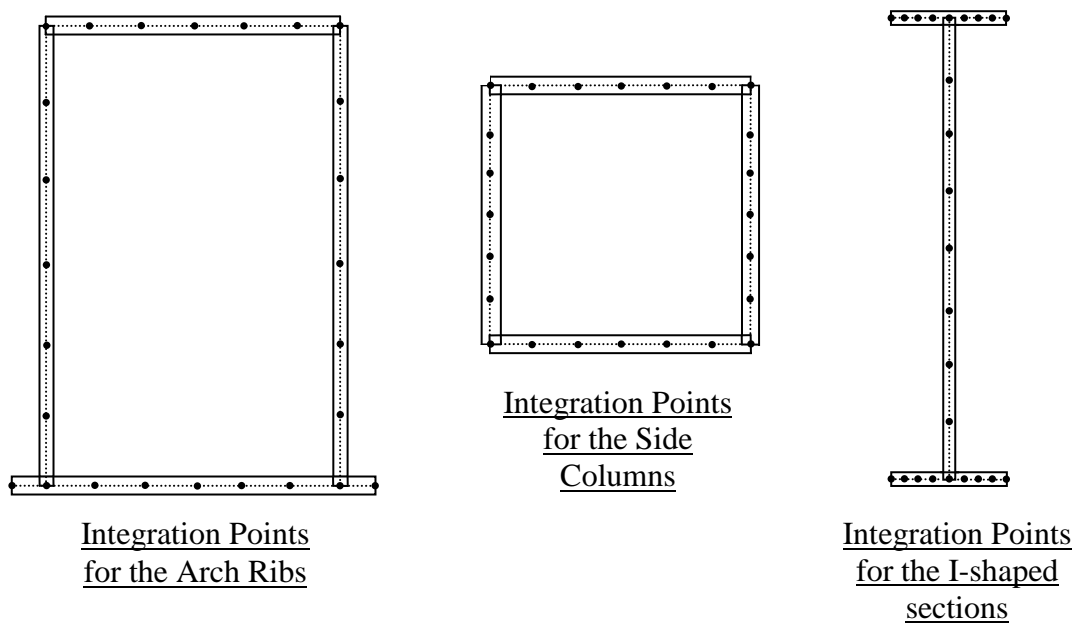


Figure 3.5: Integration Point Configurations of the Cross-Sections

The finite element mesh division is shown in **Figure 3.6.** Here two types of the beam elements can be seen with their defined cross-sections by fiber modeling. With a few exceptions finite element mesh division is made in a manner that one element is defined between each of two junction points where structural members coincide. All of the models are composed of 245 elements and 499 nodes. The figure illustrates the mesh division for only the template Model 1. The divisions and the element types are identical for all of the rest of bridge models. It should be noticed that the reinforced concrete slab was not modeled for any of the bridges although its mass is considered.

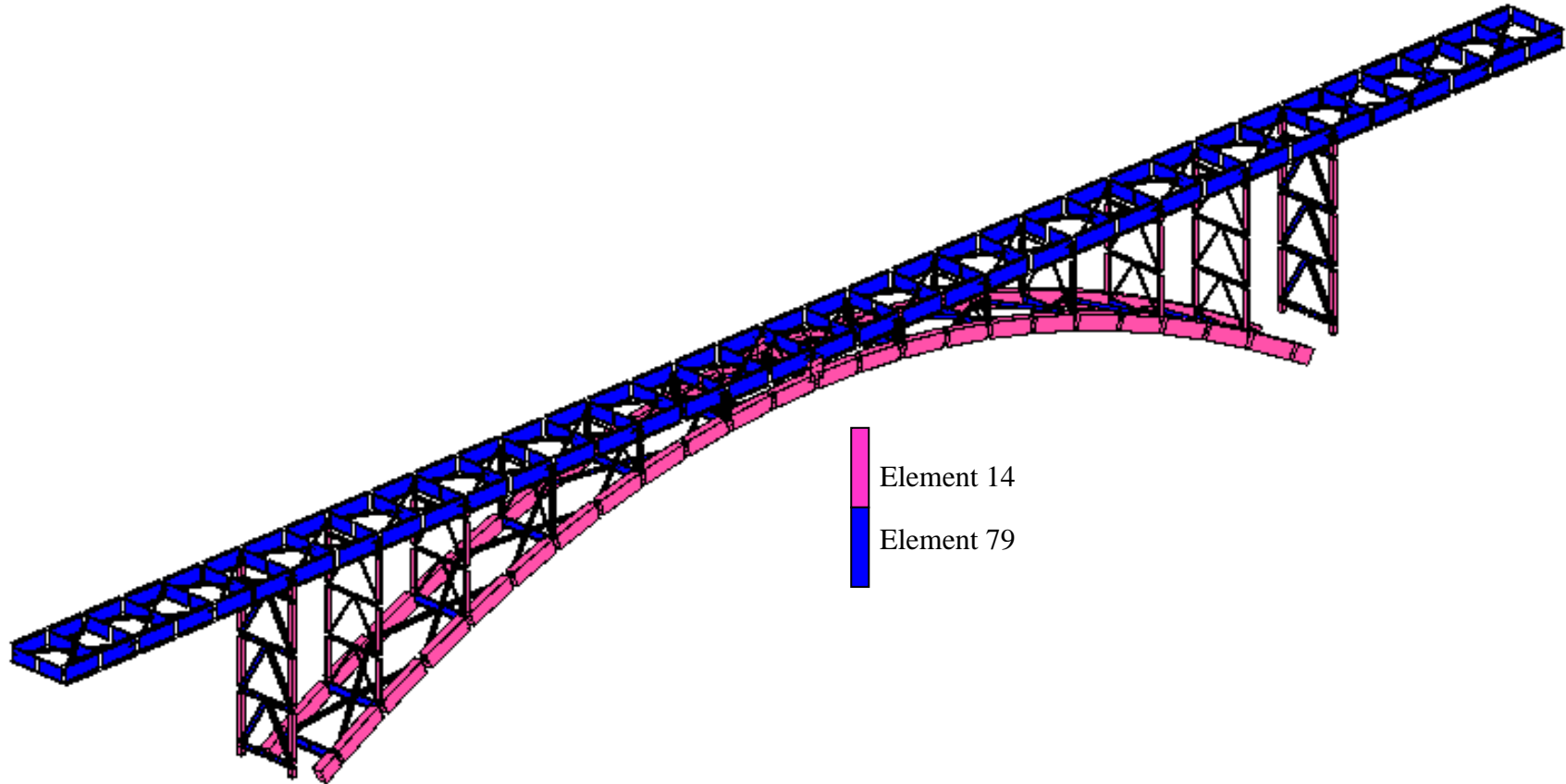


Figure 3.6: Finite Element Mesh

One type of steel, JIS-SMA490, is adopted for all of the bridge models (yield stress $\sigma_y=355$ MPa, Young's modulus, $E=206$ GPa and Poisson's ratio, $\nu=0.3$). A bilinear stress-strain relation with a strain hardening slope $E'=E/100$ and a kinematic hardening rule are assumed as seen in **Figure 3.7**.

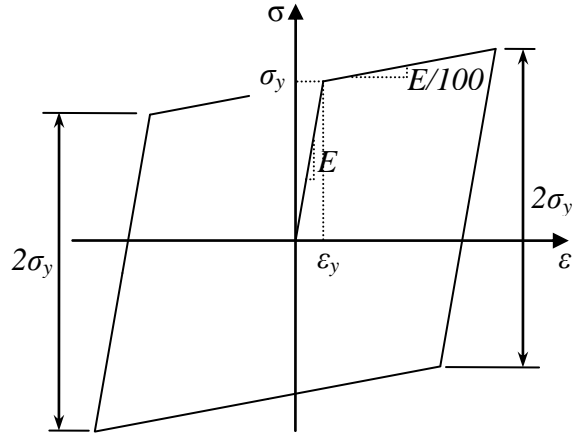
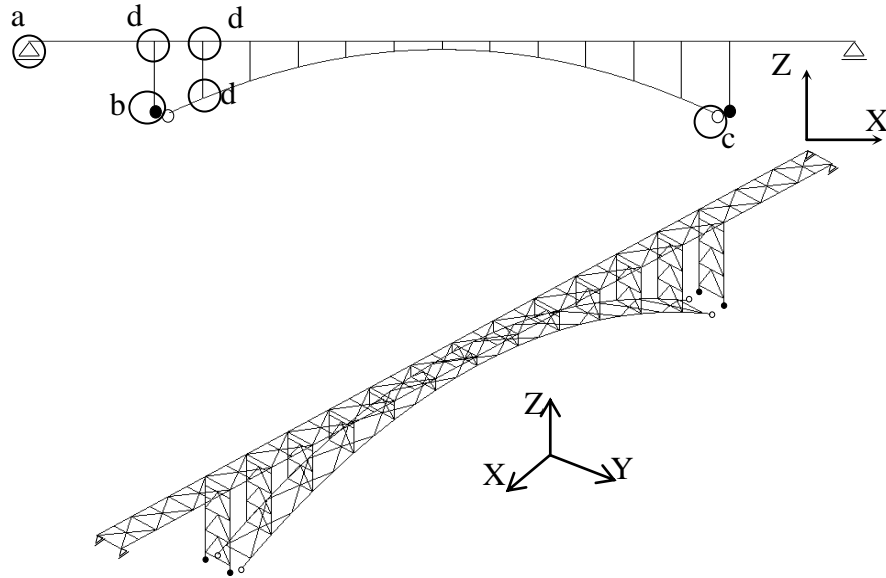


Figure 3.7: Material Models for Steel

Boundary and connection conditions of the bridge models are shown in **Figure 3.8**. Typical boundary conditions are used for all of the models. As for the abutment bearings, roller condition is assumed in the longitudinal direction. Side pier ends are of a pivot type, and the arch rib ends are pinned bearings. All the vertical members are connected rigidly to the longitudinal girders. Lateral and transverse members are also connected rigidly to the vertical members and to the longitudinal girders.



Location	Type	D_x	D_y	D_z	Θ_x	Θ_y	Θ_z
a	Roller Bearing	Free	Fixed	Fixed	Free	Free	Free
b	Pivot Bearing	Fixed	Fixed	Fixed	Fixed	Free	Fixed
c	Pin Bearing	Fixed	Fixed	Fixed	Free	Free	Free
d	Fixed Connection	Fixed	Fixed	Fixed	Fixed	Fixed	Fixed

Figure 3.8: Boundary and Connection Conditions

Lumped mass approach is used to consider the mass of the bridges. Although the reinforced concrete deck was not modeled its mass is considered and lumped to the nodal points of the stiffening girder. The reason why the reinforced concrete slab was not considered is the same as keeping the transverse and the lateral members unchanged in the generation process of the parametric models as explained in **Section 3.2.1**. It is assumed that the stiffness of the reinforced concrete slab is not essential for the assessment of the accuracy of the results estimated by the equal energy assumption. In both cases of getting the maximum nonlinear response from dynamic response analysis and estimating it by equal energy assumption the reinforced concrete deck is not considered. As the applicability of equal energy assumption is evaluated by comparing these two values, individual influence of the stiffness of the reinforced concrete deck can be negligible for the evaluation.

Mass of the stiffening girder, arch ribs and the piers are lumped along their nodal points. Additionally, the mass of the transverse and diagonal members are considered and their mass is lumped on the nodal points of the corresponding stiffening girder, arch rib or the vertical member. The mass associated to each nodal point is in X, Y, Z directions according to the global coordinate system.

3.2.3 Modal Analysis

Eigenvalue analyses of 6 bridge models are carried out to get fundamental insight into dynamic characteristics. Natural frequencies, modal participations and mode definitions of first 10 modes are listed in **Table 3.2** for models 1, 2, 3 and in **Table 3.3** for models 4, 5, 6 respectively. Since dynamic response in out-of plane direction is the concern of this research the eigenmodes in out-of plane direction are evaluated to assign the predominant modes which contribute the structural response the most. It is seen that the first three out-of plane modes are the modes having the highest contribution to the total structural dynamic response as they have the largest effective modal mass. Among them the symmetric modes have the highest contribution as the mode shapes are similar to the deflected shape of the structure in out-of-plane dynamic loading. The mode shapes of the predominant modes are shown in **Appendix B** respectively for all of the analyzed models. Although there are some differences between the six bridges such as different arch rise and deck width, they exhibit similar shapes in the corresponding eigenmodes.

Table 3.2: Eigenvalue Analysis Results for Model 1, 2 and 3

(a) Model 1

Mode	Natural Frequency (Hz)	Effective Modal Mass			Deflection Mode
		Longitudinal	Transverse	Vertical	
1	0.788	-482.1526	-0.0049	0.0001	In-plane
2	1.041	-0.0026	839.1836	-0.0014	Out-of-plane
3	1.696	0.0187	0.0006	-0.0054	Out-of-plane
4	1.846	-0.0012	-0.1589	-98.9429	In-plane
5	2.590	0.0023	-405.7658	-0.0490	Out-of-plane
6	2.960	-284.3034	-0.0082	-0.0048	In-plane
7	3.197	0.0015	0.0813	-735.4828	In-plane
8	3.356	-0.0177	-0.0057	0.0015	Out-of-plane
9	3.549	0.0006	244.2216	0.0506	In-plane
10	3.709	0.0125	-0.0967	-504.1305	Local mechanism

(b) Model 2

1	0.744	-669.9698	-0.0023	0.0001	In-plane
2	0.995	0.0016	-929.6994	0.0004	Out-of-plane
3	1.502	0.0041	0.0036	0.0022	Out-of-plane
4	1.701	-0.0016	0.0011	-37.5689	In-plane
5	2.204	0.0017	-413.4478	0.0019	Out-of-plane
6	2.745	-563.8236	-0.0029	0.0004	In-plane
7	3.026	0.0274	-0.0079	0.0090	Out-of-plane
8	3.143	-468.0344	0.0055	0.0016	Local mechanism
9	3.369	0.0041	0.0075	170.7041	Local mechanism
10	3.657	-265.3845	-1.4821	0.8353	Local mechanism

(c) Model 3

1	0.785	911.3521	0.0047	0.0000	In-plane
2	0.824	-0.0041	1011.6425	-0.0003	Out-of-plane
3	1.328	-0.0025	-0.0039	-0.0007	Out-of-plane
4	1.884	-0.0005	0.0022	49.7362	In-plane
5	2.014	-0.0005	426.4610	-0.0014	Out-of-plane
6	2.690	-130.0184	-0.0044	-0.0003	In-plane
7	2.866	-0.0032	-0.0033	0.0026	Out-of-plane
8	3.262	-0.0210	0.0111	174.8111	Local mechanism
9	3.308	-418.4561	0.0092	-0.0085	Local mechanism
10	3.679	-0.0069	158.2557	0.0232	Out-of-plane

Table 3.3: Eigenvalue Analysis Results for Model 4, 5, 6

(a) Model 4

Mode	Natural Frequency (Hz)	Effective Modal Mass			Deflection Mode
		Longitudinal	Transverse	Vertical	
1	0.580	1038.8126	0.0030	0.0000	In-plane
2	0.647	-0.0028	1071.3974	-0.0002	Out-of-plane
3	1.127	-0.0018	-0.0029	0.0001	Out-of-plane
4	1.563	-0.0002	-0.0001	106.9989	In-plane
5	1.839	0.0010	390.8759	-0.0009	Out-of-plane
6	1.952	190.0374	-0.0055	-0.0005	Local mechanism
7	2.053	-0.0007	-0.0037	-80.2438	Local mechanism
8	2.460	233.2333	-0.0001	0.0000	In-plane
9	2.671	0.0301	0.0853	-0.1195	Out-of-plane
10	2.842	-0.0012	-47.5044	0.0004	Local mechanism

(b) Model 5

1	0.811	-606.3323	-0.0017	0.0002	In-plane
2	1.315	0.0009	-1025.6148	0.0005	Out-of-plane
3	1.659	-0.0017	0.0015	-123.8532	In-plane
4	1.905	-0.0073	-0.0041	-0.0003	Out-of-plane
5	2.447	-910.4414	0.0017	-0.0004	In-plane
6	2.723	-0.0061	-467.1449	0.0040	Out-of-plane
7	3.132	447.9622	-0.0046	-0.0018	In-plane
8	3.267	0.0000	-0.0001	-896.3626	In-plane
9	3.423	-0.0001	103.4117	0.0018	Out-of-plane
10	3.825	0.0120	-0.0197	-485.8466	In-plane

(c) Model 6

1	0.777	682.0205	0.0013	0.0000	In-plane
2	1.363	0.0006	-1125.2597	0.0003	Out-of-plane
3	1.582	-0.0011	0.0025	-154.2888	In-plane
4	1.739	0.0066	0.0149	-0.0014	Out-of-plane
5	2.238	-1065.9515	0.0051	-0.0002	In-plane
6	2.323	-0.0116	-501.1985	0.0020	Out-of-plane
7	2.964	412.8626	-0.0021	-0.0035	In-plane
8	3.012	0.0009	0.0006	1013.3258	In-plane
9	3.121	0.0004	-13.5822	0.0023	Out-of-plane
10	3.777	2.1267	9.5388	-454.1864	In-plane

3.2.4 Determination of Damping Parameters

In all of the analyzed models damping effect is considered as Rayleigh damping [27] of Equation (3.1).

$$\mathbf{C} = \alpha \mathbf{M} + \beta \mathbf{K} \quad (3.1)$$

where,

C: Rayleigh damping matrix,

M: Mass matrix,

K: Stiffness matrix.

α : Mass matrix multiplier.

β : Stiffness matrix multiplier .

Rayleigh damping leads to the following relation between modal damping ratio and the frequency.

$$h_n = \frac{\alpha}{2w_n} + \frac{\beta}{2} w_n \quad (3.2)$$

where,

h_n = Damping ratio of mode n.

w_n = Angular frequency of mode n.

The coefficients of α and β are determined from specified damping ratios h_1 and h_2 for the i th and j th modes, respectively. Expressing Equation (3.2) for these two modes in matrix form leads to:

$$\frac{1}{2} \begin{bmatrix} 1/w_i & w_i \\ 1/w_j & w_j \end{bmatrix} \begin{Bmatrix} \alpha \\ \beta \end{Bmatrix} = \begin{Bmatrix} h_1 \\ h_2 \end{Bmatrix} \quad (3.3)$$

These two algebraic equations shown in matrix form in equation (3.3) are solved to determine the mass and stiffness matrix multipliers as shown in equation (3.4).

$$\alpha = 4\pi \cdot f_1 \cdot f_2 \cdot \frac{f_1 \cdot h_2 - f_2 \cdot h_1}{f_1^2 - f_2^2}$$

$$\beta = \frac{f_1 \cdot h_1 - f_2 \cdot h_2}{\pi \cdot (f_1^2 - f_2^2)}$$
(3.4)

Where, f_1 and f_2 are the first and second symmetric predominant mode frequencies shown in the previous section. h_1 and h_2 are the modal damping ratios of these modes which are both assumed as 0.03. These values are illustrated in **Table 3.4** for the corresponding model.

Table 3.4: Rayleigh Damping Coefficients of the Analyzed Models.

	f_1 (sec ⁻¹)	f_2 (sec ⁻¹)	h	α	B
Model 1	1.041	2.590	0.03	0.2799	0.0026
Model 2	0.9946	2.204	0.03	0.2584	0.0030
Model 3	0.824	2.014	0.03	0.2204	0.0034
Model 4	0.6472	1.839	0.03	0.1805	0.0038
Model 5	1.315	2.723	0.03	0.3343	0.0024
Model 6	1.363	2.323	0.03	0.3283	0.0026

3.2.5 Input Ground Motions

The ground motions used in dynamic response analysis are spectral fitted to the response spectra specified in JRA Code [1] as illustrated in **Appendix C**. Six Level-2, Type-2 ground motions, three for ground condition I and three for ground condition II, are used for the dynamic response analysis in out-of-plane direction whose names and maximum accelerations are summarized in **Table 3.5**. Additionally the acceleration records of these ground motions are plotted in **Figure 3.9** and **Figure 3.10** respectively for ground type 1 and type 2. All of the ground motions are the spectral fitted versions of the near-fault strong ground motions recorded in various places and directions during the Hyogo Ken Nanbu Earthquake. Additionally these ground motions are amplified by the coefficients in the below table. Dynamic response analyses with these newly amplified ground motions are repeated in order to obtain sufficiently inelastic response. By this way a pattern showing the effect of the increase in the intensity of the ground motion can be studied for the evaluation of the applicability of equal energy assumption in the later steps.

Table 3.5: Input Ground Motions For the Dynamic Response Analysis

Ground Condition	Name	Duration (sec)	Maximum Acceleration (Gal)	Amplification
Ground 1 (Stiff)	1995 JMA Kobe OBS N-S (Le2.t211)	30	812	1.2, 1.5, 1.7, 2, 5
	1995 JMA Kobe OBS E-W (Le2.t212)	30	766	1.5, 2, 5
	1995 HEPC Inagawa N-S (Le2.t213)	30	780	1.5, 2, 5
Ground 2 (Moderate)	1995 JR Takatori Sta. N-S (Le2.t221)	40	687	1.5, 2
	1995 JR Takatori Sta. E-W (Le2.t222)	40	673	1.5, 2
	1995 OGAS Fukiai N27W (Le2.t223)	40	736	1.5, 2

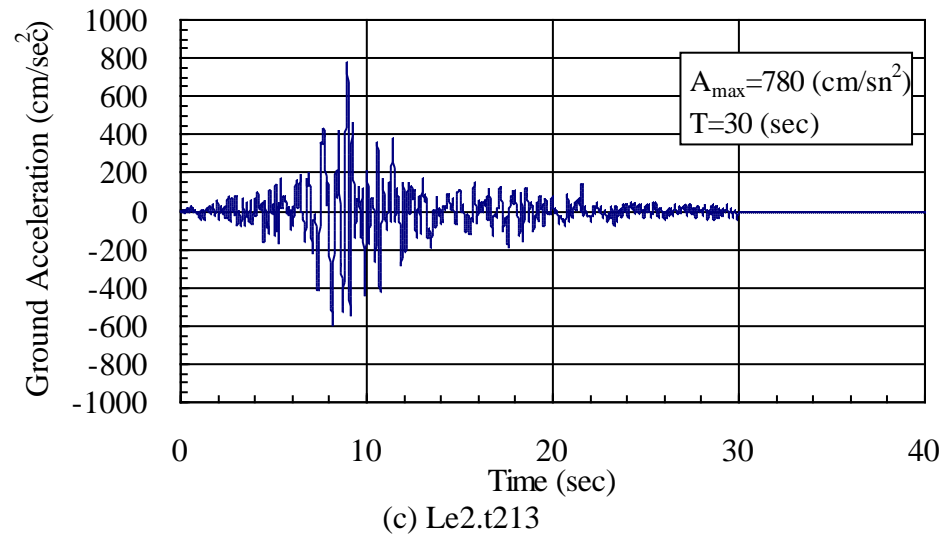
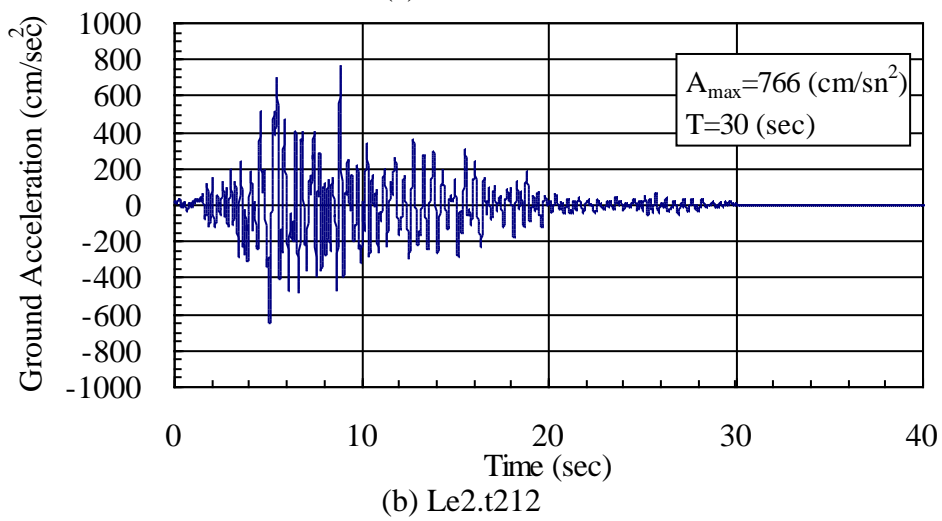
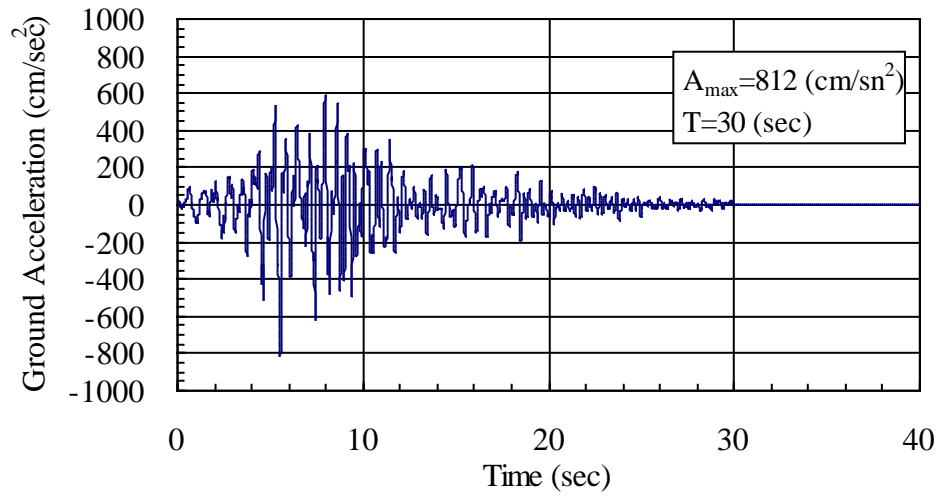
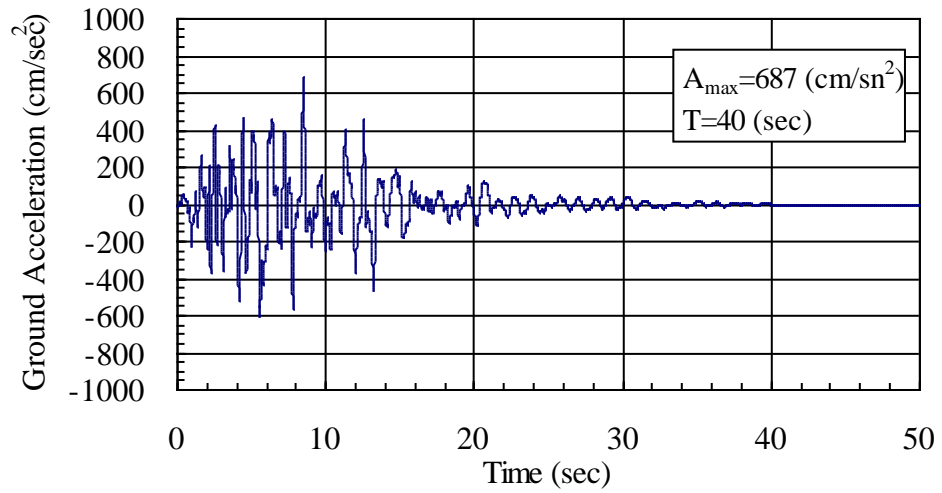
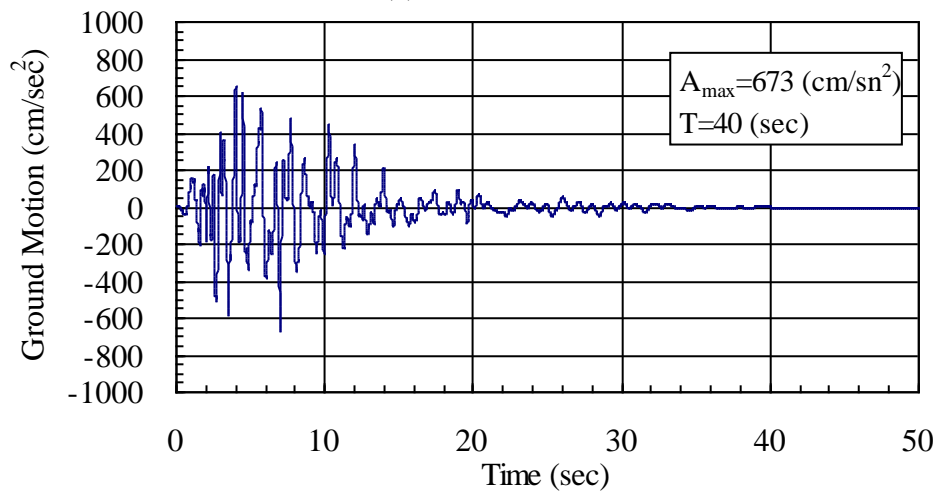


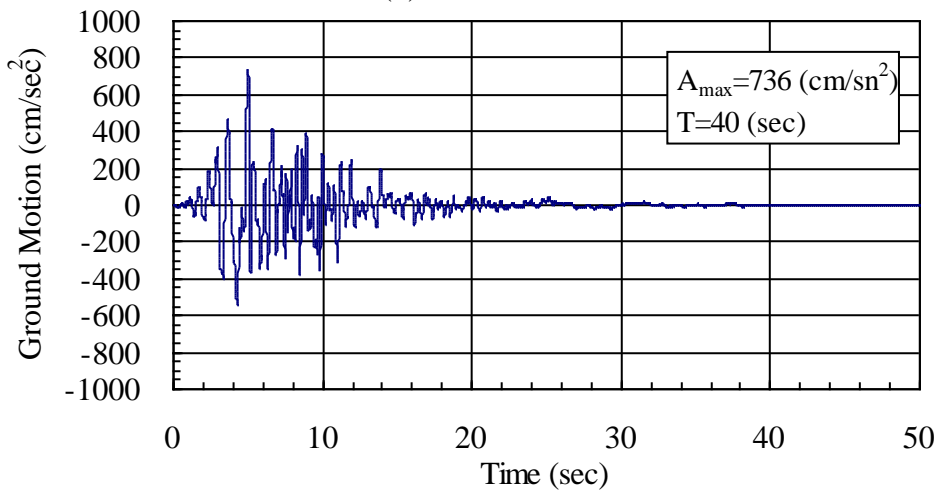
Figure 3.9: Ground Acceleration Record of Level 2 Type 1 Earthquake for Ground Type 1



(a) Le2.t221



(b) Le2.t222



(c) Le2.t223

Figure 3.10: Ground Acceleration Record of Level 2 Type 1 Earthquake for Ground Type 2

3.3 Numerical Analysis

3.3.1 Examination Procedure

The equal energy assumption as a prediction tool for the maximum nonlinear dynamic response is evaluated by a numerical analysis procedure summarized in **Figure 3.11**. Its applicability is examined by comparing the estimated maximum inelastic response with that of nonlinear dynamic response analysis result.

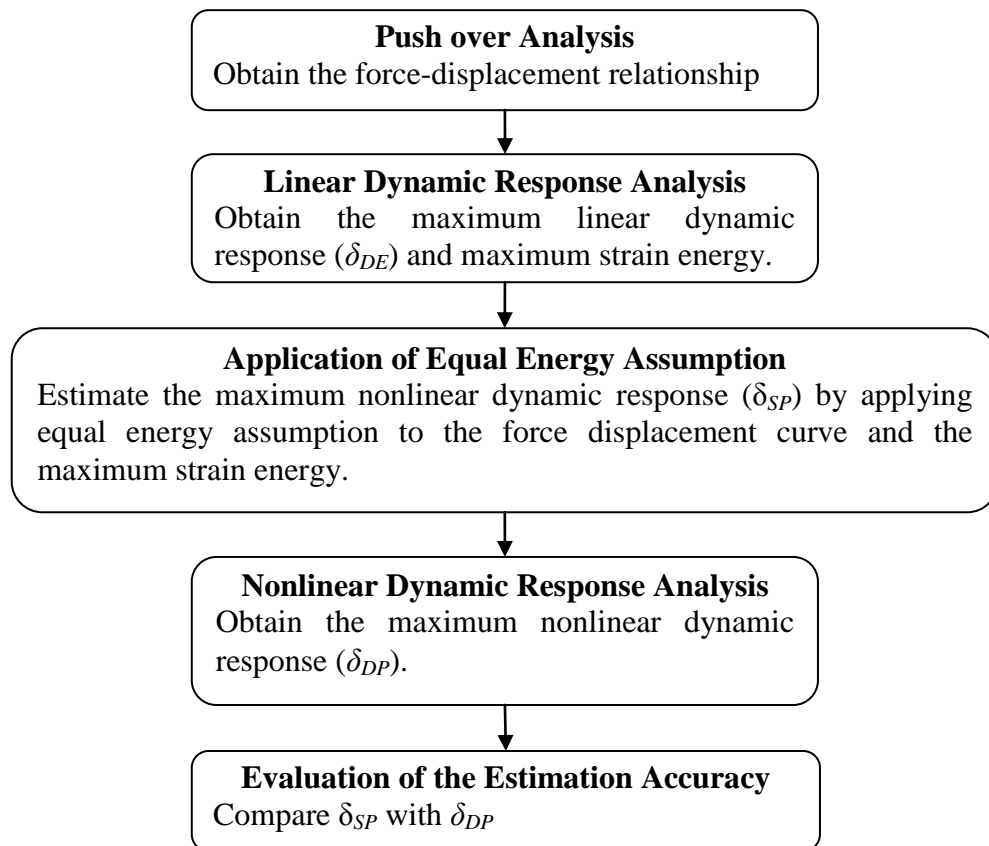


Figure 3.11: Flowchart of the Numerical Analysis Procedure

Pushover analysis, linear and nonlinear dynamic response analysis, application of equal energy assumption and the evaluation of the estimation results are explained in the following sections.

3.3.2 Pushover Analysis

Elasto-plastic finite displacement pushover analysis of each model is performed in order to obtain the force-displacement relation curves. A modal force distribution from the single dominant mode of the transverse direction (first symmetric out-of-plane mode) is adopted as the lateral force distribution pattern expressed as:

$$\{H_i\} = \{m_i \phi_i\} \quad (3.5)$$

in which m_i is the mass component of the structural mass matrix and ϕ_i is the transverse component of the eigenvector $\{\phi_i\}$ at each node.

The mid point of the stiffening girder is used as reference point for the pushover analysis since the maximum transverse displacements for all models are observed in this point. The reference point is shown in **Figure 3.12** together with the load distribution pattern.

Force-displacement relationship of each model is illustrated in **Figure 3.13, 3.14, 3.15, 3.16, 3.17 3.18** in terms of the transverse displacement of the reference point and the base shear force. Also the yield displacements (σ_y) obtained geometrically from the curves as being the points where the initial slope change are given. Here it should be noted that no failure criteria is employed to determine the lateral displacement capacity of the structure because the concern of the pushover analysis conducted in this research is only to get the nonlinear displacement-force relationship of each model to be used for the prediction of the maximum nonlinear dynamic response by the equal energy assumption.

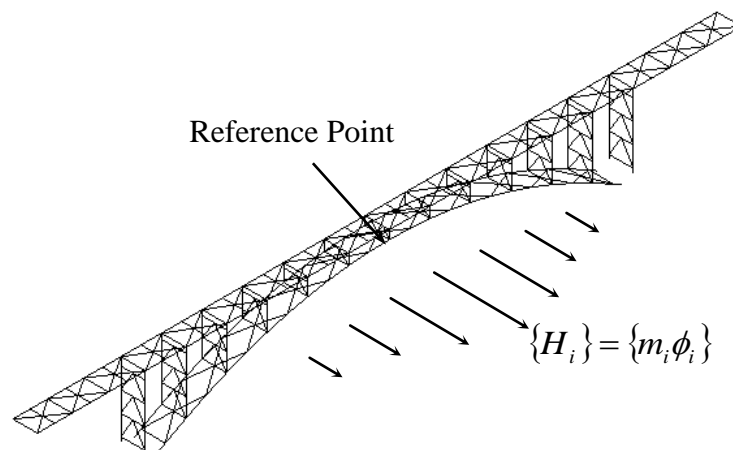


Figure 3.12: Reference Point and the Load Distribution Pattern

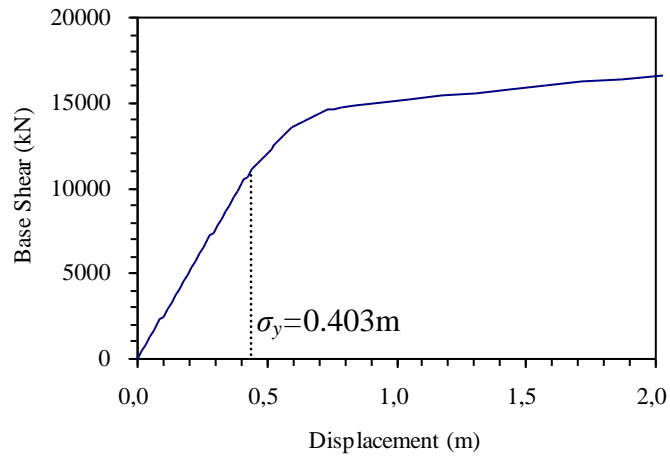


Figure 3.13: Force Displacement Relationship for Model 1

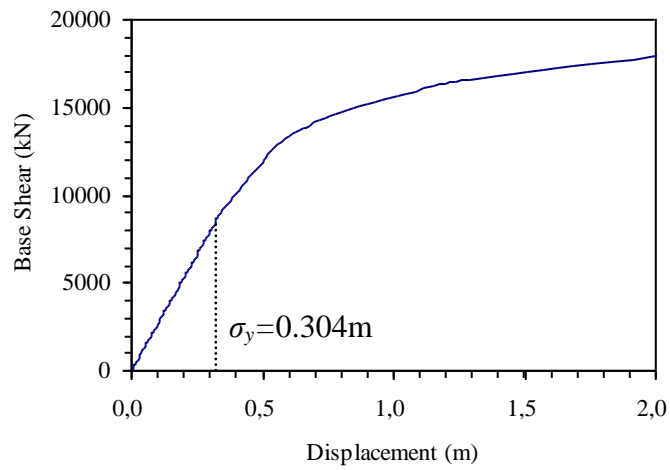


Figure 3.14: Force Displacement Relationship for Model 2

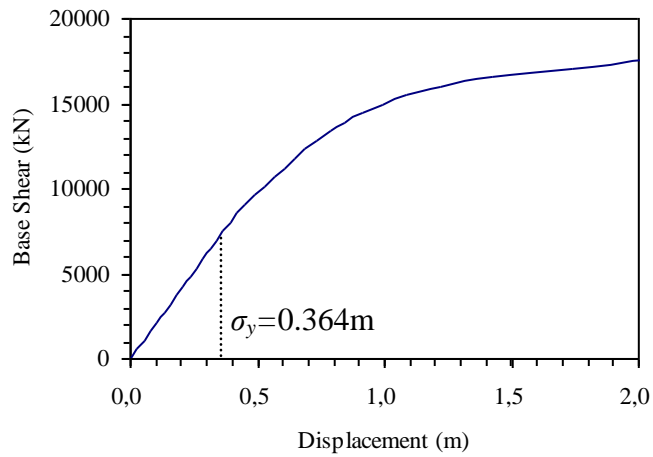


Figure 3.15: Force Displacement Relationship for Model 3

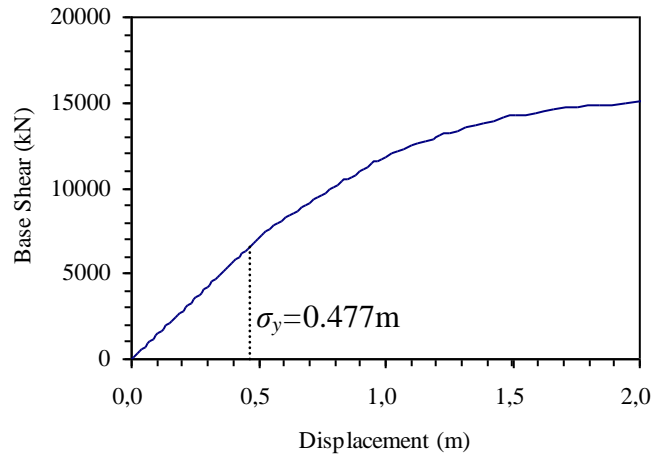


Figure 3.16: Force Displacement Relationship for Model 4

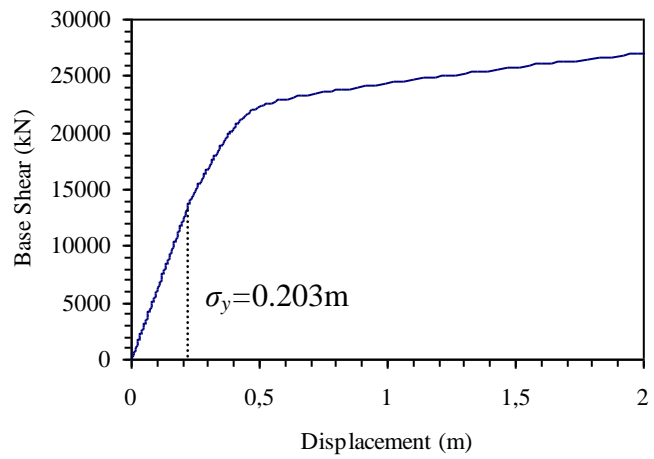


Figure 3.17: Force Displacement Relationship for Model 5

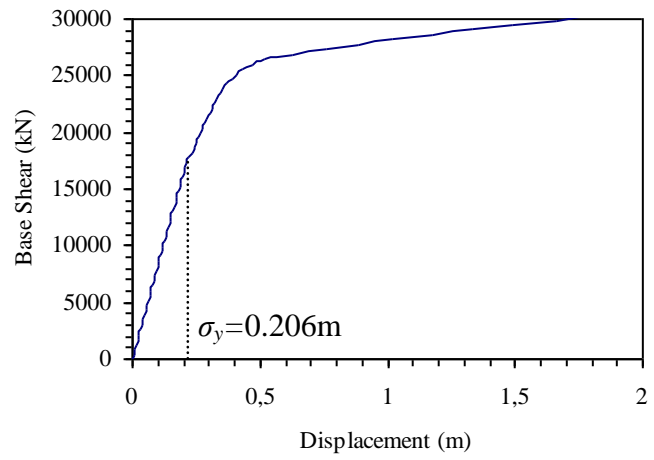


Figure 3.18: Force Displacement Relationship for Model 6

3.3.3 Linear and Nonlinear Dynamic Response Analysis

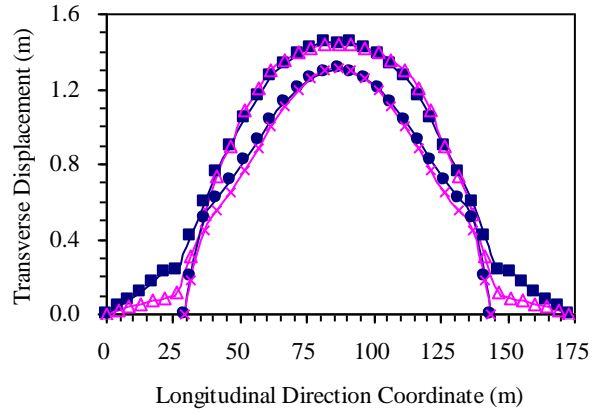
Linear and nonlinear dynamic response analyses are conducted in order to get the maximum elastic and inelastic responses.

Maximum linear response (δ_{DE}) is obtained by performing linear dynamic response analysis. Additionally maximum strain energy stored in the system is calculated as it is necessary for the application of equal energy assumption to estimate the maximum nonlinear response (δ_{SP}). Nonlinear dynamic response analysis is conducted to get the maximum inelastic response (δ_{DP}). This value is considered as the actual maximum nonlinear response and used as the reference value for evaluating the accuracy of the estimation results by the equal energy assumption. All of these response displacements are obtained for the reference point which is the mid point of the stiffening girder.

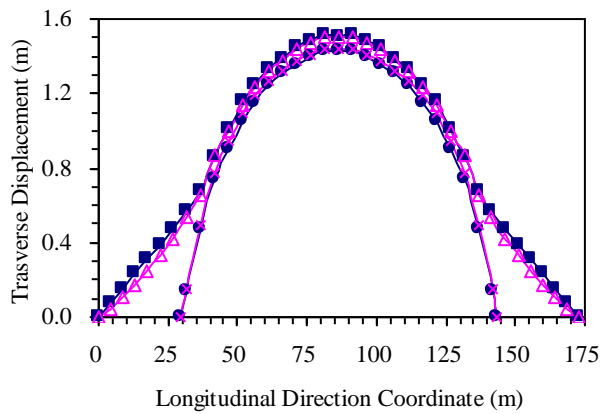
Newmark's β method [27] is employed to solve the equation of motion for both linear and nonlinear dynamic response analysis. The β value is taken as 1/4. Rayleigh damping is employed for all of the models as explained in **Section 3.2.4**.

It is another concern that whether the force-displacement relationship obtained by pushover analysis can represent the dynamic behavior. For this purpose displacement distribution of the pushover analysis is compared with that of the nonlinear dynamic response. Comparison is conducted for the most severe dynamic excitation for each model. The displacement distribution of the dynamic response at the time increment when the maximum response arise at the reference point is compared with that of the pushover analysis at the static force increment at which the same displacement occur at the reference point. These comparisons are given in **Figure 3.19** and **3.20** for the stiffening girder and the arch rib for each model respectively.

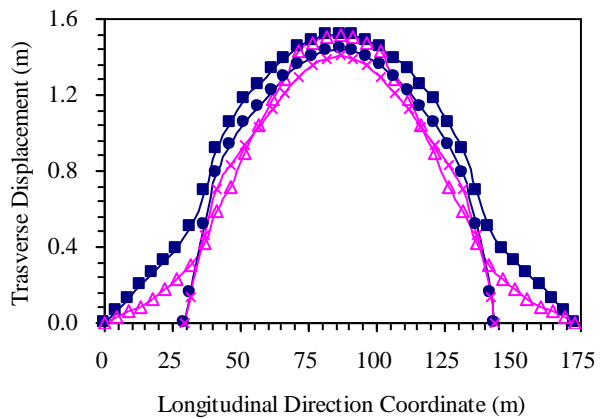
It is seen in these figures that the displacement distributions quite match each other (although some differences are seen for Model 3). So it is possible to say that the displacement pattern obtained statically by pushover analysis is also valid for the nonlinear dynamic response.



(a) Model 1



(b) Model 2



(c) Model 3

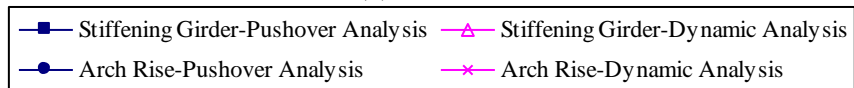
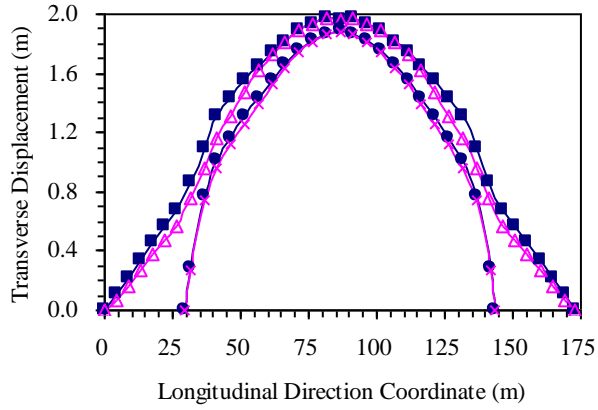
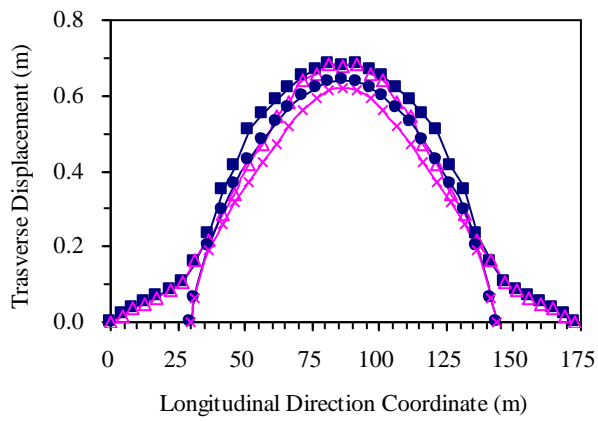


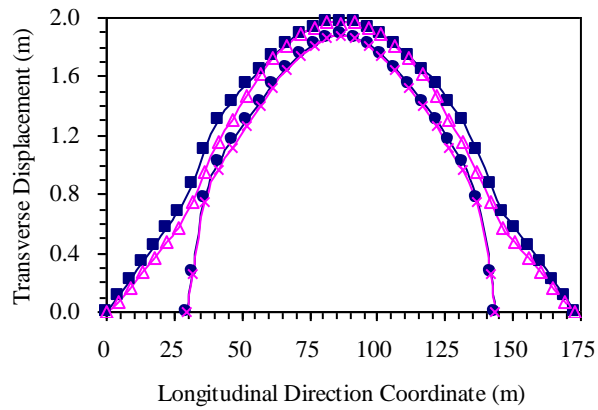
Figure 3.19: Displacement Distributions for Pushover and Dynamic Response Analyses (Model 1, 2 and 3)



(a) Model 4



(b) Model 5



(c) Model 6

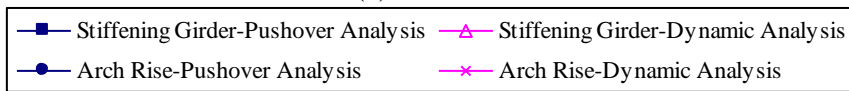


Figure 3.20: Displacement Distributions for Pushover and Dynamic Response Analyses (Model 4, 5 and 6)

3.3.4 Application of Equal Energy Assumption

In the equal energy assumption it is assumed that the energy stored in the elastic and inelastic systems for a given excitation are equal to each other. By this way it is possible to estimate the nonlinear response from the results of elastic system without the need of nonlinear dynamic response analysis.

In this research the equal energy assumption is applied to the force-displacement relation curve obtained by pushover analysis and the maximum strain energy obtained by linear dynamic response analysis. The maximum nonlinear response (δ_{SP}) is estimated by equating the elastic strain energy to the energy stored in the nonlinear system as illustrated in **Figure 3.21**.

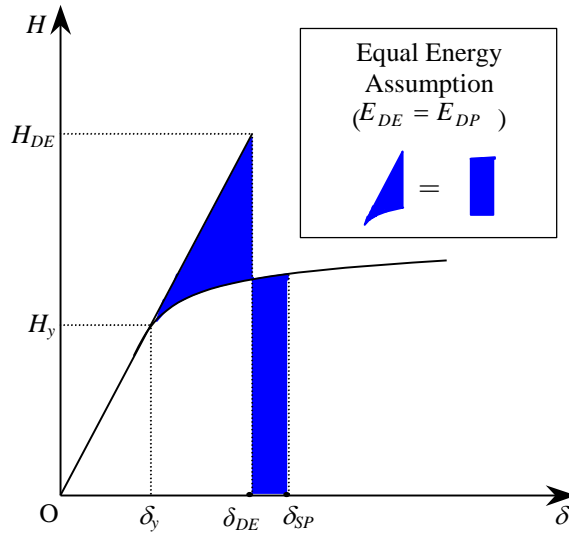


Figure 3.21: Equal Energy Assumption

3.3.5 Evaluation of Estimation Accuracy

Estimation accuracy is indicated by comparing the estimated maximum response (δ_{SP}) with the actual dynamic response (δ_{DP}). The ratio of δ_{SP} to δ_{DP} is used as an index that shows the accuracy of the estimation. Applicability of the assumption is studied by evaluating the estimation accuracy (δ_{SP}/δ_{DP}) - estimated ductility factor (μ_E) relationship. Estimated ductility factor is expressed as

$$\mu_E = \delta_{SP} / \delta_Y \quad (3.6)$$

in which δ_{SP} is the estimated maximum nonlinear response and δ_Y is the yield displacement.

4 APPLICABILITY OF EQUAL ENERGY ASSUMPTION

4.1 Estimation Accuracy of the Equal Energy Assumption

The numerical analysis results are given for each model respectively in the tables in **Appendix D**. Based on these results $\delta_{SP}/\delta_{DP}-\mu_E$ relationships of all models are illustrated in **Figure 4.1, 4.2, 4.3, 4.4, 4.5, 4.6**. It can be seen that regardless the ground condition type all of the estimation results are in conservative side as the δ_{SP}/δ_{DP} values are always larger than 1. δ_{SP}/δ_{DP} values ranging between 1 and 5.3 point out that the equal energy assumption results in too conservative estimation. In all of the cases the estimation accuracy is found to be decreasing with the increase in the estimated ductility factor μ_E causing very poor estimation results especially for the high ductility factors.

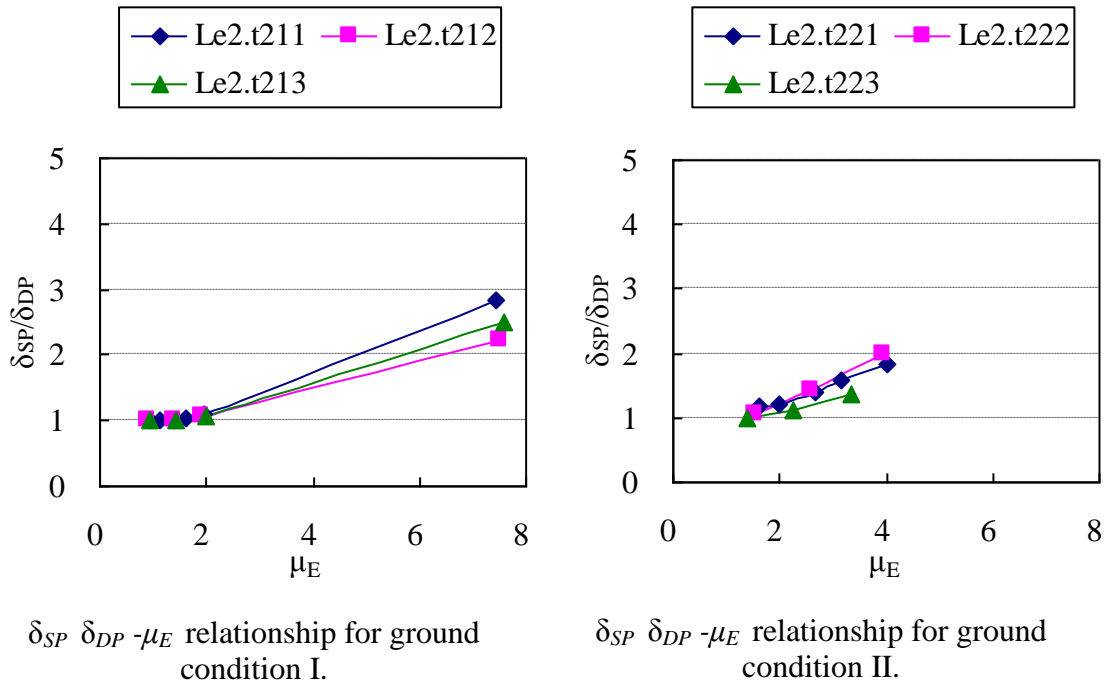


Figure 4.1: Numerical Analysis Results for Model 1

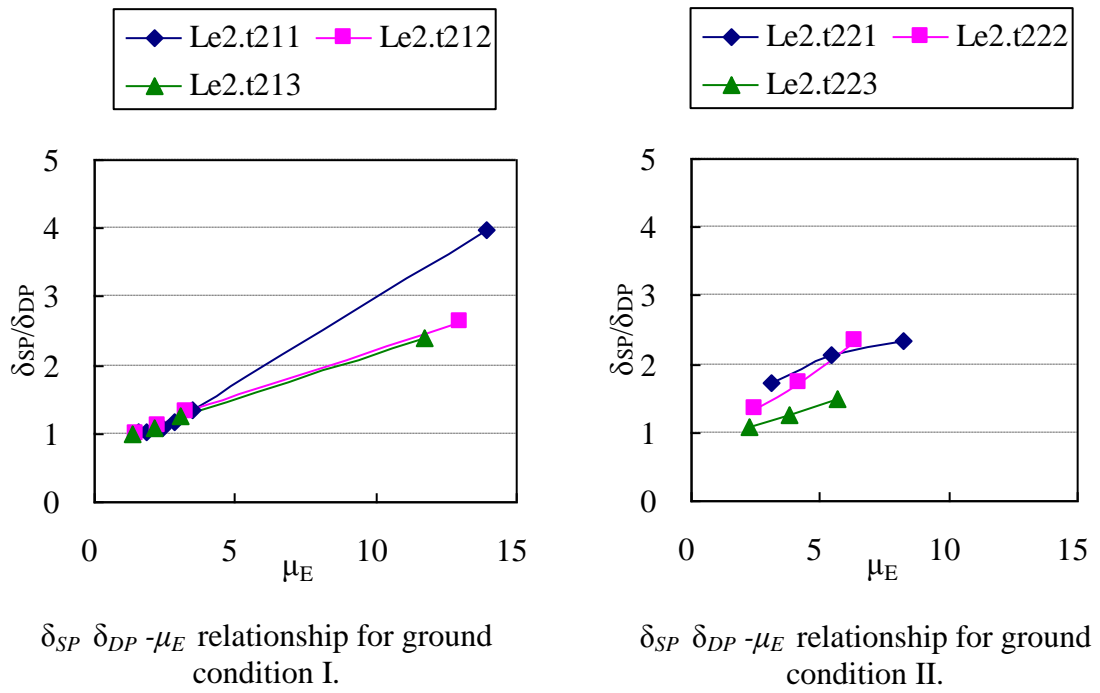


Figure 4.2: Numerical Analysis Results for Model 2

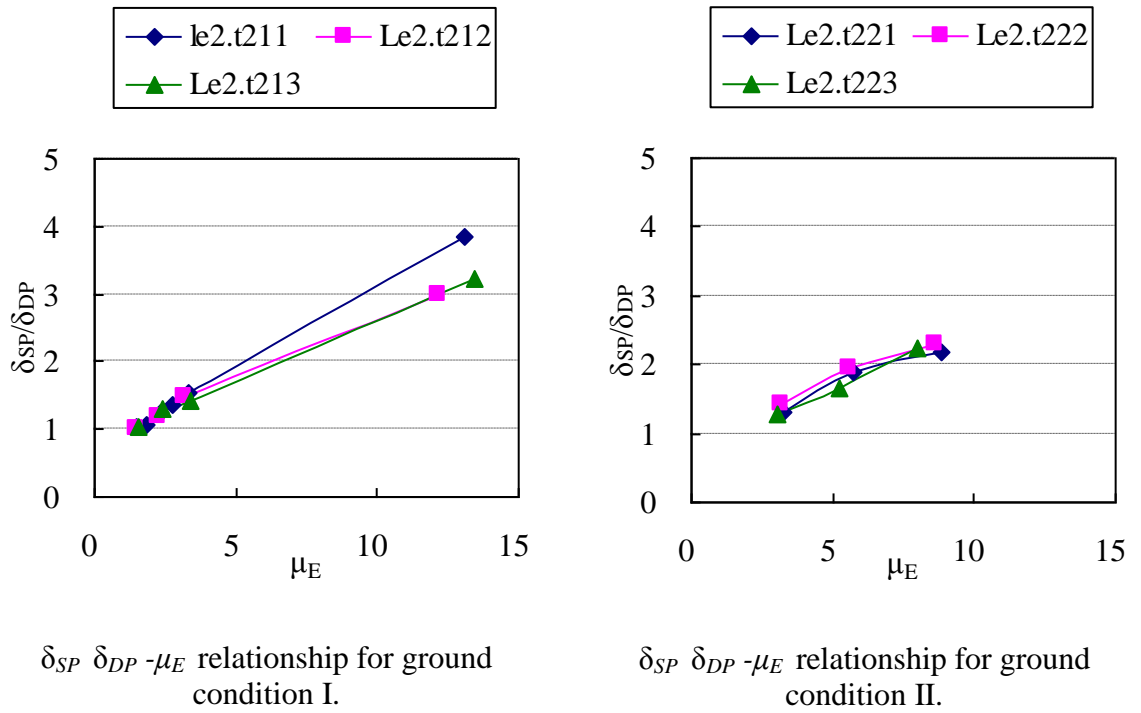


Figure 4.3: Numerical Analysis Results for Model 3

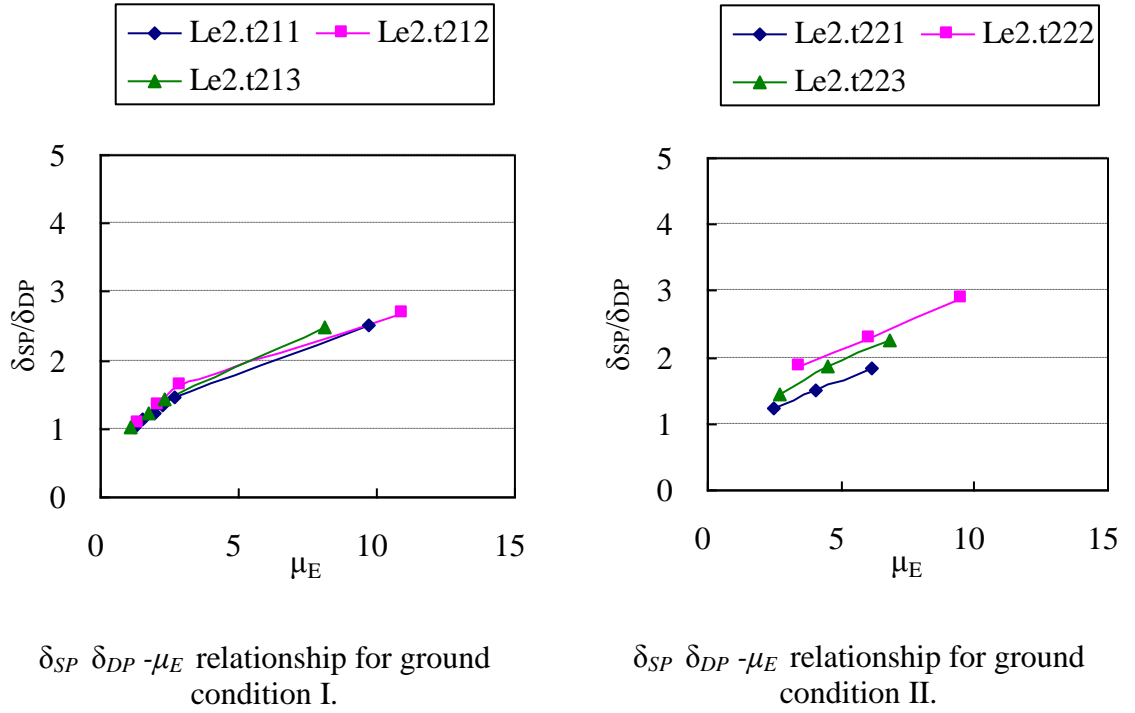


Figure 4.4: Numerical Analysis Results for Model 4

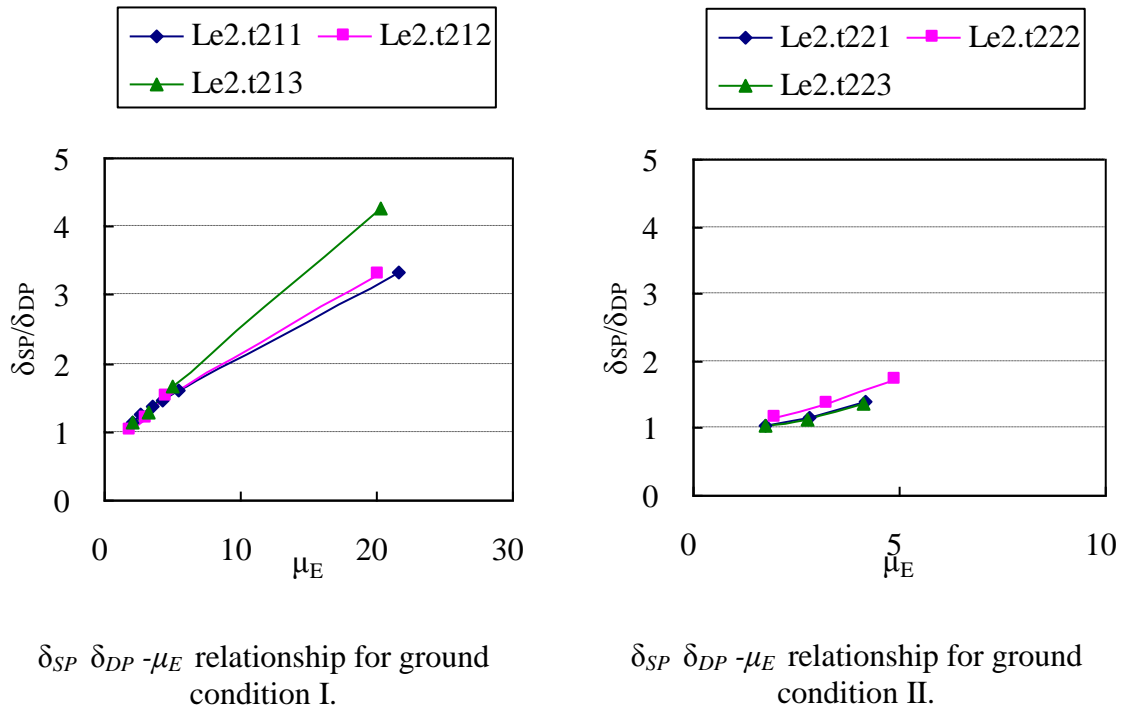
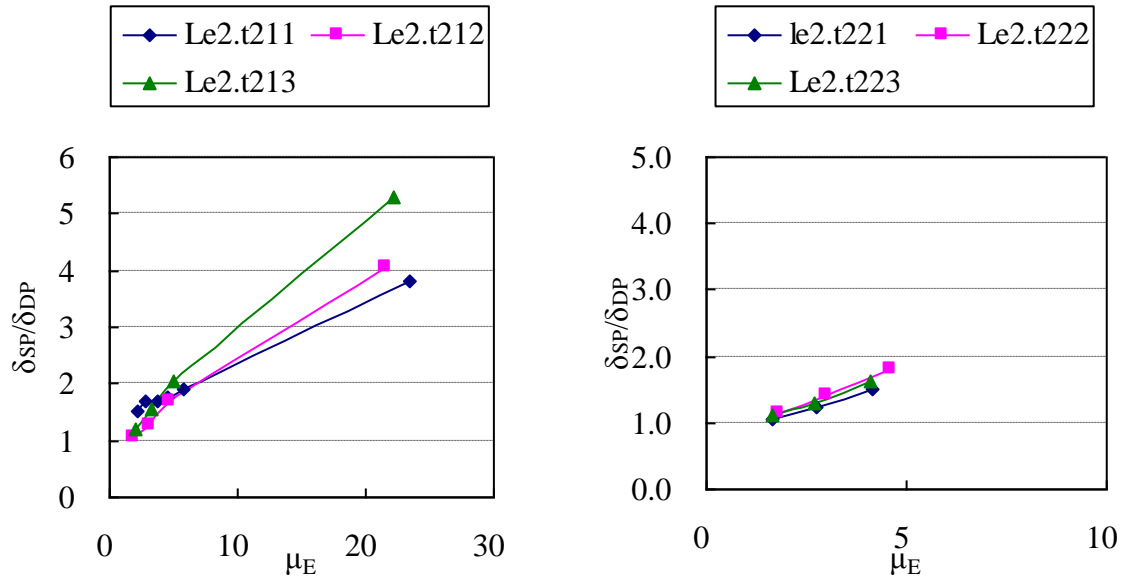


Figure 4.5: Numerical Analysis Results for Model 5



$\delta_{SP} \delta_{DP} - \mu_E$ relationship for ground condition I.

$\delta_{SP} \delta_{DP} - \mu_E$ relationship for ground condition II.

Figure 4.6: Numerical Analysis Results for Model 6

4.2 Relationship between Accuracy of the Estimation and some Parameters

The numerical analysis results illustrated in the last section showed out that the equal energy assumption results in conservative side estimation of the maximum nonlinear response. But the estimation accuracies are so poor in many cases that it cannot be used directly for the design procedure. However, it is favorable to further investigate estimation results in order to find some relationships that can be used to improve the estimation accuracy of equal energy assumption.

Firstly the factors that are considered to affect the estimation accuracy are investigated. The natural frequency and the structural parameters such as Arch Rise/Span Length ratio and the distance between the two arch ribs can be considered to have an influence on the applicability of the equal energy assumption. The relationship between these parameters and δ_{SP}/δ_{DP} , which is the basic factor expressing the accuracy of the estimation, is examined.

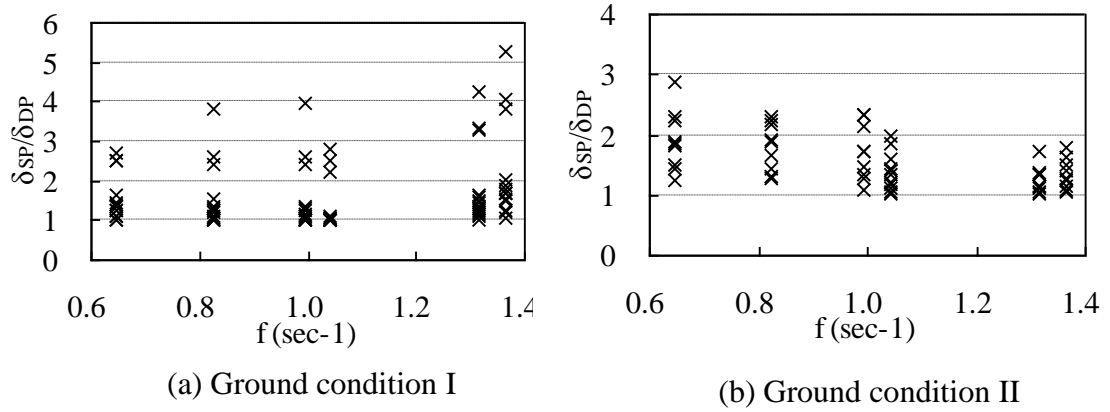


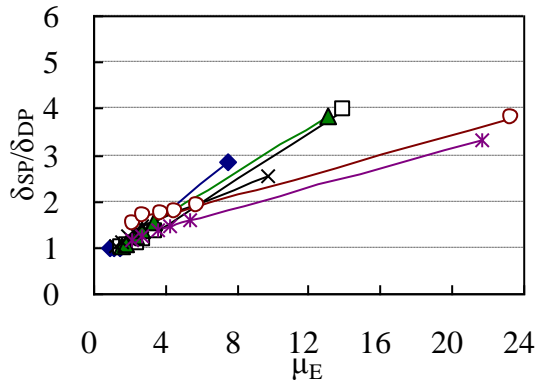
Figure 4.7: δ_{SP}/δ_{DP} – Natural Frequency Relationship

Figure 4.7 illustrates the relationship between δ_{SP}/δ_{DP} and 1st symmetric predominant mode frequency for the ground motions of ground condition I and ground condition II. The plots gathered along a column, represent the estimation accuracy results for a model under different input ground motions. The values that have lower accuracy are for the more intensified ground motions. Any correlation between δ_{SP}/δ_{DP} and natural frequencies can not be found in these graphs, suggesting that the natural frequency of the structure has no apparent effect on the accuracy of the estimation.

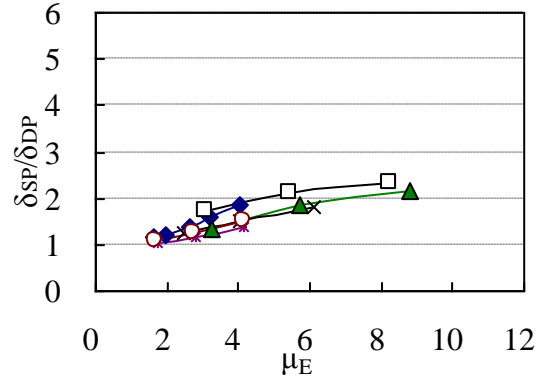
The estimation accuracy values of all models are plotted together on the same graph in order to investigate the effect of the considered structural parameters on the estimation accuracy as shown in **Figure 4.8**. Here $\delta_{SP}/\delta_{DP}-\mu_E$ relationships of different models are illustrated together for different input ground motions. The results residing on the right side represent the estimation accuracy for more intensively amplified ground motions. The ductility factors may seem to be too large to be practical for any design procedure. But it should be noted that the μ_E is the estimated ductility factor, not the actual ductility factor μ ($\mu = \delta_{DP}/\delta_y$), containing the error of the estimation which becomes more than 300% in some cases. However for the models 5 and 6, the actual ductility factors are also too large for the ground condition I ground motions amplified by 5 especially under the Le2.t211 ground motion. Their actual ductility factors range from 5 to 6 which are unpractical values for the design procedure. These values can simply be excluded from consideration. It

should be noticed that excluding these results the scale of the relationship would be quite similar.

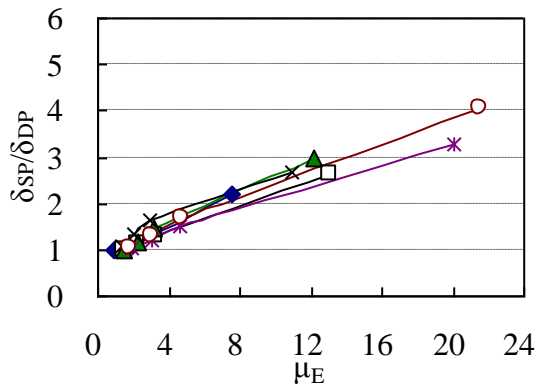
A similar decreasing tendency in estimation accuracy with the increase in estimated ductility factor μ_E is observed for all of the input ground motions. The tendency is almost the same for all models although they possess different structural parameters. This suggests that the considered structural parameters which are the Arch Rise/Span Length ratio and the distance between the arch ribs do not have any significant influence on the applicability of the assumption. When the estimation accuracy of all models for respective ground condition are compared it is seen that although the estimation accuracy for different models could be very diverging from each other under the same input ground motion, the estimation results in similar accuracy for any given estimated ductility factor, following a general tendency regardless the type of the model. This makes it possible to predict the accuracy of the estimation for a given estimated ductility factor without depending on any parameters.



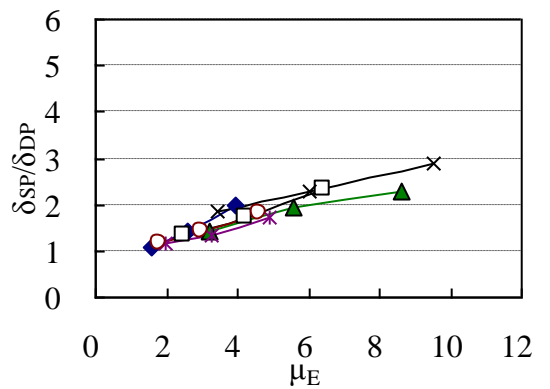
(a) Le2.t211, $\times 1.2, \times 1.5, \times 1.7, \times 2, \times 5$
(Ground Condition I)



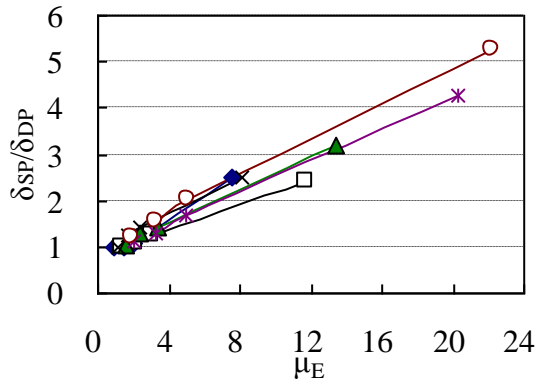
(d) Le2.t221, $\times 1.5, \times 2$
(Ground Condition II)



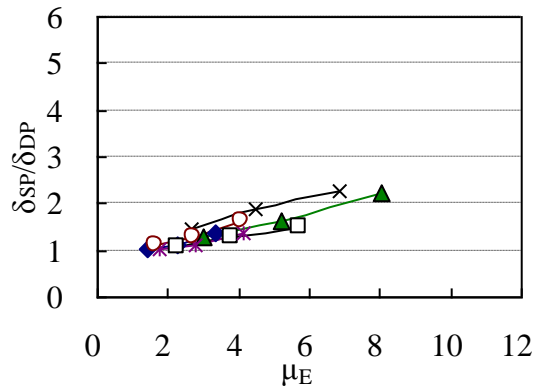
(b) Le2.t212, $\times 1.5, \times 2, \times 5$
(Ground Condition I)



(e) Le2.t222, $\times 1.5, \times 2$
(Ground Condition II)



(c) Le2.t213, $\times 1.5, \times 2, \times 5$
(Ground Condition I)



(f) Le2.t223, $\times 1.5, \times 2$
(Ground Condition II)

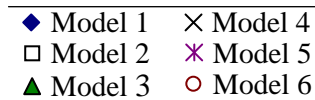


Figure 4.8: $\delta_{SP} - \delta_{DP} - \mu_E$ Relationships for Individual Ground Motions

The JRA [1] code recommends using at least three ground motions per dynamic analysis, and taking an average of them to evaluate the response for the seismic design. So it is necessary to calculate the average of the estimated responses of three ground motions for the considered ground conditions respectively. This is also done for a better understanding of the influence of the considered structural parameters. In **Figure 4.9** $\delta_{SP}/\delta_{DP} - \mu_E$ relationship for the average estimated response displacements are shown for the both ground conditions. It is clearly seen that there is no significant difference of the estimation accuracy for different models as the estimation accuracy results are scattered roughly along a linear tendency with the increase in the estimated ductility factor μ_E . Also the tendency is similar for both ground conditions, suggesting that the estimation accuracy is not significantly influenced by the considered structural parameters and the input ground conditions.

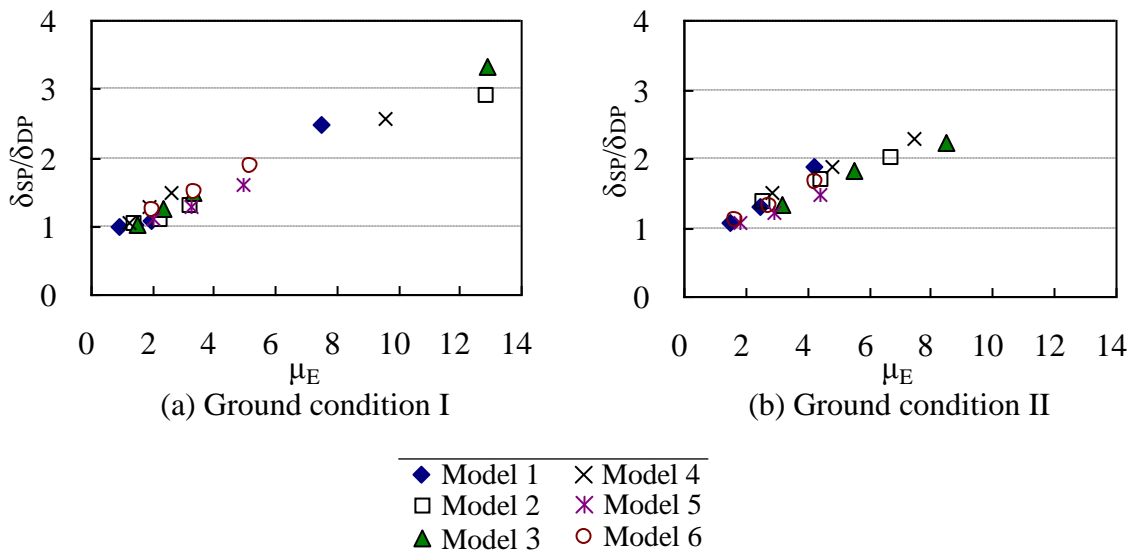


Figure 4.9: $\delta_{SP}/\delta_{DP} - \mu_E$ Relationships for Average Response Displacements

4.3 Approximation of $\delta_{SP}/\delta_{DP} - \mu_E$ Relationship

With the finding that the estimation accuracy is not dependent on model and ground condition type, it is possible to approximate the $\delta_{SP}/\delta_{DP} - \mu_E$ relationship by a single function $f(\mu_E)$ that represents the general tendency which is valid for different ground motions and structural parameters. This approximation is carried out by considering only the average response displacement results, as recommended by JRA code [1]. Average and lower bound values of δ_{SP}/δ_{DP} are expressed by lines as shown in **Figure 4.10**. The average approximation is the optimum line between δ_{SP}/δ_{DP} values

calculated by least squares method. On the other hand the lower bound approximation is the bottom boundary line of $\delta_{SP}/\delta_{DP} - \mu_E$ relationship. By the help of these lines it is possible to predict the estimation accuracy for any given μ_E values.

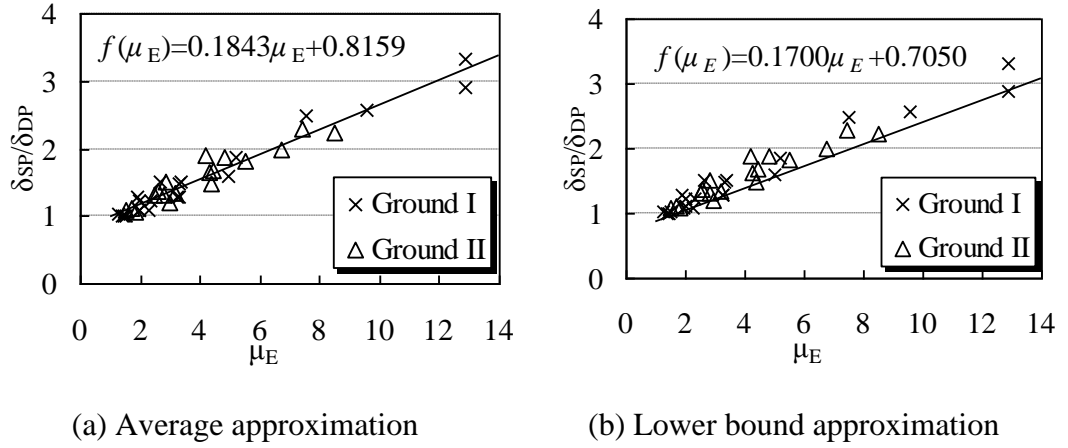


Figure 4.10: Approximation of $\delta_{SP}/\delta_{DP} - \mu_E$ Relationship

4.4 Correction Functions for Equal Energy Assumption

The poor estimation accuracy of equal energy assumption can be improved by modifying the approximation function which represents the estimation accuracy for all cases for a given μ_E . The principle of modification is simply urging the estimation accuracy toward the ideal precise estimation expressed as;

$$\begin{aligned}
 f(\mu_E).C &= 1 \\
 \Rightarrow C &= \frac{1}{f(\mu_E)}
 \end{aligned}
 \tag{4.1}$$

where C is defined as the correction function. This states that the correction function is simply the reciprocal of the approximation function.

Two kinds of correction functions are proposed. One of them is average estimation correction function shown in equation (4.2) which is used for the most optimum estimation results. The other one is lower bound estimation correction function which assures a safe side estimation where the estimated value is always larger than or equal to the actual maximum response δ_{DP} . These correction functions are derived from the corresponding $f(\mu_E)$ approximation functions respectively.

Average Estimation

$$C = 1/(0.1843\mu_E + 0.8159), \text{ for } 0 < C \leq 1 \quad (4.2)$$

Lower Bound Estimation

$$C = 1/(0.1700\mu_E + 0.7050), \text{ for } 0 < C \leq 1 \quad (4.3)$$

Both of the correction functions should be used if the corrected value is less than 1. Otherwise no correction is needed and the estimated value can be used directly. This is generally encountered in the very small values of μ_E or when the response is completely elastic.

By the same manner with the definition of correction function the estimated ductility factor μ_E is corrected as

$$\mu_E C = \mu_C \quad (4.4)$$

in which μ_C is the corrected ductility factor. The corrected estimated maximum response δ_{SP}' can be obtained as

$$\delta_{SP}' = \mu_E \times C \times \delta_y \quad (4.5)$$

which is simply multiplying the corrected ductility factor with the yield displacement.

It should be noted that the accuracy of this correction depends on the degree how much the originally estimated value can be represented by the approximation function $f(\mu_E)$. If the value coincides with the line defined by $f(\mu_E)$ the correction will lead to a 100% estimation where δ_{SP}' would be equal to δ_{DP} . The accuracy will tend to decrease as the estimation value gets far from the line.

Correction results of the estimation for average estimation and lower bound estimation are given respectively in the tables in **Appendix E** and **Appendix F**. Although the correction functions are generated by considering only the average response displacements, the average estimation correction functions is also applied to the results of the individual ground motions. The correction functions for lower bound estimations are only applied to the average response displacements since it is

meaningful only in design procedure in which the average of the response displacements of three ground motions should be taken. It can be seen in these tables that the correction functions for both average and lower bound estimations fairly improves the estimation results. The δ_{SP}/δ_{DP} value ranging between 1 and 5.3 before the correction settles between 0.9 and 1.2 for the average estimation and between 1 and 1.3 for the lower bound estimation. When the average estimation correction functions are applied to the results of individual ground motions, the estimation accuracy is improved as well, ranging from 0.8 to 1.3. This suggests that the average estimation correction functions can be also applied to the estimation for the individual ground motions.

4.5 Validity of the Correction Functions

In order to demonstrate the efficiency of the correction functions the corrected values are compared with the original ones by plotting the both estimation results on the same graph. For this purpose the corrected values of the estimated ductility factor calculated from the average response displacements for the both ground conditions are plotted in **Figure 4.11** together with the values without correction, versus the actual ductility factor μ . The corrected estimation results of the individual ground motions by the application of the average estimation correction functions are also illustrated as in **Figure 4.12**. It can be seen in these figures that the accuracy of the estimation is significantly improved.

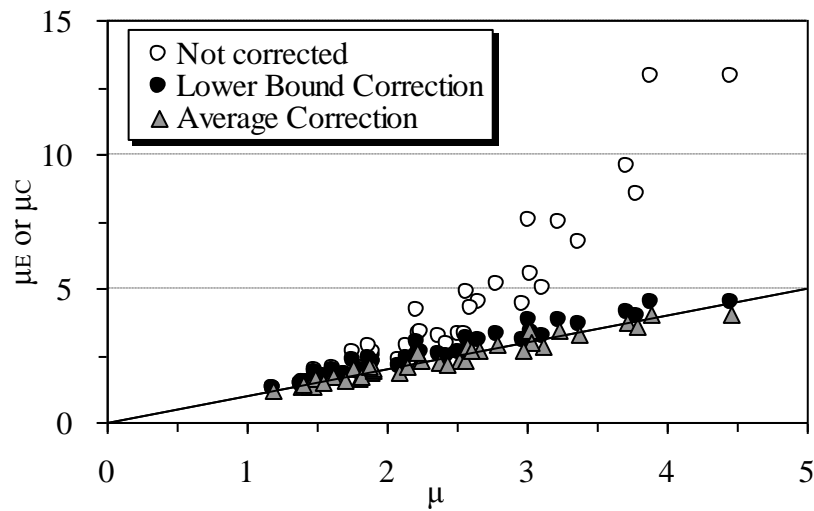


Figure 4.11: Correction Results for the Average Response Displacements

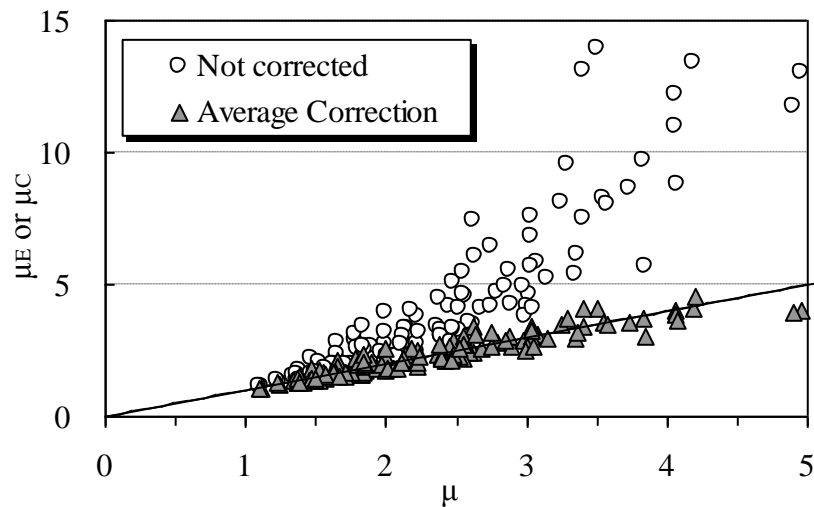
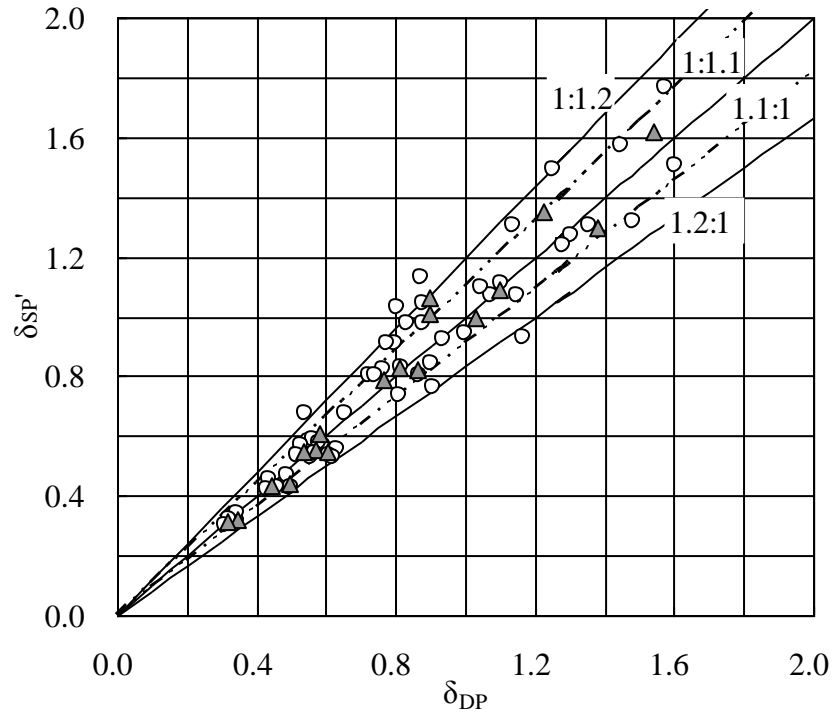


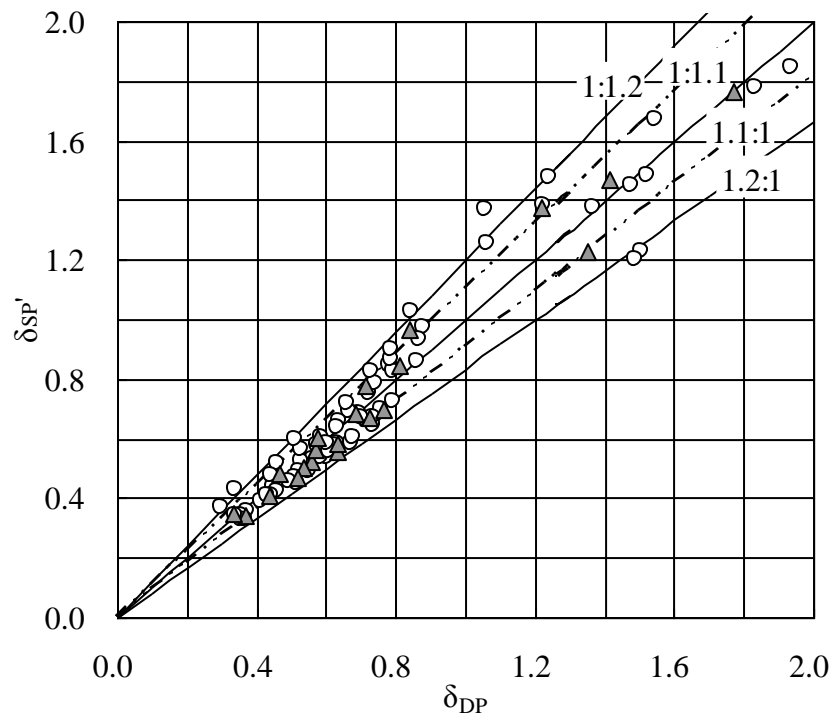
Figure 4.12: Correction Results for the Individual Ground Motions

Figure 4.13 represents the relationship between the calculated (δ_{DP}) and the estimated (δ_{SP}) maximum responses for the average estimation. Fairly good results are obtained for average response displacements. Their error mostly ranges from -10% to 10%. For the individual ground motions, the average estimation with the error ranging from -20% to 20% is obtained with the exception of a few cases. **Figure 4.14** represents the similar relationship for the lower bound estimations. Lower bound estimation is plotted only for the average response displacements. All of the lower bound estimation results are conservative side, and its estimation error is less than 20% except a few cases.

Within these acceptable error ranges it could be concluded that the proposed correction functions are valid for the maximum inelastic response estimation of steel arch bridges in out-of-plane direction.



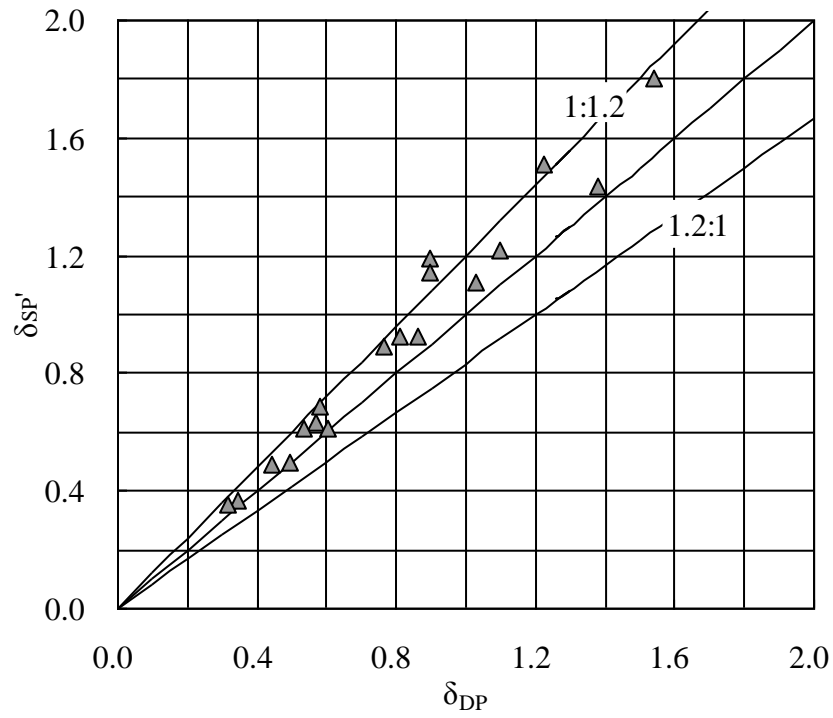
Ground Condition I



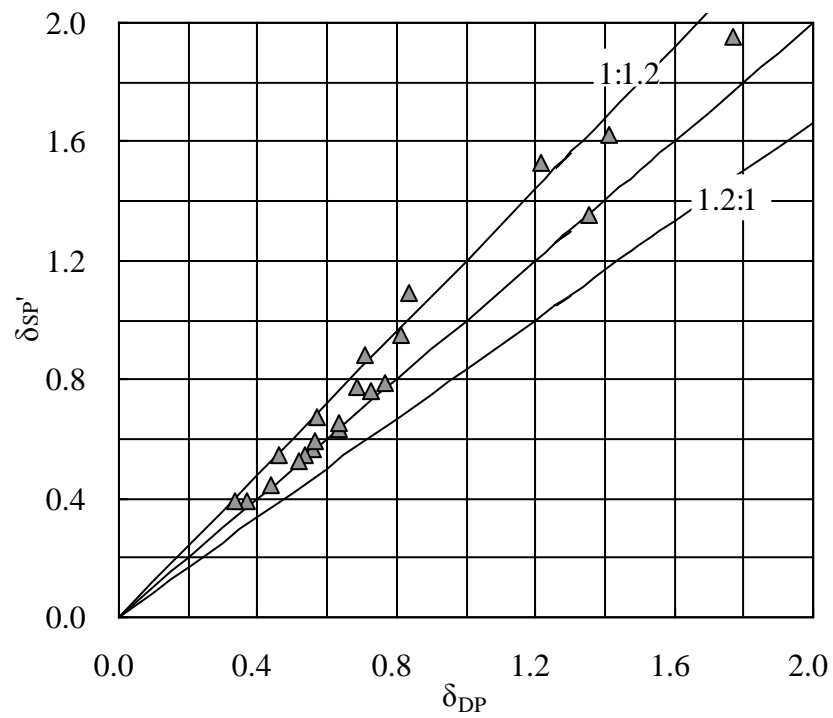
Ground Condition II

-
- Average Estimation Results for the Individual Ground Motions
 - ▲ Average Estimation Results for Average Response Displacements
-

Figure 4.13: Average Estimation Results by the Proposed Correction Functions



Ground Condition I



Ground Condition II

▲ Lower Bound Estimation Results
(Average Response Displacements)

Figure 4.14: Lower Bound Estimation Results by the Proposed Correction Functions

5 CONCLUDING REMARKS

Static pushover analysis, linear and nonlinear dynamic response analysis of six deck-type steel arch bridges were carried out. The applicability of the equal energy assumption for the out-of-plane response of the structure was examined based on the results of these analysis, and correction functions were proposed to improve the estimation accuracy of the maximum response displacement. The validity of the correction functions was evaluated through numerical examples. Main findings in this research are summarized as:

- 1) The predicted maximum inelastic response displacement based on the equal energy assumption is conservative for deck-type steel arch bridges. But too conservative results may be obtained in many cases.
- 2) The ground condition type and structural parameters considered in this research which are the Arch Rise/ Span Length ratio and the distance between the arch ribs do not have any significant influence on the applicability of equal energy assumption.
- 3) The prediction accuracy of the equal energy assumption can be improved by using the proposed correction functions. The presented correction functions can be successfully applied to the deck-type steel arch bridges to predict their maximum inelastic response without the need of inelastic dynamic response analysis like numerical examples

In this study maximum elastic response to predict the maximum inelastic response by equal energy assumption is obtained by dynamic response analysis. If the elastic maximum response is obtained by using response spectra, it will be possible to achieve the estimation of maximum inelastic response displacement without dynamic response analysis. On the basis of this concept, development of a static-analysis-based prediction method of maximum inelastic seismic response of steel arch bridges

will be tried in the future work. Also the scope of the study will be broadened to the in-plane response estimation of the structure by considering more ground conditions.

.

REFERENCES

- [1] **Kawashima, K. and Unjoh, S.**, 1997. The damage of highway bridges in the 1995 Hyogo-ken nanbu earthquake and its impact on Japanese seismic design, *Journal of Earthquake Engineering*, **1(3)**, 505-541.
- [2] **Gao, S. Usami, T. and Ge, H. B.**, 1998. Ductility of steel short cylinders in compression and bending, *Journal of Engineering Mechanics (ASCE)*, **124(2)**, 176-183.
- [3] **Liu, Q. Kasai, A. and Usami, T.**, 2001. Two hysteretic models for thin walled pipe-section steel bridge piers, *Engineering Structures*, **23(2)**, 186-197.
- [4] **Usami, T. Gao, S. and Ge, H.**, 2000. Elastoplastic analysis of steel members and frames subjected to cyclic loading, *Engineering Structures*, **22(2)**, 135-145.
- [5] **Li, X. S. and Goto, Y.**, 1998. A three dimensional nonlinear seismic analysis of frames considering panel zone deformation, *Journal of Structural Mechanics and Earthquake Engineering (Japanese Society of Civil Engineers-JSCE)*, **605(I-45)**, 1-13.
- [6] **Nonaka, T. Usami, T. Sakamoto, Y. and Iwamura, M.**, 2003. Inelastic seismic behavior of upper-deck steel truss bridges under major earthquakes and a proposal for its seismic upgrading, *Journal of Structural Engineering (JSCE)*, **49A**, 531-542 (in Japanese).
- [7] **Nonaka, T. Usami, T. Yoshino, H. Sakamoto, Y. and Torigoe, T.**, 2003. Elasto-plastic behavior and improvement of seismic performance for upper-upper-deck steel arch bridge models, *Journal of Structural Mechanics and Earthquake Engineering (JSCE)*, **731(I-63)**, 31-49.
- [8] **Nonaka, T. and Ali, A.**, 2001. Dynamic response of half-through steel arch bridge using fiber model, *Journal of Bridge Engineering (American Society of Civil Engineers - ASCE)*, **6(6)**, 482-488.
- [9] **Yanagi, T. Nakajima, A. and Saiki, I.**, 2003. Two-dimensional elasto-plastic behavior of upper-deck steel arch bridge and its modeling, *Journal of Structural Engineering (JSCE)*, **49A**, 543-552 (in Japanese).
- [10] **Okumura, T. Goto, Y. and Ozawa, K.**, 2000. Ultimate in-plane behavior of upper-upper-deck steel arch bridges under seismic loads, *Journal of Structural Engineering (JSCE)*, **46A**, 1333-1342 (in Japanese).

- [11] **Sakakibara, Y. Kawashima, K. and Shoji, G.**, 2000. Analytical evaluation of an upper-upper-deck two-hinge steel arch bridge, *Journal of Structural Engineering (JSCE)*, **46A**, 1333-1342 (in Japanese).
- [12] **Usami, T. Lu, Z. Ge, H. and Kono, T.**, 2004. Steel performance evaluation of steel arch bridges against major earthquakes. Part 1: Dynamic analysis approach, *Journal of Earthquake Engineering and Structural Dynamics*, **33**, 1337-1354.
- [13] **Lu, Z. Usami, T. and Ge, H.**, 2004. Seismic performance evaluation of steel arch bridges against major earthquakes. Part 2: Simplified verification procedure, *Journal of Earthquake Engineering and Structural Dynamics*, **33**, 1355-1372.
- [14] **Lu, Z. Ge, H. and Usami T.**, 2004. Applicability of pushover analysis-based seismic performance evaluation procedure for steel arch bridges. *Engineering Structures*, **26**, 1957-1977.
- [15] **Kudo, T. Saiki, I. and Nakajima, A.**, 2002. Elasto-plastic behavior of viaduct system under bi-directional earthquake motions, *Proceedings of the third international workshop on performance-based seismic design and retrofit of transportation facilities*, Tokyo, Japan, 89-99.
- [16] **Zhu, P. Abe, M. and Fujino, Y.**, 2002. Modeling of three-dimensional non-linear seismic performance of elevated bridges with emphasis on pounding of girders, *Journal of Earthquake Engineering and Structural Dynamics*, **31(11)**, 1891-1913.
- [17] **Chaudhary, M. T. A. Abe, M. and Fujino Y.**, 2002. Investigation of a typical seismic response of a base-isolated bridge, *Engineering Structures*, **24(7)**, 945-953
- [18] **Japan Road Association**, 1996. Specifications for highway bridges-Part V Seismic Design, Tokyo, Japan.
- [19] **Japan Road Association**, 2002. Specifications for highway bridges-Part V Seismic Design, Tokyo, Japan.
- [20] **Veletsos, A. S. and Newmark, N. M.**, 1960. Effect of inelastic behavior on the response of simple systems to earthquake motions, *Proceedings of the Second World Conference on Earthquake Engineering*, Tokyo, Japan, 895-912.
- [21] **Usami, T. Saizuka, K. Kiso, E. and Ito, Y.**, 1995. Pseudo-dynamic tests of steel bridge pier models under severe earthquake, *Journal of Structural Mechanics and Earthquake Engineering*, **519/I-32**, 101-113 (In Japanese).
- [22] **Nakajima, A. and Onodera, O.**, 1998. A study on elasto-plastic behavior of steel portal frames under severe earthquake and applicability of equal energy assumption to its seismic design, *Proceedings of the Second*

Symposium on Nonlinear Numerical Analysis and its Application to Seismic Design of Steel Structures, 135-142 (In Japanese).

- [23] **Nakamura, S. Ida, Y. Takahashi, K.**, 2001. A prediction method of maximum inelastic seismic response for steel portal frame bridge piers. *Proceedings of the First International Conference on Steel & Composite Structures*, **2**, 1047-1054.

- [24] **Usami, T.** editor, 2003. Seismic performance evaluation procedures and upgrading measures for steel bridges, *Task Committee of Performance-Based Seismic Design Methods for Steel Bridges (Japan Society of Steel Construction -JSCE)*. Tokyo, Japan (in Japanese).

- [25] **JIP Techno Science Corporation**, 2002. Input Manual for JSW-15W version 2.04 (in Japanese).

- [26] **MARC Analysis Research Corporation**, 1997. MARC User Manual Volume A- Volume E, version K7.

- [27] **Chopra, A. K.**, 2001. Dynamics of structures, 2nd ed. Prentice Hall, Upper Saddle River NJ.

APPENDIXES

Appendix A: Generated Models

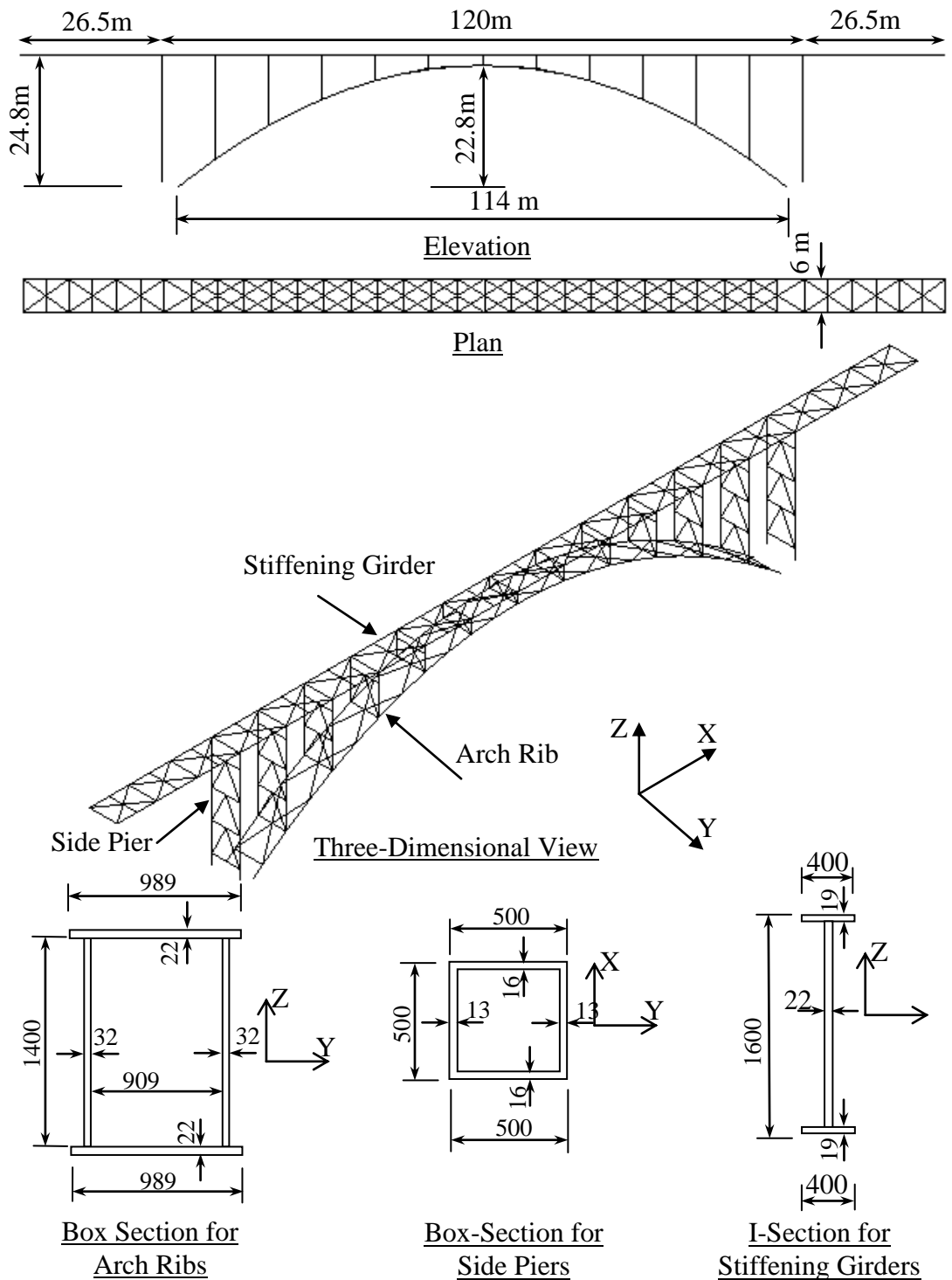


Figure A.1: Model 2

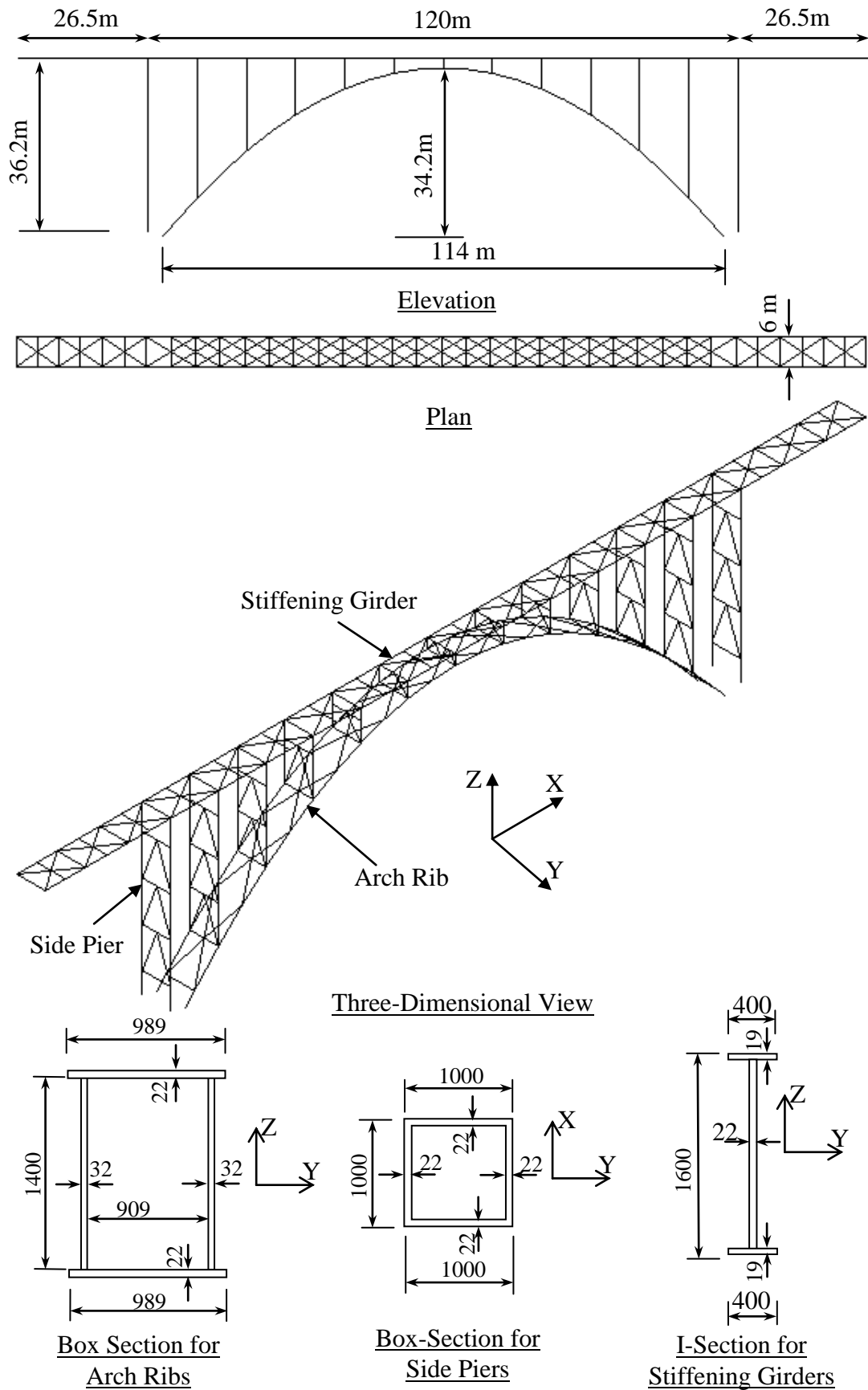


Figure A.2: Model 3

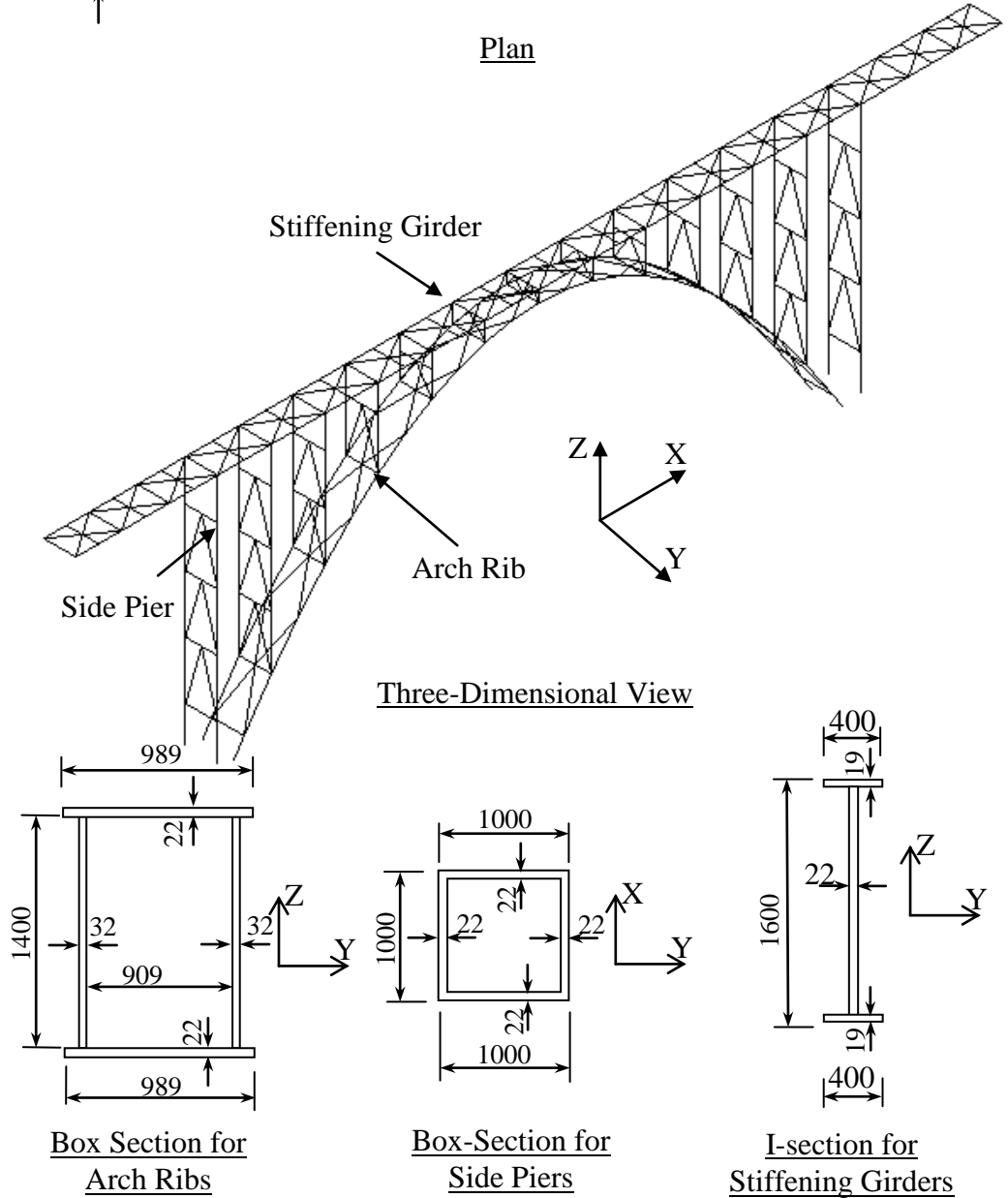
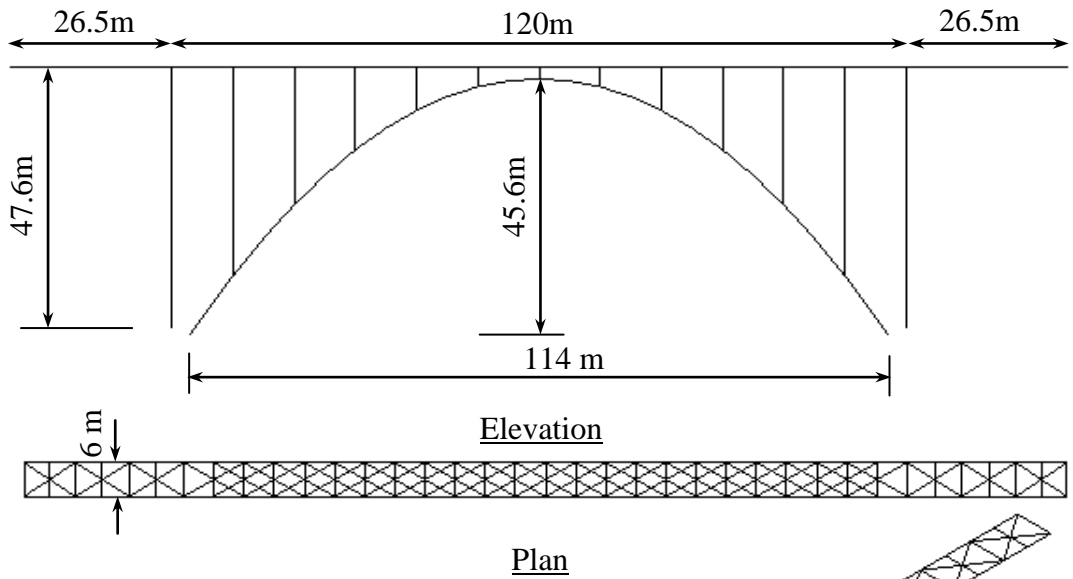


Figure A.3: Model 4

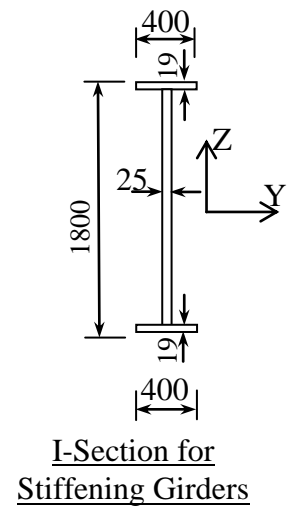
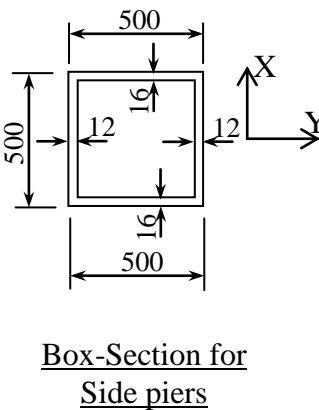
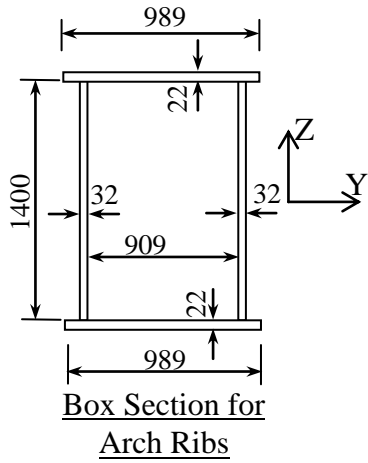
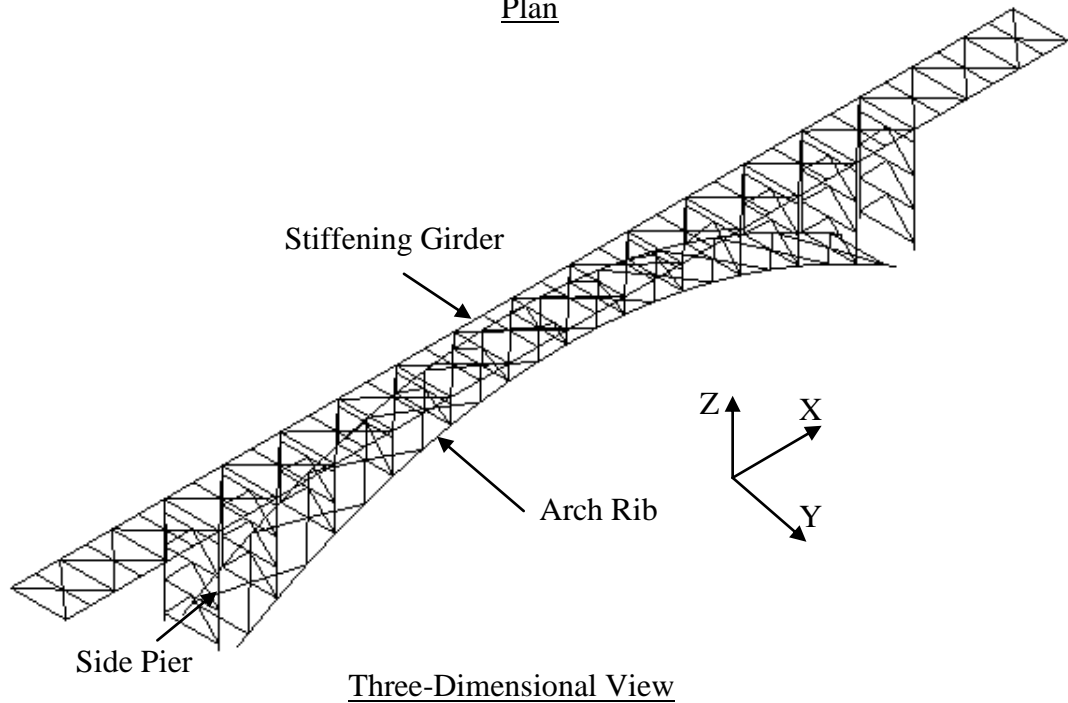
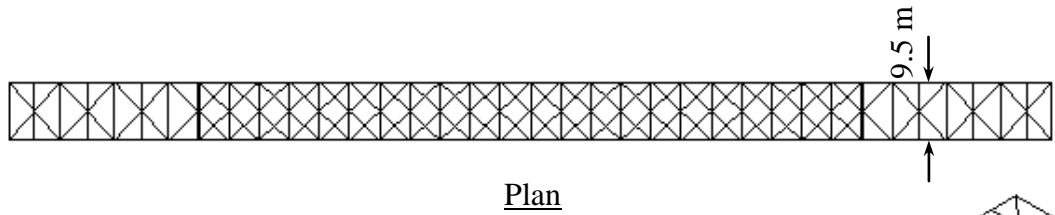
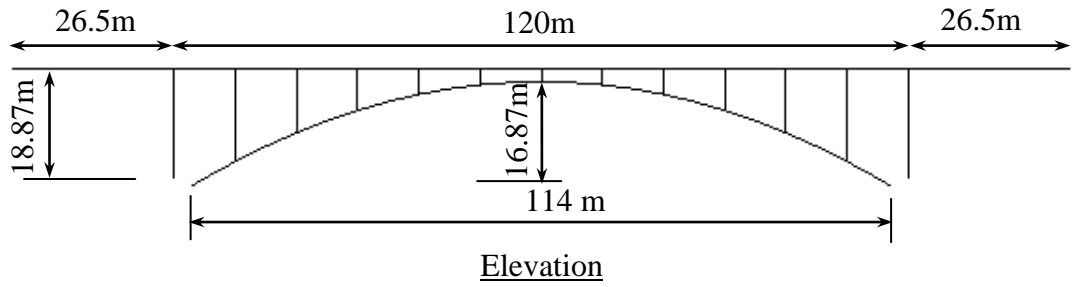


Figure A.4: Model 5

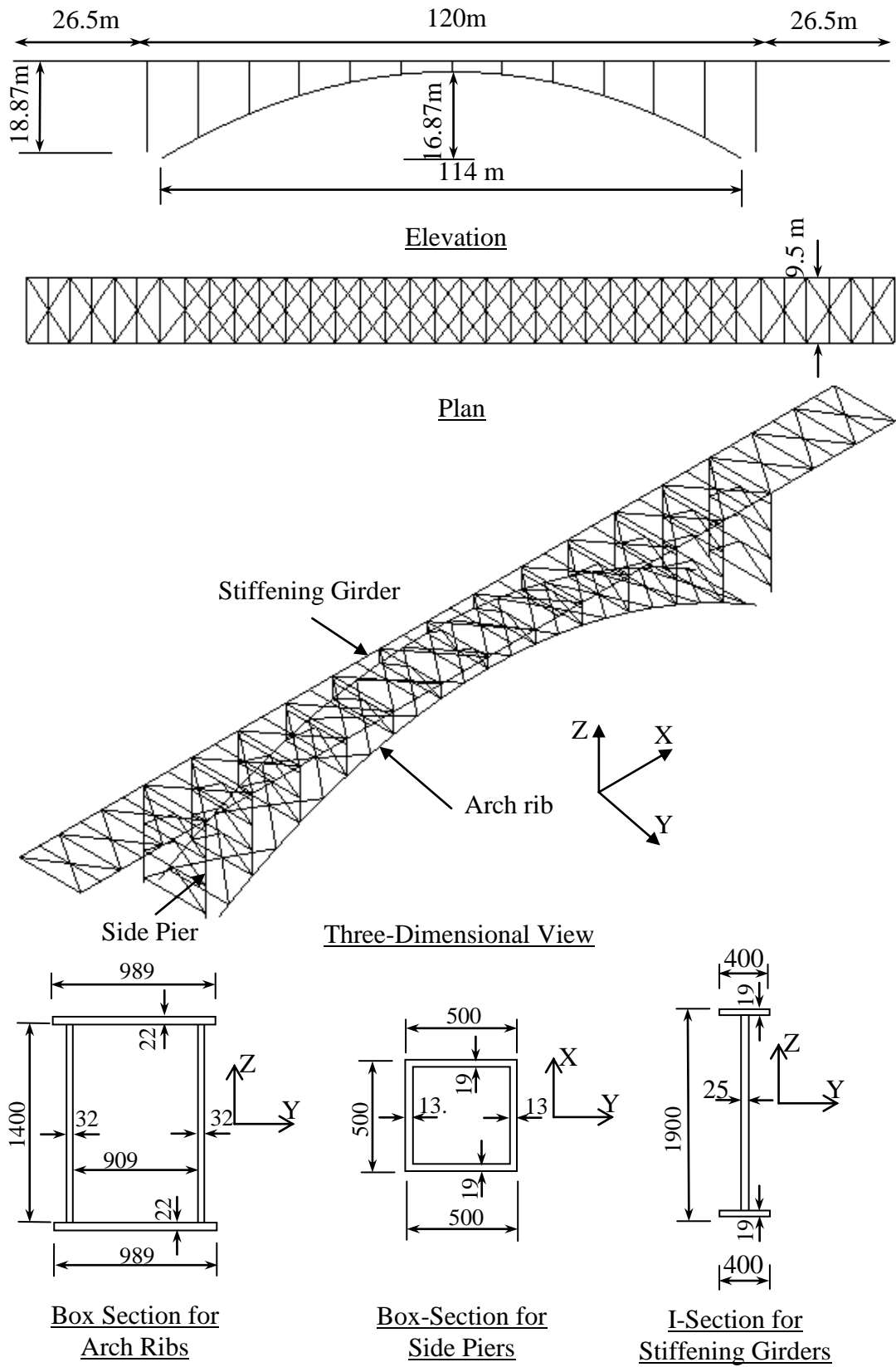
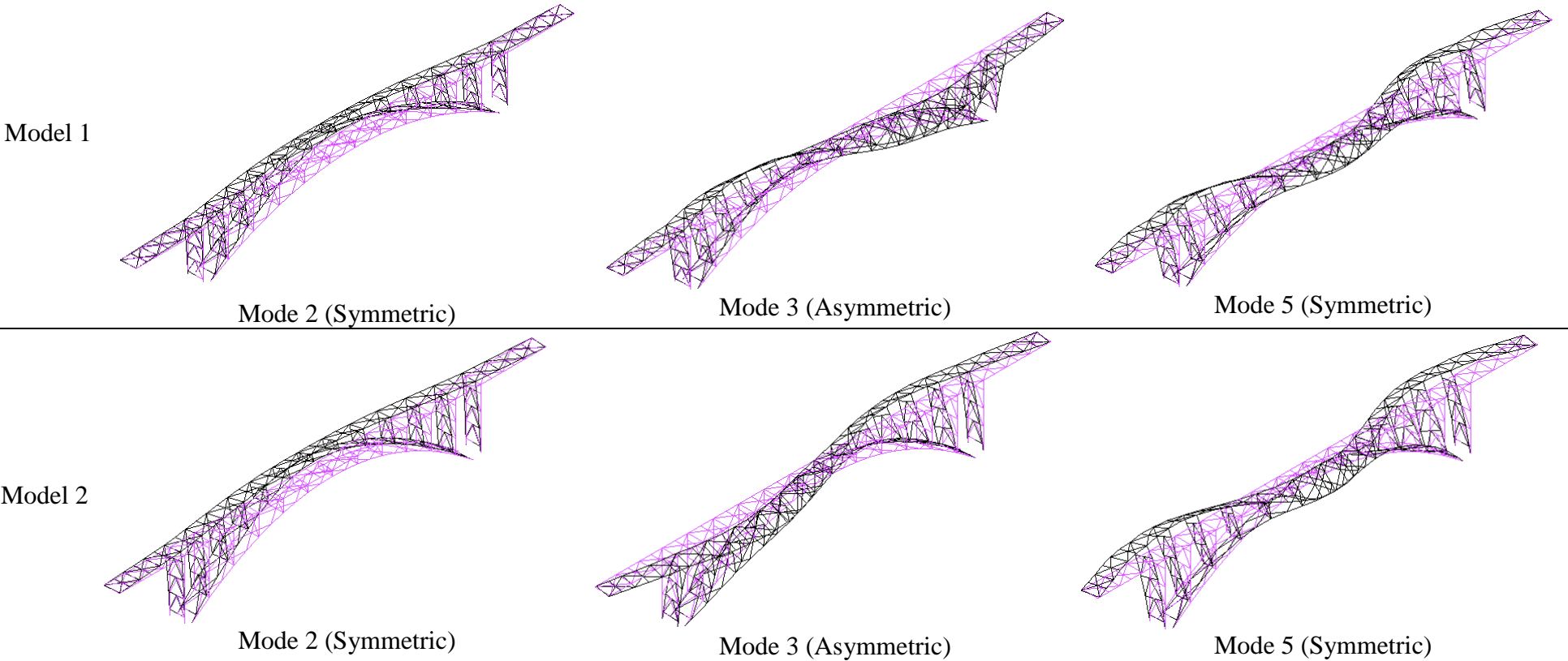


Figure A.5: Model 6

Appendix B: Predominant Eigenmodes



70

Figure B.1: Predominant Eigenmodes (Model 1, Model 2)

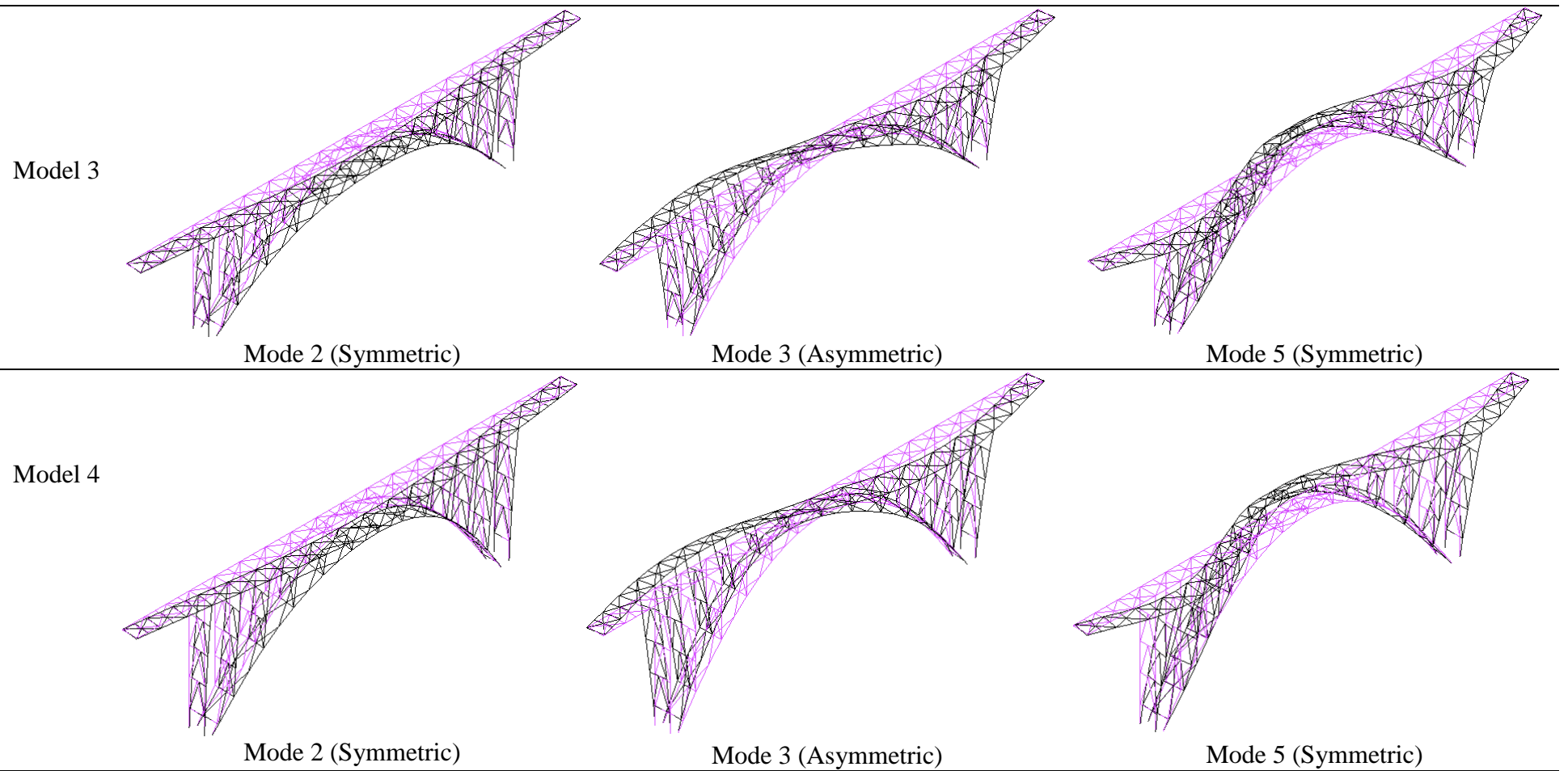


Figure B.2: Predominant Eigenmodes (Model 3, Model 4)

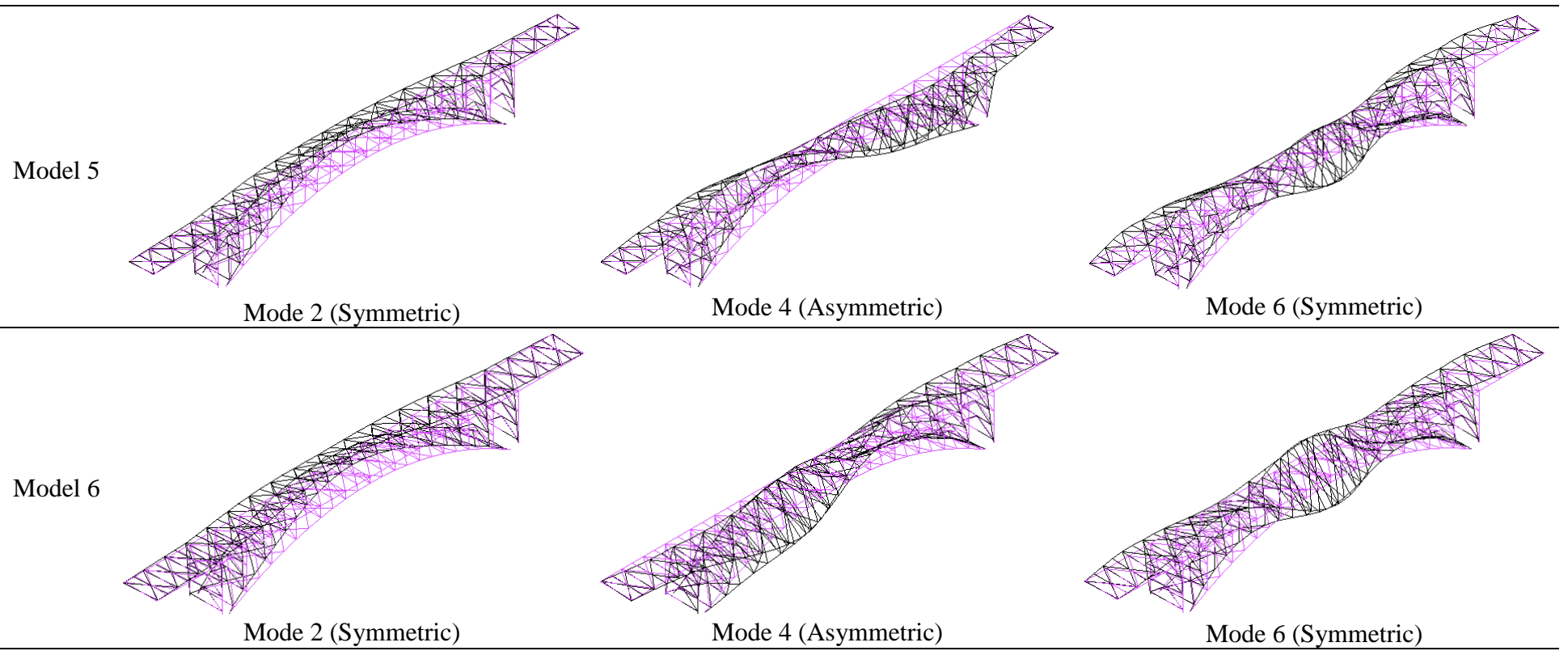


Figure B.3: Predominant Eigenmodes (Model 5, Model 6)

Appendix C: Specified Response Spectra by the JRA [1] code

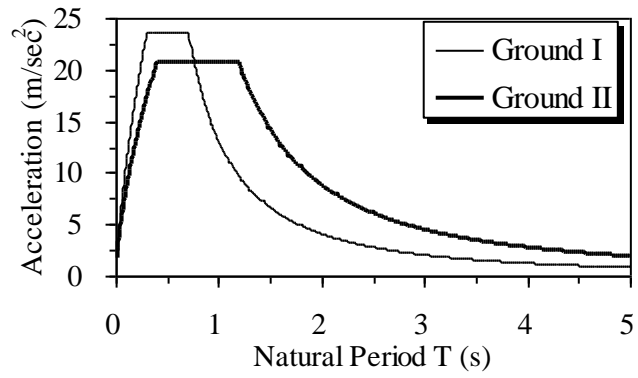


Figure C.1: The specified response spectrum for level 2 Type 2 Earthquake Ground Motions ($\xi=0.03$).

Appendix D: Numerical Analysis Results

Table D.1: Numerical Analysis Results for Model 1

Ground Condition	Ground Motion	$\delta_{DE}(m)$	$\delta_{DP}(m)$	$\delta_{SP}(m)$	μ_E	δ_{SP}/δ_{DP}
Ground I	L2.t211	0.4204	0.3017	0.453	2.198	1.501
	L2.t211×1.2	0.5028	0.3404	0.571	2.774	1.679
	L2.t211×1.5	0.6245	0.4570	0.780	3.784	1.706
	L2.t211×1.7	0.7044	0.5280	0.937	4.549	1.775
	L2.t211×2	0.8218	0.6331	1.197	5.810	1.890
	L2.t211×5	1.8920	1.2630	4.815	23.373	3.812
	L2.t212	0.359	0.356	0.375	1.820	1.053
	L2.t212×1.5	0.539	0.492	0.629	3.054	1.279
	L2.t212×2	0.719	0.576	0.968	4.697	1.680
	L2.t212×5	1.802	1.098	4.441	21.558	4.045
	L2.t213	0.382	0.338	0.403	1.957	1.193
	L2.t213×1.5	0.569	0.440	0.680	3.300	1.545
	L2.t213×2	0.753	0.510	1.041	5.052	2.040
	L2.t213×5	1.832	0.865	4.564	22.157	5.277
Ground II	Le2.t221	0.333	0.322	0.344	1.670	1.068
	Le2.t221x1.5	0.499	0.458	0.566	2.748	1.236
	Le2.t221x2	0.664	0.567	0.855	4.150	1.508
	Le2.t222	0.356	0.323	0.371	1.801	1.149
	Le2.t222x1.5	0.533	0.436	0.619	3.005	1.420
	Le2.t222x2	0.709	0.526	0.947	4.597	1.800
	Le2.t223	0.330	0.309	0.341	1.655	1.104
	Le2.t223x1.5	0.493	0.433	0.556	2.699	1.284
	Le2.t223x2	0.657	0.518	0.842	4.087	1.625

Table D.2: Numerical Analysis Results for Model 2

Ground Condition	Ground Motion	$\delta_{DE}(m)$	$\delta_{DP}(m)$	$\delta_{SP}(m)$	μ_E	δ_{SP}/δ_{DP}
Ground I	L2.t211	0.463	0.462	0.468	1.540	1.013
	L2.t211×1.2	0.555	0.553	0.570	1.873	1.030
	L2.t211×1.5	0.694	0.675	0.736	2.421	1.091
	L2.t211×1.7	0.786	0.735	0.859	2.824	1.168
	L2.t211×2	0.923	0.795	1.059	3.483	1.332
	L2.t211×5	2.286	1.064	4.238	13.942	3.983
	L2.t212	0.440	0.440	0.443	1.458	1.008
	L2.t212×1.5	0.660	0.622	0.693	2.281	1.115
	L2.t212×2	0.881	0.760	0.995	3.274	1.309
	L2.t212×5	2.195	1.506	3.958	13.019	2.628
	L2.t213	0.416	0.415	0.418	1.374	1.005
	L2.t213×1.5	0.623	0.605	0.648	2.133	1.072
L2.t213×2	0.830	0.737	0.921	3.028	1.249	
L2.t213×5	2.065	1.488	3.573	11.754	2.401	
Ground II	Le2.t221	0.843	0.540	0.939	3.089	1.739
	Le2.t221×1.5	1.266	0.776	1.655	5.444	2.133
	Le2.t221×2	1.661	1.077	2.506	8.243	2.327
	Le2.t222	0.705	0.563	0.750	2.467	1.332
	Le2.t222×1.5	1.058	0.743	1.277	4.201	1.719
	Le2.t222×2	1.412	0.836	1.949	6.411	2.331
	Le2.t223	0.655	0.634	0.687	2.260	1.084
	Le2.t223×1.5	0.982	0.908	1.152	3.789	1.269
	Le2.t223×2	1.307	1.168	1.735	5.707	1.485

Table D.3: Numerical Analysis Results for Model 3

Ground Condition	Ground Motion	$\delta_{DE}(m)$	$\delta_{DP}(m)$	$\delta_{SP}(m)$	μ_E	δ_{SP}/δ_{DP}
Ground I	L2.t211	0.544	0.536	0.549	1.508	1.024
	L2.t211×1.2	0.653	0.625	0.668	1.835	1.069
	L2.t211×1.5	0.817	0.695	0.857	2.354	1.233
	L2.t211×1.7	0.927	0.727	0.993	2.727	1.365
	L2.t211×2	1.090	0.783	1.210	3.324	1.545
	L2.t211×5	2.75	1.24	4.766	13.094	3.844
	L2.t212	0.529	0.528	0.533	1.464	1.009
	L2.t212×1.5	0.793	0.699	0.828	2.275	1.185
	L2.t212×2	1.056	0.792	1.163	3.195	1.468
	L2.t212×5	2.628	1.479	4.426	12.159	2.993
	L2.t213	0.553	0.543	0.559	1.535	1.029
	L2.t213×1.5	0.830	0.665	0.872	2.397	1.312
	L2.t213×2	1.107	0.861	1.234	3.390	1.433
	L2.t213×5	2.792	1.522	4.886	13.424	3.210
	Ground II	Le2.t221	1.078	0.903	1.193	3.277
Le2.t221×1.5		1.616	1.105	2.074	5.698	1.877
Le2.t221×2		2.15	1.481	3.208	8.813	2.166
Le2.t222		1.061	0.814	1.170	3.214	1.437
Le2.t222×1.5		1.590	1.048	2.026	5.566	1.933
Le2.t222×2		2.117	1.356	3.131	8.602	2.309
Le2.t223		1.010	0.870	1.101	3.025	1.266
Le2.t223x1.5		1.518	1.148	1.894	5.203	1.650
Le2.t223x2		2.026	1.304	2.923	8.030	2.242

Table D.4: Numerical Analysis Results for Model 4

Ground Condition	Ground Motion	$\delta_{DE}(m)$	$\delta_{DP}(m)$	$\delta_{SP}(m)$	μ_E	δ_{SP}/δ_{DP}
Ground I	L2.t211	0.596	0.588	0.597	1.252	1.015
	L2.t211×1.2	0.715	0.636	0.723	1.515	1.136
	L2.t211×1.5	0.893	0.744	0.920	1.929	1.237
	L2.t211×1.7	1.012	0.786	1.057	2.216	1.345
	L2.t211×2	1.190	0.880	1.274	2.671	1.448
	L2.t211×5	2.967	1.831	4.624	9.695	2.526
	L2.t212	0.638	0.586	0.641	1.343	1.093
	L2.t212×1.5	0.956	0.730	0.992	2.080	1.359
	L2.t212×2	1.275	0.847	1.384	2.901	1.633
	L2.t212×5	3.197	1.938	5.223	10.949	2.695
	L2.t213	0.533	0.526	0.533	1.118	1.013
	L2.t213×1.5	0.799	0.659	0.815	1.708	1.236
	L2.t213×2	1.064	0.785	1.119	2.346	1.425
	L2.t213×5	2.653	1.546	3.865	8.102	2.500
	Ground II	Le2.t221	1.106	0.936	1.170	2.453
Le2.t221x1.5		1.660	1.280	1.935	4.057	1.512
Le2.t221x2		2.214	1.601	2.921	6.124	1.824
Le2.t222		1.460	0.875	1.636	3.430	1.870
Le2.t222x1.5		2.195	1.255	2.883	6.044	2.297
Le2.t222x2		2.935	1.572	4.544	9.526	2.891
Le2.t223		1.189	0.877	1.273	2.669	1.452
Le2.t223x1.5		1.785	1.138	2.137	4.480	1.878
Le2.t223x2		2.382	1.448	3.265	6.845	2.255

Table D.5: Numerical Analysis Results for Model 5

Ground Condition	Ground Motion	$\delta_{DE}(m)$	$\delta_{DP}(m)$	$\delta_{SP}(m)$	μ_E	δ_{SP}/δ_{DP}
Ground I	L2.t211	0.413	0.3756	0.431	2.124	1.148
	L2.t211×1.2	0.4959	0.4301	0.535	2.637	1.244
	L2.t211×1.5	0.6193	0.5253	0.718	3.536	1.367
	L2.t211×1.7	0.7013	0.5883	0.858	4.226	1.458
	L2.t211×2	0.8236	0.6796	1.093	5.383	1.608
	L2.t211×5	1.937	1.321	4.398	21.664	3.329
	L2.t212	0.369	0.369	0.380	1.871	1.030
	L2.t212×1.5	0.555	0.517	0.618	3.047	1.196
	L2.t212×2	0.741	0.612	0.931	4.585	1.521
	L2.t212×5	1.851	1.237	4.081	20.105	3.299
	L2.t213	0.390	0.355	0.404	1.988	1.137
	L2.t213×1.5	0.585	0.513	0.664	3.269	1.294
	L2.t213×2	0.780	0.603	1.005	4.953	1.667
	L2.t213×5	1.863	0.967	4.125	20.320	4.266
Ground II	Le2.t221	0.348	0.346	0.356	1.754	1.029
	Le2.t221x1.5	0.521	0.492	0.570	2.808	1.159
	Le2.t221x2	0.695	0.611	0.847	4.172	1.386
	Le2.t222	0.390	0.347	0.404	1.990	1.164
	Le2.t222x1.5	0.583	0.487	0.661	3.256	1.357
	Le2.t222x2	0.774	0.579	0.994	4.897	1.717
	Le2.t223	0.346	0.339	0.353	1.739	1.041
	Le2.t223x1.5	0.518	0.500	0.565	2.783	1.130
	Le2.t223x2	0.690	0.618	0.838	4.128	1.356

Table D.6: Numerical Analysis Results for Model 6

Ground Condition	Ground Motion	$\delta_{DE}(m)$	$\delta_{DP}(m)$	$\delta_{SP}(m)$	μ_E	δ_{SP}/δ_{DP}
Ground I	L2.t211	0.4204	0.3017	0.453	2.198	1.501
	L2.t211×1.2	0.5028	0.3404	0.571	2.774	1.679
	L2.t211×1.5	0.6245	0.4570	0.780	3.784	1.706
	L2.t211×1.7	0.7044	0.5280	0.937	4.549	1.775
	L2.t211×2	0.8218	0.6331	1.197	5.810	1.890
	L2.t211×5	1.8920	1.2630	4.815	23.373	3.812
	L2.t212	0.359	0.356	0.375	1.820	1.053
	L2.t212×1.5	0.539	0.492	0.629	3.054	1.279
	L2.t212×2	0.719	0.576	0.968	4.697	1.680
	L2.t212×5	1.802	1.098	4.441	21.558	4.045
	L2.t213	0.382	0.338	0.403	1.957	1.193
	L2.t213×1.5	0.569	0.440	0.680	3.300	1.545
	L2.t213×2	0.753	0.510	1.041	5.052	2.040
	L2.t213×5	1.832	0.865	4.564	22.157	5.277
Ground II	Le2.t221	0.333	0.322	0.344	1.670	1.068
	Le2.t221x1.5	0.499	0.458	0.566	2.748	1.236
	Le2.t221x2	0.664	0.567	0.855	4.150	1.508
	Le2.t222	0.356	0.323	0.371	1.801	1.149
	Le2.t222x1.5	0.533	0.436	0.619	3.005	1.420
	Le2.t222x2	0.709	0.526	0.947	4.597	1.800
	Le2.t223	0.330	0.309	0.341	1.655	1.104
	Le2.t223x1.5	0.493	0.433	0.556	2.699	1.284
	Le2.t223x2	0.657	0.518	0.842	4.087	1.625

Appendix E: Correction Results for the Average Estimation

Table E.1: Average Estimation Results for Model 1

Ground Condition I

Ground Motion	$\delta_{DP}(m)$	$\delta_{SP}(m)$	δ_{SP}/δ_{DP}	μ_E	C	μ_c	$\delta_{SP}'(m)$	δ_{SP}'/δ_{DP}
L2.t211	0.373	0.373	1.000	0.926	1.014	No Correction		
L2.t211×1.2	0.448	0.448	1.000	1.112	0.980	1.089	0.439	0.980
L2.t211×1.5	0.558	0.565	1.013	1.402	0.931	1.305	0.526	0.943
L2.t211×1.7	0.630	0.647	1.027	1.605	0.899	1.444	0.582	0.924
L2.t211×2	0.714	0.782	1.095	1.940	0.852	1.654	0.666	0.933
L2.t211×5	1.058	2.992	2.828	7.424	0.458	3.399	1.370	1.295
L2.t212	0.369	0.369	1.000	0.916	1.016	No Correction		
L2.t212×1.5	0.553	0.560	1.013	1.390	0.933	1.296	0.522	0.945
L2.t212×2	0.722	0.776	1.075	1.926	0.854	1.645	0.663	0.918
L2.t212×5	1.370	3.034	2.215	7.529	0.454	3.417	1.377	1.005
L2.t213	0.378	0.378	1.000	0.938	1.011	No Correction		
L2.t213×1.5	0.566	0.573	1.012	1.422	0.928	1.319	0.532	0.939
L2.t213×2	0.743	0.795	1.070	1.973	0.848	1.673	0.674	0.907
L2.t213×5	1.223	3.051	2.495	7.571	0.452	3.424	1.380	1.128
Average	0.373	0.373	1.000	0.926	1.014	No Correction		
Average×1.5	0.559	0.566	1.013	1.404	0.930	1.307	0.527	0.942
Average×2	0.726	0.785	1.081	1.948	0.851	1.658	0.668	0.920
Average×5	1.217	3.026	2.486	7.509	0.455	3.413	1.376	1.130

Ground Condition II

Ground Motion	$\delta_{DP}(m)$	$\delta_{SP}(m)$	δ_{SP}/δ_{DP}	μ_E	C	μ_c	$\delta_{SP}'(m)$	δ_{SP}'/δ_{DP}
Le2.t221	0.552	0.646	1.170	1.603	0.900	1.442	0.581	1.053
Le2.t221×1.2	0.656	0.800	1.220	1.985	0.846	1.680	0.677	1.032
Le2.t221×1.5	0.763	1.070	1.402	2.655	0.766	2.034	0.820	1.074
Le2.t221×7	0.801	1.277	1.594	3.169	0.714	2.264	0.912	1.139
Le2.t221×2	0.879	1.622	1.845	4.025	0.642	2.584	1.041	1.185
Le2.t222	0.590	0.627	1.063	1.556	0.907	1.411	0.569	0.964
Le2.t222×1.5	0.724	1.038	1.433	2.576	0.775	1.996	0.804	1.111
Le2.t222×2	0.803	1.585	1.974	3.933	0.649	2.553	1.029	1.281
Le2.t223	0.559	0.564	1.009	1.400	0.931	1.303	0.525	0.940
Le2.t223×1.5	0.809	0.907	1.121	2.251	0.813	1.829	0.737	0.911
Le2.t223×2	0.999	1.353	1.354	3.357	0.697	2.340	0.943	0.944
Average	0.567	0.612	1.079	1.519	0.913	1.386	0.559	0.985
Average×1.5	0.765	1.004	1.312	2.491	0.784	1.954	0.787	1.029
Average×2	0.894	1.695	1.896	4.206	0.629	2.643	1.065	1.192

Table E.2: Average Estimation Results for Model 2*Ground Condition I*

Ground Motion	$\delta_{DP}(m)$	$\delta_{SP}(m)$	δ_{SP}/δ_{DP}	μ_E	C	μ_c	$\delta_{SP}'(m)$	δ_{SP}'/δ_{DP}
L2.t211	0.462	0.468	1.013	1.540	0.909	1.400	0.426	0.922
L2.t211×1.2	0.553	0.570	1.030	1.873	0.861	1.613	0.490	0.887
L2.t211×1.5	0.675	0.736	1.091	2.421	0.792	1.918	0.583	0.864
L2.t211×1.7	0.735	0.859	1.168	2.824	0.748	2.113	0.642	0.874
L2.t211×2	0.795	1.059	1.332	3.483	0.686	2.389	0.726	0.914
L2.t211×5	1.064	4.238	3.983	13.942	0.295	4.118	1.252	1.177
L2.t212	0.440	0.443	1.008	1.458	0.922	1.344	0.409	0.929
L2.t212×1.5	0.622	0.693	1.115	2.281	0.809	1.845	0.561	0.902
L2.t212×2	0.760	0.995	1.309	3.274	0.705	2.307	0.701	0.923
L2.t212×5	1.506	3.958	2.628	13.019	0.311	4.049	1.231	0.817
L2.t213	0.415	0.418	1.005	1.374	0.935	1.285	0.391	0.940
L2.t213×1.5	0.605	0.648	1.072	2.133	0.827	1.764	0.536	0.886
L2.t213×2	0.737	0.921	1.249	3.028	0.728	2.204	0.670	0.909
L2.t213×5	1.488	3.573	2.401	11.754	0.335	3.941	1.198	0.805
Average	0.439	0.444	1.010	1.459	0.922	1.345	0.409	0.931
Average×1.5	0.634	0.692	1.092	2.277	0.809	1.843	0.560	0.884
Average×2	0.764	0.991	1.297	3.259	0.706	2.301	0.699	0.915
Average×5	1.353	3.918	2.896	12.890	0.313	4.039	1.228	0.907

Ground Condition II

Ground Motion	$\delta_{DP}(m)$	$\delta_{SP}(m)$	δ_{SP}/δ_{DP}	μ_E	C	μ_c	$\delta_{SP}'(m)$	δ_{SP}'/δ_{DP}
Le2.t221	0.540	0.939	1.739	3.089	0.722	2.230	0.678	1.255
Le2.t221×1.5	0.776	1.655	2.133	5.444	0.550	2.992	0.910	1.172
Le2.t221×2	1.077	2.506	2.327	8.243	0.428	3.530	1.073	0.996
Le2.t222	0.563	0.750	1.332	2.467	0.787	1.942	0.590	1.048
Le2.t222×1.5	0.743	1.277	1.719	4.201	0.629	2.642	0.803	1.081
Le2.t222×2	0.836	1.949	2.331	6.411	0.501	3.210	0.976	1.167
Le2.t223	0.634	0.687	1.084	2.260	0.811	1.834	0.557	0.879
Le2.t223×1.5	0.908	1.152	1.269	3.789	0.660	2.502	0.761	0.838
Le2.t223×2	1.168	1.735	1.485	5.707	0.535	3.056	0.929	0.795
Average	0.579	0.788	1.361	2.592	0.773	2.004	0.609	1.052
Average×1.5	0.809	1.353	1.672	4.451	0.611	2.720	0.827	1.022
Average×2	1.027	2.050	1.996	6.743	0.486	3.276	0.996	0.970

Table E.3: Average Estimation Results for Model 3*Ground Condition I*

Ground Motion	δ_{DP} (m)	δ_{SP} (m)	δ_{SP}/δ_{DP}	μ_E	C	μ_c	δ_{SP}' (m)	δ_{SP}'/δ_{DP}
L2.t211	0.536	0.549	1.024	1.508	0.914	1.379	0.502	0.936
L2.t211×1.2	0.625	0.668	1.069	1.835	0.866	1.590	0.579	0.926
L2.t211×1.5	0.695	0.857	1.233	2.354	0.800	1.883	0.686	0.986
L2.t211×1.7	0.727	0.993	1.365	2.727	0.758	2.068	0.753	1.036
L2.t211×2	0.783	1.210	1.545	3.324	0.700	2.327	0.847	1.082
L2.t211×5	1.24	4.766	3.844	13.094	0.310	4.055	1.476	1.190
L2.t212	0.528	0.533	1.009	1.464	0.921	1.348	0.491	0.930
L2.t212×1.5	0.699	0.828	1.185	2.275	0.810	1.842	0.670	0.959
L2.t212×2	0.792	1.163	1.468	3.195	0.712	2.274	0.828	1.045
L2.t212×5	1.479	4.426	2.993	12.159	0.327	3.978	1.448	0.979
L2.t213	0.543	0.559	1.029	1.535	0.910	1.397	0.508	0.936
L2.t213×1.5	0.665	0.872	1.312	2.397	0.795	1.906	0.694	1.043
L2.t213×2	0.861	1.234	1.433	3.390	0.694	2.353	0.857	0.995
L2.t213×5	1.522	4.886	3.210	13.424	0.304	4.080	1.485	0.976
Average	0.536	0.547	1.020	1.502	0.915	1.375	0.500	0.934
Average×1.5	0.686	0.852	1.242	2.341	0.802	1.877	0.683	0.996
Average×2	0.812	1.202	1.480	3.301	0.702	2.318	0.844	1.039
Average×5	1.414	4.690	3.317	12.885	0.313	4.038	1.470	1.040

Ground Condition II

Ground Motion	δ_{DP} (m)	δ_{SP} (m)	δ_{SP}/δ_{DP}	μ_E	C	μ_c	δ_{SP}' (m)	δ_{SP}'/δ_{DP}
Le2.t221	0.903	1.193	1.321	3.277	0.704	2.308	0.840	0.930
Le2.t221x1.5	1.105	2.074	1.877	5.698	0.536	3.053	1.111	1.006
Le2.t221x2	1.481	3.208	2.166	8.813	0.410	3.612	1.315	0.888
Le2.t222	0.814	1.170	1.437	3.214	0.710	2.282	0.831	1.021
Le2.t222x1.5	1.048	2.026	1.933	5.566	0.543	3.022	1.100	1.050
Le2.t222x2	1.356	3.131	2.309	8.602	0.416	3.582	1.304	0.962
Le2.t223	0.870	1.101	1.266	3.025	0.728	2.202	0.802	0.921
Le2.t223x1.5	1.148	1.894	1.650	5.203	0.563	2.932	1.067	0.930
Le2.t223x2	1.304	2.923	2.242	8.030	0.436	3.498	1.273	0.976
Average	0.862	1.155	1.340	3.173	0.714	2.265	0.825	0.957
Average×1.5	1.100	1.998	1.816	5.489	0.547	3.004	1.093	0.994
Average×2	1.380	3.087	2.237	8.481	0.420	3.565	1.298	0.940

Table E.4: Average Estimation Results for Model 4*Ground Condition I*

Ground Motion	$\delta_{DP}(m)$	$\delta_{SP}(m)$	δ_{SP}/δ_{DP}	μ_E	C	μ_c	$\delta_{SP}'(m)$	δ_{SP}'/δ_{DP}
L2.t211	0.588	0.597	1.015	1.252	0.955	1.196	0.570	0.970
L2.t211×1.2	0.636	0.723	1.136	1.515	0.913	1.384	0.660	1.038
L2.t211×1.5	0.744	0.920	1.237	1.929	0.854	1.647	0.785	1.056
L2.t211×1.7	0.786	1.057	1.345	2.216	0.817	1.810	0.863	1.098
L2.t211×2	0.88	1.274	1.448	2.671	0.764	2.042	0.974	1.107
L2.t211×5	1.831	4.624	2.526	9.695	0.384	3.725	1.777	0.970
L2.t212	0.586	0.641	1.093	1.343	0.940	1.263	0.602	1.028
L2.t212×1.5	0.730	0.992	1.359	2.080	0.834	1.734	0.827	1.133
L2.t212×2	0.847	1.384	1.633	2.901	0.740	2.148	1.025	1.210
L2.t212×5	1.938	5.223	2.695	10.949	0.353	3.864	1.843	0.951
L2.t213	0.526	0.533	1.013	1.118	0.979	1.094	0.522	0.992
L2.t213×1.5	0.659	0.815	1.236	1.708	0.884	1.511	0.721	1.093
L2.t213×2	0.785	1.119	1.425	2.346	0.801	1.879	0.896	1.142
L2.t213×5	1.546	3.865	2.500	8.102	0.433	3.509	1.674	1.083
Average	0.567	0.590	1.040	1.237	0.958	1.185	0.565	0.997
Average×1.5	0.711	0.909	1.278	1.905	0.857	1.633	0.779	1.095
Average×2	0.837	1.256	1.501	2.634	0.768	2.024	0.965	1.154
Average×5	1.772	4.554	2.570	9.547	0.388	3.707	1.768	0.998

Ground Condition II

Ground Motion	$\delta_{DP}(m)$	$\delta_{SP}(m)$	δ_{SP}/δ_{DP}	μ_E	C	μ_c	$\delta_{SP}'(m)$	δ_{SP}'/δ_{DP}
Le2.t221	0.936	1.170	1.250	2.453	0.789	1.934	0.923	0.986
Le2.t221×1.5	1.280	1.935	1.512	4.057	0.640	2.595	1.238	0.967
Le2.t221×2	1.601	2.921	1.824	6.124	0.514	3.149	1.502	0.938
Le2.t222	0.875	1.636	1.870	3.430	0.691	2.369	1.130	1.291
Le2.t222×1.5	1.255	2.883	2.297	6.044	0.518	3.132	1.494	1.190
Le2.t222×2	1.572	4.544	2.891	9.526	0.389	3.704	1.767	1.124
Le2.t223	0.877	1.273	1.452	2.669	0.765	2.041	0.973	1.110
Le2.t223×1.5	1.138	2.137	1.878	4.480	0.609	2.729	1.302	1.144
Le2.t223×2	1.448	3.265	2.255	6.845	0.481	3.295	1.572	1.085
Average	0.896	1.354	1.511	2.839	0.747	2.120	1.011	1.129
Average×1.5	1.224	2.299	1.878	4.820	0.587	2.828	1.349	1.102
Average×2	1.540	3.542	2.300	7.426	0.458	3.399	1.621	1.053

Table E.5: Average Estimation Results for Model 5*Ground Condition I*

Ground Motion	δ_{DP} (m)	δ_{SP} (m)	δ_{SP}/δ_{DP}	μ_E	C	μ_c	δ_{SP}' (m)	δ_{SP}'/δ_{DP}
L2.t211	0.376	0.431	1.148	2.124	0.828	1.759	0.357	0.951
L2.t211×1.2	0.430	0.535	1.244	2.637	0.768	2.025	0.411	0.956
L2.t211×1.5	0.525	0.718	1.367	3.536	0.681	2.410	0.489	0.931
L2.t211×1.7	0.588	0.858	1.458	4.226	0.627	2.650	0.538	0.914
L2.t211×2	0.680	1.093	1.608	5.383	0.553	2.977	0.604	0.889
L2.t212	0.369	0.380	1.030	1.871	0.861	1.612	0.327	0.887
L2.t212×1.5	0.517	0.618	1.196	3.047	0.726	2.212	0.449	0.868
L2.t212×2	0.612	0.931	1.521	4.585	0.602	2.760	0.560	0.916
L2.t213	0.355	0.404	1.137	1.988	0.846	1.681	0.341	0.962
L2.t213×1.5	0.513	0.664	1.294	3.269	0.705	2.305	0.468	0.912
L2.t213×2	0.603	1.005	1.667	4.953	0.578	2.865	0.582	0.965
Average	0.367	0.405	1.103	1.994	0.845	1.685	0.342	0.932
Average×1.5	0.518	0.665	1.284	3.277	0.704	2.308	0.469	0.904
Average×2	0.632	1.009	1.597	4.972	0.577	2.870	0.583	0.922

Ground Condition II

Ground Motion	δ_{DP} (m)	δ_{SP} (m)	δ_{SP}/δ_{DP}	μ_E	C	μ_c	δ_{SP}' (m)	δ_{SP}'/δ_{DP}
Le2.t221	0.346	0.356	1.029	1.754	0.878	1.540	0.313	0.903
Le2.t221×1.5	0.492	0.570	1.159	2.808	0.750	2.106	0.427	0.869
Le2.t221×2	0.611	0.847	1.386	4.172	0.631	2.633	0.534	0.875
Le2.t222	0.347	0.404	1.164	1.990	0.846	1.683	0.342	0.984
Le2.t222×1.5	0.487	0.661	1.357	3.256	0.706	2.300	0.467	0.959
Le2.t222×2	0.579	0.994	1.717	4.897	0.582	2.850	0.578	0.999
Le2.t223	0.339	0.353	1.041	1.739	0.880	1.530	0.311	0.916
Le2.t223×1.5	0.500	0.565	1.130	2.783	0.753	2.094	0.425	0.850
Le2.t223×2	0.618	0.838	1.356	4.128	0.634	2.618	0.531	0.860
Average	0.344	0.370	1.076	1.823	0.868	1.582	0.321	0.934
Average×1.5	0.493	0.598	1.213	2.946	0.736	2.168	0.440	0.893
Average×2	0.603	0.892	1.479	4.394	0.615	2.703	0.549	0.910

Table E.6: Average Estimation Results for Model 6*Ground Condition I*

Ground Motion	δ_{DP} (m)	δ_{SP} (m)	δ_{SP}/δ_{DP}	μ_E	C	μ_c	δ_{SP}' (m)	δ_{SP}'/δ_{DP}
L2.t211	0.302	0.453	1.501	2.198	0.819	1.800	0.371	1.229
L2.t211×1.2	0.340	0.571	1.679	2.774	0.754	2.090	0.431	1.265
L2.t211×1.5	0.457	0.780	1.706	3.784	0.661	2.501	0.515	1.127
L2.t211×1.7	0.528	0.937	1.775	4.549	0.604	2.750	0.566	1.073
L2.t211×2	0.633	1.197	1.890	5.810	0.530	3.079	0.634	1.002
L2.t212	0.356	0.375	1.053	1.820	0.869	1.581	0.326	0.915
L2.t212×1.5	0.492	0.629	1.279	3.054	0.725	2.215	0.456	0.928
L2.t212×2	0.576	0.968	1.680	4.697	0.595	2.793	0.575	0.999
L2.t213	0.338	0.403	1.193	1.957	0.850	1.663	0.343	1.014
L2.t213×1.5	0.440	0.680	1.545	3.300	0.702	2.317	0.477	1.085
L2.t213×2	0.510	1.041	2.040	5.052	0.572	2.892	0.596	1.168
L2.t213×5	0.865	4.564	5.277	22.157	0.204	4.522	0.932	1.077
Average	0.332	0.409	1.233	1.988	0.846	1.681	0.346	1.043
Average×1.5	0.463	0.695	1.502	3.376	0.695	2.347	0.484	1.044
Average×2	0.573	1.067	1.862	5.180	0.565	2.926	0.603	1.052

Ground Condition II

Ground Motion	δ_{DP} (m)	δ_{SP} (m)	δ_{SP}/δ_{DP}	μ_E	C	μ_c	δ_{SP}' (m)	δ_{SP}'/δ_{DP}
Le2.t221	0.322	0.344	1.068	1.670	0.890	1.486	0.306	0.951
Le2.t221×1.5	0.458	0.566	1.236	2.748	0.756	2.078	0.428	0.935
Le2.t221×2	0.567	0.855	1.508	4.150	0.633	2.626	0.541	0.954
Le2.t222	0.323	0.371	1.149	1.801	0.871	1.569	0.323	1.001
Le2.t222×1.5	0.436	0.619	1.420	3.005	0.730	2.194	0.452	1.037
Le2.t222×2	0.526	0.947	1.800	4.597	0.601	2.764	0.569	1.083
Le2.t223	0.309	0.341	1.104	1.655	0.892	1.477	0.304	0.984
Le2.t223×1.5	0.433	0.556	1.284	2.699	0.761	2.055	0.423	0.978
Le2.t223×2	0.518	0.842	1.625	4.087	0.637	2.605	0.537	1.036
Average	0.318	0.352	1.107	1.709	0.884	1.511	0.311	0.979
Average×1.5	0.442	0.579	1.310	2.811	0.750	2.107	0.434	0.982
Average×2	0.537	0.881	1.641	4.277	0.623	2.666	0.549	1.023

Appendix F: Correction Results for the Lower Bound Estimation

Table F.1: Lower Bound Estimation Results for Model 1

<i>Ground Condition I</i>								
Ground Motion	$\delta_{DP}(m)$	$\delta_{SP}(m)$	δ_{SP}/δ_{DP}	μ_E	C	μ_c	$\delta_{SP}'(m)$	δ_{SP}'/δ_{DP}
Average	0.373	0.373	1.000	0.926	1.160	No Correction		
Average×1.5	0.559	0.566	1.013	1.404	1.060	No Correction		
Average×2	0.726	0.785	1.081	1.948	0.965	1.880	0.758	1.044
Average×5	1.217	3.026	2.486	7.509	0.505	3.789	1.527	1.255
<i>Ground Condition II</i>								
Average	0.567	0.612	1.079	1.519	1.038	No Correction		
Average×1.5	0.765	1.004	1.312	2.491	0.886	2.208	0.890	1.163
Average×2	0.894	1.695	1.896	4.206	0.704	2.962	1.194	1.335

Table F.2: Lower Bound Estimation Results for Model 2

<i>Ground Condition I</i>								
Ground Motion	$\delta_{DP}(m)$	$\delta_{SP}(m)$	δ_{SP}/δ_{DP}	μ_E	C	μ_c	$\delta_{SP}'(m)$	δ_{SP}'/δ_{DP}
Average	0.439	0.444	1.010	1.459	1.049	No Correction		
Average×1.5	0.634	0.692	1.092	2.277	0.916	2.085	0.634	1.000
Average×2	0.764	0.991	1.297	3.259	0.794	2.588	0.787	1.030
Average×5	1.353	3.918	2.896	12.890	0.345	4.450	1.353	1.000
<i>Ground Condition II</i>								
Average	0.579	0.788	1.361	2.592	0.873	2.263	0.688	1.188
Average×1.5	0.809	1.353	1.672	4.451	0.684	3.045	0.926	1.144
Average×2	1.027	2.050	1.996	6.743	0.540	3.642	1.107	1.078

Table F.3: Lower Bound Estimation Results for Model 3

<i>Ground Condition I</i>								
Ground Motion	$\delta_{DP}(m)$	$\delta_{SP}(m)$	δ_{SP}/δ_{DP}	μ_E	C	μ_c	$\delta_{SP}'(m)$	δ_{SP}'/δ_{DP}
Average	0.536	0.547	1.020	1.502	1.041	No Correction		
Average×1.5	0.686	0.852	1.242	2.341	0.907	2.122	0.772	1.126
Average×2	0.812	1.202	1.480	3.301	0.790	2.607	0.949	1.169
Average×5	1.414	4.690	3.317	12.885	0.345	4.450	1.620	1.146
<i>Ground Condition II</i>								
Average	0.862	1.155	1.340	3.173	0.804	2.550	0.928	1.077
Average×1.5	1.100	1.998	1.816	5.489	0.610	3.351	1.220	1.109
Average×2	1.380	3.087	2.237	8.481	0.466	3.951	1.438	1.042

Table F.4: Lower Bound Estimation Results for Model 4

<i>Ground Condition I</i>								
Ground Motion	$\delta_{DP}(m)$	$\delta_{SP}(m)$	δ_{SP}/δ_{DP}	μ_E	C	μ_c	$\delta_{SP}'(m)$	δ_{SP}'/δ_{DP}
Average	0.567	0.590	1.040	1.237	1.093	No Correction		
Average×1.5	0.711	0.909	1.278	1.905	0.972	1.852	0.883	1.242
Average×2	0.837	1.256	1.501	2.634	0.867	2.285	1.090	1.302
Average×5	1.772	4.554	2.570	9.547	0.430	4.101	1.956	1.104
<i>Ground Condition II</i>								
Ground Motion	$\delta_{DP}(m)$	$\delta_{SP}(m)$	δ_{SP}/δ_{DP}	μ_E	C	μ_c	$\delta_{SP}'(m)$	δ_{SP}'/δ_{DP}
Average	1.224	2.299	1.878	4.820	0.656	3.162	1.508	1.232
Average×1.5	1.540	3.542	2.300	7.426	0.508	3.774	1.800	1.169

Table F.5: Lower Bound Estimation Results for Model 5

<i>Ground Condition I</i>								
Ground Motion	$\delta_{DP}(m)$	$\delta_{SP}(m)$	δ_{SP}/δ_{DP}	μ_E	C	μ_c	$\delta_{SP}'(m)$	δ_{SP}'/δ_{DP}
Average	0.367	0.405	1.103	1.994	0.958	1.910	0.388	1.056
Average×1.5	0.518	0.665	1.284	3.277	0.792	2.597	0.527	1.018
Average×2	0.632	1.009	1.597	4.972	0.645	3.207	0.651	1.030
<i>Ground Condition II</i>								
Ground Motion	$\delta_{DP}(m)$	$\delta_{SP}(m)$	δ_{SP}/δ_{DP}	μ_E	C	μ_c	$\delta_{SP}'(m)$	δ_{SP}'/δ_{DP}
Average	0.344	0.370	1.076	1.823	0.985	1.796	0.365	1.060
Average×1.5	0.493	0.598	1.213	2.946	0.829	2.443	0.496	1.006
Average×2	0.603	0.892	1.479	4.394	0.689	3.026	0.614	1.019

Table F.6: Lower Bound Estimation Results for Model 6

<i>Ground Condition I</i>								
Ground Motion	$\delta_{DP}(m)$	$\delta_{SP}(m)$	δ_{SP}/δ_{DP}	μ_E	C	μ_c	$\delta_{SP}'(m)$	δ_{SP}'/δ_{DP}
Average	0.332	0.409	1.233	1.988	0.959	1.906	0.393	1.183
Average×1.5	0.463	0.695	1.502	3.376	0.782	2.640	0.544	1.174
Average×2	0.573	1.067	1.862	5.180	0.631	3.267	0.673	1.174
<i>Ground Condition II</i>								
Ground Motion	$\delta_{DP}(m)$	$\delta_{SP}(m)$	δ_{SP}/δ_{DP}	μ_E	C	μ_c	$\delta_{SP}'(m)$	δ_{SP}'/δ_{DP}
Average	0.318	0.352	1.107	1.709	1.005	1.716	0.354	1.112
Average×1.5	0.442	0.579	1.310	2.811	0.845	2.376	0.490	1.107
Average×2	0.537	0.881	1.641	4.277	0.698	2.986	0.615	1.146

CURRICULUM VITAE

Osman Tunc CETINKAYA was born in 1979 in Erzurum, Turkey. He has completed his high school education in TED Ankara College, and graduated from Yildiz Technical University, Department of Civil Engineering in 2001. He still continues his post graduate education in Istanbul Technical University.